



# Durham E-Theses

---

## *The electrification of hail*

Church, Christopher, R.

### How to cite:

---

Church, Christopher, R. (1966) *The electrification of hail*, Durham theses, Durham University.  
Available at Durham E-Theses Online: <http://etheses.dur.ac.uk/8779/>

### Use policy

---

The full-text may be used and/or reproduced, and given to third parties in any format or medium, without prior permission or charge, for personal research or study, educational, or not-for-profit purposes provided that:

- a full bibliographic reference is made to the original source
- a [link](#) is made to the metadata record in Durham E-Theses
- the full-text is not changed in any way

The full-text must not be sold in any format or medium without the formal permission of the copyright holders.

Please consult the [full Durham E-Theses policy](#) for further details.

THE ELECTRIFICATION OF HAIL

by

Christopher R. Church, B.Sc., Grad. Inst. P.

Thesis submitted in candidature for the degree of Doctor  
of Philosophy in the University of Durham.



August, 1966.

ABSTRACT.

Reynolds, Brook and Gourley (1957) derived a value of  $5 \times 10^{-4}$  e.s.u. for the charge separated per crystal collision when a simulated hailstone rotated in a cloud consisting of ice crystals together with supercooled water droplets of some  $5 \mu$  size. From this estimate they concluded that the electrification of thunderclouds could be explained in terms of the electrification of hail by impacting ice crystals. Latham and Mason (1961 B) performed similar experiments in the absence of water droplets and obtained an estimate which was 5 orders of magnitude less than Reynolds' value. They also measured the electrification of an iced probe by supercooled water droplets shattering on it and derived a value of  $4 \times 10^{-6}$  e.s.u. for the mean charge separated per droplet diameter range  $40 \pm 100 \mu$ . They concluded from these experiments that the charge separated by ice crystal impacts was not sufficient to explain thunderstorm electrification. They proposed instead that the droplet shattering mechanism offered a satisfactory explanation of the magnitude of the charge separated in thunderclouds. It was the purpose of this thesis to investigate the results of these two authorities and in particular to seek an explanation for the large discrepancy between their results on ice crystal impactations.

In this laboratory similar experiments to Reynolds, Brook and Gourley were performed, and it was concluded that the results could be explained qualitatively in terms of the temperature gradient theory, but quantitatively the charge separated was larger than predicted by

the theory.

Experiments similar to those of Latham and Mason on crystal impacts were performed. The quantity of charge separated per crystal collision and how it depended on the sign and magnitude of the measured temperature difference between the iced probe and the crystals, the presence of impurities in the probe, and the impact velocity of the ice crystals was determined. An estimate of  $2.5 \times 10^{-7}$  e.s.u. was obtained for an impact velocity of  $20 \text{ m sec}^{-1}$  and measured temperature difference of  $10^{\circ} \text{ C}$ . This was 50 times greater than the value found by Latham and Mason but it was shown that the two values could be reconciled. It was shown that they could also be reconciled with the previous value of  $5 \times 10^{-6}$  e.s.u. It was further observed that the charge separated per crystal collision increased markedly as the impact velocity increased.

Apparatus was built which enabled stable streams of uniformly sized uncharged water droplets in the radius range  $50 - 150 \mu$  to be produced. Smaller droplets down to  $30 \mu$  radius were produced in unstable streams. Droplets were made to encounter a rotating iced probe connected to an electrometer. It was found that appreciable quantities of charge were separated only for the larger droplets. If the droplets were above about  $0^{\circ} \text{ C}$  they charged the probe positively and if they were supercooled they charged it negatively. The quantity of negative charge separated decreased as the degree of supercooling increased. The maximum mean charge separated for a  $150 \mu$  radius droplet was  $10^{-5}$  e.s.u. and for a  $90 \mu$  radius droplet was  $4 \times 10^{-7}$  e.s.u. It was concluded that the charge was separated by the

droplets splashing.

Droplets which were in the process of freezing were allowed to encounter the probe. The droplets always charged the probe negatively and mean charges of up to  $2 \times 10^{-4}$  e.s.u. per 150  $\mu$  radius droplet were separated. The charge separated appeared to be proportional to the cube of the droplet radius. Although the results were not directly comparable with the results of Iatham and Mason, it was considered that a similar charge separation mechanism was operative, and that it could be explained more readily by the Workman - Reynolds effect than by the temperature gradient theory.

## CONTENTS.

	<u>Page</u>
<u>CHAPTER 1.</u> <u>THE THUNDERSTORM</u>	
1. Introduction.	1
2. Meteorological and Physical Aspects of a Typical Thunderstorm.	1
3. Electrical Aspects of the Typical Thundercloud.	4
4. Thunderstorm Theories.	6
 <u>CHAPTER 2.</u> <u>THE ELECTRIFICATION OF HAIL</u>	
1. Introduction.	19
2. The Electrification Produced on Melting.	19
3. Electrification Associated with Temperature Gradients in Ice.	23
4. Collisions between Supercooled Water Droplets and Hailstones.	29
5. Electrification by Evaporation of Ice.	31
6. Other Electrification Processes	33
7. Comparison of Field Measurements.	33
 <u>CHAPTER 3.</u> <u>SOME THEORY CONCERNING THE ELECTRIFICATION OF ICE AND WATER</u>	
1. Introduction.	36
2. Electrification Processes in Ice and Water.	36
3. The Structure of Ice and Water.	38
4. Charge Transport in Water and Ice.	39
5. The Temperature Gradient Theory for Ice.	43

CONTENTS (Continued)

	<u>Page</u>
<u>CHAPTER 4.</u> <u>MEASUREMENTS WITH A ROTATING PROBE</u>	
1. Introduction and Apparatus.	47
2. Electrification Produced by Water Droplets Only.	53
3. Electrification Produced by Water Droplets and Ice Crystals Together.	55
4. Correlation of Rate of Charging with Temperature Difference.	62
5. Summary.	70
<u>CHAPTER 5</u> <u>MEASUREMENTS WITH A STATIONARY PROBE</u>	
1. Introduction.	79
2. Apparatus.	79
3. Variation of Charging with Temperature Difference.	87
4. Variation of Charging with Impact Velocity.	97
5. Effects of Contaminants on Electrification.	101
6. A Discussion of the Results of Reynolds Brook and Courley, Latham and Mason and the Present Results.	109
<u>APPENDIX 1</u> Formvar Slide Technique.	117
<u>CHAPTER 6</u> <u>APPARATUS FOR PRODUCING UNIFORMLY SIZED SUPERCOOLED WATER DROPLETS.</u>	
1. Introduction.	121
2. The Vibrating Needle Device.	121
3. The Other Apparatus.	128

CONTENTS (Continued)

	<u>Page</u>
<u>CHAPTER 7</u>	
<u>THEORETICAL DETERMINATION OF DROPLET TEMPERATURES.</u>	
1. Introduction.	132
2. Measurement of Lapse Rate in Tube.	132
3. Calculation of Reynolds Numbers and Terminal Velocities.	133
4. Calculation of Thermal Relaxation Times.	138
5. Calculation of Surface Temperatures.	140
6. Calculation of the Higher Degrees of Supercooling.	141
7. Conclusion.	142
<u>APPENDIX 2</u>	
Variation of Reynolds Numbers with Temperature.	144
<u>APPENDIX 3</u>	
Effect of Room Temperature on the Cooling of the Droplets.	145
<u>CHAPTER 8</u>	
<u>EXPERIMENTAL WORK ON WATER DROPLETS</u>	
1. Introduction.	148
2. General Procedure.	148
3. Variation of Charging with Droplet Temperature.	150
4. Variation of Charging with Impact Velocity.	159
5. Variation of Charging with Droplet Size.	160
6. Charging by Droplets which had been Nucleated Before Encountering the Probe.	163
7. Summary.	171



CONTENTS (Continued)

		<u>Page</u>
<u>APPENDIX 4</u>	Calculations of Droplet Freezing Times.	173
<u>CHAPTER 9</u>	<u>CONCLUSIONS AND SUGGESTIONS FOR FURTHER WORK.</u>	177
<u>ACKNOWLEDGEMENTS</u>		
<u>REFERENCES.</u>		

CHAPTER 1

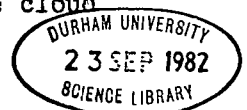
THE THUNDERSTORM.

1. INTRODUCTION.

In attempting to give an account of the various aspects of the thunderstorm, one is cautious in presenting a general picture of a typical thunderstorm. This is because the scale of the storms varies over such a wide range, and in attempting to explain thunderstorm electrification, the theorist must be sure that the parameter he has chosen not only explains the electrification of a typical thunderstorm, but are also applicable to the extreme cases as well. Also, there are clouds which exhibit thunderstorm activity, and yet in some respects do not comply with the general meteorological picture..

2. METEOROLOGICAL AND PHYSICAL ASPECTS OF A TYPICAL THUNDERSTORM.

Byers and Braham (1949), using radar techniques, established the cellular structure of thunderclouds. A thundercloud can be considered to consist of one or more active cells which may range from 0.5 to 10 km in horizontal extent. Küttner (1950) has suggested the existence of even smaller sub-cells which are only 100 m. in diameter. The cell represents the region in the cloud



in which precipitation and lightning activity occur. Each cell has a life cycle, and is detected during the mature stage of the cycle which lasts 15 to 20 minutes. During this period there is a strong central updraft of air in the cell, which may typically be  $10 \text{ m sec.}^{-1}$ , but which may be as high as  $50 \text{ m sec.}^{-1}$ , and sometimes displaying a pulse-like nature (Workman and Holzer, 1942). The columnar updraught is surrounded by a region of strong down-draught. Lightning activity and intense precipitation also occur during the mature stage. Hail falls from the regions where the updraught is too weak to support it, and may reach the ground either in solid form or as rain. In tropical thunderstorms very large hailstones can be produced by recirculation, but elsewhere the most usual form is as small hail and soft hail, which have rounded or conical shapes and measure from 4 to 6 mm. across. Precipitation in the form of hail is usually intense, and rates may be as high as  $5 \text{ cm. hr.}^{-1}$  (Latham and Mason, 1961 B). During the latter part of the storm, hail may give way to snow.

Also characteristic of the typical thundercloud are its great vertical depth and the very wide temperature range which it spans. The bases are usually warmer than  $0^{\circ} \text{ C.}$  and the tops may extend to the  $-40^{\circ} \text{ C.}$  isotherm, and occasionally beyond into the tropopause. The vertical depth is up to  $10 \text{ km.}$  The cloud top is characterised by an anvil-shaped mass of ice crystals which has the diffuse outline

of cirrus cloud. A number of cases have been reported, however, of lightning activity from clouds having a different physical appearance and dimensions to this picture, and which have tops warmer than  $0^{\circ}$  C. (Moore, 1965). Although the evidence for such occurrences is as yet not well detailed, the large number of instances of warm cloud lightning is sufficient indication that it really happens.

The particular sizes and concentrations of the cloud particles found in thunderclouds are present only in thunderclouds, and they have been involved in various theories to explain the electrification of the cloud. Jones (1960) measured the size spectra of ice crystals in such clouds and found that the most numerous were between 80 and 175  $\mu$  in diameter, and of concentration  $10^5 \text{ m}^{-3}$ . Crystal sizes were measured up to 5 mm, but the concentration fell off rapidly with increasing size, and the largest crystals were only to be found near to the  $0^{\circ}$  C isotherm. Information concerning the size spectra of droplets appears to be less well documented, probably because of the greater difficulties involved in sampling, but in general, the larger cloud droplets are more numerous than in other types of cloud. Latham and Mason (1961 B) quote that droplets of diameters greater than 50  $\mu$  are present in concentrations of at least  $10^6 \text{ m}^{-3}$ .

### 3. ELECTRICAL ASPECTS OF THE TYPICAL THUNDERCLOUD.

It is difficult to determine the charge distribution in a thundercloud because electrostatic measurements at the ground do not present a unique picture. However, the results of many workers employing many different techniques (see Mason, Physics of Clouds, Pages 372-5) have shown that the charge distribution in a typical thundercloud can be represented as a simple electric dipole with the positive charge uppermost. Often a region of smaller positive charge is situated below the main negative charge, and is usually also below the  $0^{\circ}$  C. isotherm. It has yet to be shown definitely whether the lower positive charge is common to all thunderclouds. The magnitudes of the charges neutralised by a lightning discharge were calculated from the charge in electric moment caused by the discharge. The charge in electric moment was deduced from field measurements at the ground. The average electric moment destroyed per lightning flash was shown by Pierce (1955) to be 100 C km. For a charge separation of 5 km. this meant that the magnitude of the segregated charges is 20 C. The region between the segregated charges may contain approximately 1000 C. of unsegregated positive and negative charges. The presence of charge of this magnitude is necessary if the charging current in the cloud is to be explained in terms of the gravitational separation of precipitation elements. The expression relating the charge being separated after a flash

to the relative velocity  $V$  of the charge carriers has been worked out as  $3000/v.c.$

When a lightning discharge occurs, the field inside the cloud falls to zero and immediately begins to redevelop, increasing exponentially with a time constant of about 7 seconds. Wormell (1953) showed that this could be explained in terms of a constant charging current in conjunction with a dissipating current proportional to the charge separated. It is the constant current which theories attempt to account for. Wormell calculated its value to be 3 A. This is the value for a typical thunderstorm, and to indicate how other thunderstorms can deviate from this, the observations of Vonnegut and Moore (1958) can be mentioned. They observed storms in which there were 10 to 20 discharges per second. This meant that there must have been a charging current of about 100 A.

In addition to the internal currents there are external currents. There is a point discharge current of positive ions to the base of the cloud. Chalmers (1953) has calculated this to be less than 0.5 A. There is also a negative conduction current to the top of the cloud from the ionosphere. Gish and Wait (1950) obtained an average value of 0.5 A. and Stergis, Rein and Kangas (1957) measured the current to be 1.3 A.

It has been stated above that the electrical activity in a thunderstorm cell occurs in the same part of the life-cycle as

violent convection and the growth of precipitation particles large enough to give radar returns. It is of great importance that this information should be expressed more precisely and in fact the earlier radar results of Workman and Reynolds (1949) had indicated that the electrical activity did not begin until several minutes had elapsed since the first radar returns, from which it was deduced that charge was being segregated by falling precipitation. However, Moore (1965) has now observed that precipitation appears to follow a lightning flash rather than to precede it, and this result would seem to affect opinions about the temporal relationship between the growth of hail and the onset of lightning activity. However, this is an issue which will not be finally settled without many more observations.

#### 4. THUNDERSTORM THEORIES.

The following list gives the names of those who have proposed theories of cloud and thundercloud electrification during this century.

Gerdien	1905	Rossmann	1948
Simpson	1909	Workman & Reynolds	1948
Elster & Geitel	1913	Wall	1948
Wilson	1929	Vonnegut	1955
Gunn	1935	Wilson	1956

Simpson & Sêrase	1937	Reynolds, Brook & Gôurley.	1957
Findeisen	1940	Latham & Mason	1961
Frenkel	1944	Sartor	1961
Dinger & Gunn	1946	Magono & Takahashi	1963
Grenet	1947	Reiter	1965

This list is eloquent of the many ways in which electrification phenomena in ice and water are manifest. The eventual success of a thunderstorm theory, must depend on its being able to explain all aspects of all thunderstorms. For this a very intimate knowledge of the correspondence between meteorological, physical and electrical phenomena is required. Many of the above theories are no longer accepted because they were based on ideas which experiments later showed to be either incorrect or to give insufficient electrification. However a large number of them, including some of the earliest theories have not yet been fully evaluated. It is quite clear that several of these mechanisms will cause electrification in clouds but it may be that there is only one mechanism, which may not yet have been proposed, which will satisfactorily explain thunderstorms on any scale.

Charge production mechanisms can be divided into three categories depending on the origin of the positive and negative charges:

(i) Classical, in which charge is separated by the interaction of initially neutral cloud particles.



(ii) Influence, in which positive and negative charges are already available as atmospheric ions.

(iii) Convection, in which the origin of the charges is outside the cloud. It is also possible to have a combination of these processes. The charge may be segregated by either electrical, convective or gravitational forces and recently Chalmers (1965) has suggested segregation by a centrifugal force. Most current theories favour classical separation and gravitational segregation, in which charges are separated by the interaction between cloud particles of different sizes and which are segregated because of the different fall-speeds of the particles. In the following pages are described some of the theories which have been subjects of considerable interest and great controversy in recent years.

(a) Wilson's Theory (1929)

The ideas embodied in the theories of C.T.R. Wilson are very powerful. In the earlier (1929) theory it is suggested that the weak atmospheric electric field is capable of steering and building up electrification of the vast, unwieldy thundercloud. It is an influence theory and like other influence theories it has fallen into disregard, mainly because it fails to account for the required rate of charge production in a thundercloud in terms of the available data. The principle of the method is that falling water

drops, polarised in the atmospheric electric field so that their lower surfaces have a positive charge, will repel positive ions and selectively capture negative ions and on falling towards the bottom of the cloud will thereby enhance the existing electric field, which in turn will cause further falling drops to acquire greater charges, and so the electric field will be built up in this manner. The theory of the ion capture process has been worked out by Whipple and Chalmers (1944), and Chalmers (1947) has shown that the process applies very similarly to falling ice particles. There are, however, limitations to the theory. For drops to acquire a net negative charge, they must be moving faster than the downward moving positive ions, and this is no longer true in fields of about  $500 \text{ Vcm.}^{-1}$ . In spite of this there could still be selective ion capture if the ions were attached to cloud droplets, although the quantity of charge segregated ultimately depends on the quantity of charge present on ions throughout the whole cloud, and even if all the ions were intercepted before recombination could occur, it was shown by Wormell (1953) that the charge separation would be only  $6 \text{ C km.}^{-3} \text{ hr.}^{-1}$  compared with the required rate of  $50 \text{ C km.}^{-3} \text{ hr.}^{-1}$ . It was also shown by Mason (1953) that unless the conductivity of the air is unusually high, falling cloud particles will acquire only a small fraction of their maximum charge during the lifetime of the average thunderstorm cell. The conductivity of the air inside thunderclouds has apparently not been measured. If it were found that the conductivity was unusually high,

then the origin of the charges would have to be in some other process such as point discharge. However it is not currently thought that the conductivity in thunderclouds is sufficiently high for the Wilson process to be considered as the principal charge segregation mechanism although it may well be of importance in determining the sign and magnitude of the charge carried by precipitation which has fallen through the region of dense space charge below the thundercloud base.

(b) The Dinger- Gunn Effect (1946)

As described on Page 20, the experiments of Dinger and Gunn (1946) on the electrification produced by the melting of samples of ice showed that for each gram of ice melted, a sample acquired a positive charge of 1.25 e.s.u., and the air an equal negative charge. Thus, qualitatively, the charge separated by melting hail is of the wrong sign to account for the observed polarity of thunderclouds. Whereas it would be difficult to estimate the charging current produced by melting hail in a thundercloud, a straightforward calculation shows that the maximum concentration of charge in a cloud containing  $2 \text{ gm m}^{-3}$  of solid precipitation particles would be only  $0.8 \text{ C. km}^{-3}$ , much smaller than the required concentration of  $20 \text{ C km}^{-3}$ . Although the results are both qualitatively and quantitatively unsatisfactory in accounting for thunderstorm electrification it has been suggested that the charge acquired by melting hail contributes

to the lower positive charge in thunderclouds.

(c) The Workman-Reynolds Effect (1943)

Costa Ribeiro (1945) discovered that large potential differences were set up across the ice-water boundary of freezing dilute aqueous solutions. Workman and Reynolds made more extensive studies of the effect, and applied it to atmospheric electricity. They measured the freezing potentials for very pure water and for dilute solutions containing a variety of added impurities. They found that potential differences of a few hundred volts could be attained, the sign of which depended on the nature of the added impurity. The potentials were very sensitive to small amounts of impurity, and it was difficult to get reproducible results for very pure water. Whether there is a freezing potential for the purest water has not been settled. The mechanism of the effect has not been fully described, but it is thought to be due to ions whose structures are isomorphous with the  $H_3 O^+$  ion being preferentially incorporated into the ice surface. Workman and Reynolds applied their results to a theory of thundercloud electrification in which they envisaged the wet hailstone as the charge generator: if a hailstone collects supercooled water droplets containing the usual cloud contaminants at a rate such as to maintain a liquid film on its surface, then it is suggested that this liquid film will become positively charged with respect to the ice. As the hailstone tends to grow beyond its stable size, small positively charged

droplets will be torn off and carried away in the updraft. The hailstone acquires a negative charge which increases to a value such that further droplets torn off also carry a negative charge. Since the hailstone has been falling continuously the positive and negative droplets have been spatially separated.

There have been a number of objections to this theory. Reynolds et al (1957) showed that there was no electrification caused by the riming of simulated hailstones in a cloud of supercooled water droplets of  $5 \mu$  diameter. Latham & Mason (1961 B) observed no electrification when the hailstone was wet for droplets in the diameter range 30-120  $\mu$ . Apart from these results, the mechanism is very sensitive to the nature and concentration of contaminants, and the success of the theory would seem to depend on ideal concentrations of specific impurities being present in the atmosphere. Also, this glazing process, if it occurs, will only be operative in a narrow temperature region near the freezing level in the thundercloud. Attempts to inhibit the development of electrical effects in cumulonimbus clouds by adding various impurities were briefly mentioned by Workman and Reynolds (1950), but no conclusions favourable to the theory have since appeared in published material.

(d) Convection Theories.

The suggestion that convection was responsible for cloud electrification was proposed by Grenet (1947), and supported in

greater detail by Vonnegut (1955). Vonnegut put forward several arguments against precipitation being the principal charge generating mechanism. The main ones are that during thunderstorms there is no relation between the intensity of precipitation and the intensity of electrification, the measured charge on precipitation from thunderclouds is very small and usually of the wrong sign, and that the violent updraught would interfere with any orderly charge segregation.

In Vonnegut's theory charges are transported by currents of air at several times the speed of gravitational segregation, the source of electricity being outside the cloud. A process is envisaged in which a relatively small concentration of positive charge is carried in the updraft to the top of the cloud where it causes a current of negative ions to flow from the ionosphere. These negative ions are carried in the downdraft to the bottom of the cloud where they are left. This lower negative charge causes a point discharge current of positive ions from the ground, which is carried in the updraft to enhance the upper positive charge.

Wilson (1956) proposed a theory which combined his earlier influence theory with convection theory. It was considered that a field which had been built up by the influence mechanism would cause negative ions to be attracted from above the cloud and positive ions from below. Positive ions entering the cloud base become attached to cloud droplets and are carried in the updraft to the main positive charge. Downward moving negative ions become attached to precipitation

elements and are thus brought down in this manner to form the lower negative charge.

These theories have been slow to win support, mainly because of the lack of convincing experimental evidence. It is probably more difficult to obtain results for convection theories than for precipitation theories, because laboratory experiments for the former are not feasible. In general, not sufficient information has been obtained about the air movements in thunderclouds, and these theories are attempting to explain charge segregation in terms of the air movements, and also without indicating how ions of different signs are apparently treated in a preferential manner. A further objection to Vonnegut's theory is that the charging current inside the thundercloud has been shown to be greater than the sum of the external currents, which is not what would be expected if the source of the charging current were outside the cloud.

(e) The Theory of Reynolds, Brook and Gourley

From laboratory measurements Reynolds, Brooke and Gourley (1957) estimated that when ice crystals collided with hailstones in the presence of cloud droplets, the mean charge separated by a rebounding ice crystal was  $5 \times 10^{-4}$  e.s.u., leaving the hailstone negatively charged. Applying this result to a model thundercloud containing a crystal concentration of  $10^4 \text{ m}^{-3}$  and a liquid water concentration of  $1 \text{ gm. m}^{-3}$ , they showed that hail in concentrations of  $10 \text{ gm. m}^{-3}$

falling at  $10 \text{ m. sec.}^{-1}$  relative to the ice crystals was capable of producing a 20 C. discharge in a cell 1 km. in diameter in about 14 minutes. In a thundercloud of volume  $50 \text{ km}^3$  sufficient charge would be separated to account for the repetition of lightning discharges.

The experimental techniques gave substantial errors, and it was clear that the results would only be accepted if they were confirmed by other authorities. Latham and Mason (1961 B) performed similar experiments, and concluded that the electrification of hailstones by ice crystals was five orders of magnitude less than the results of Reynolds, Brook and Gourley, clearly indicating that the mechanism was insufficient to explain thunderstorm electrification. This work is described in more detail in Chapter 2.

(f) The Theory of Latham and Mason.

Latham and Mason (1961 B) estimated the charge separated by supercooled water droplets shattering on hailstones, and concluded that the electrification of thunderclouds could be explained by the splintering of droplets in the diameter range  $40\text{-}100 \mu$  on hailstones. It was estimated that this process would separate charge at the rate of  $1 \text{ C km}^{-3} \text{ min}^{-1}$ , which is sufficient for the average thunderstorm although it does not account for very violent thunderstorms in which the rate of charge separation may be 100 times higher. This is a matter which cannot readily be resolved by scaling up either the droplet concentration or the hailstone concentration.



(g) Sartor's Theory

Sartor (1961) proposed an inductive thunderstorm theory, in which cloud particles, either ice crystals or water droplets, are polarised in the atmospheric electric field, and when they touch without coalescing, or pass within a short distance of each other, charge is separated, and then segregated by gravity. This theory is a more general form of the theories of Elster and Geitel (1913) who considered the charge separation between polarised water drops which collided but did not coalesce, and of Müller-Hillebrand (1954) who considered the charge separation between ice crystals and hailstones polarised in an electric field. It is also similar to Wilson's influence theory (1929). Sartor showed that the larger polarised cloud particles would acquire a negative charge, and if they grew by absorbing smaller charged cloud particles, both their charge and their fall-speed would be enhanced, thus causing a rapid increase in the field. It was considered that ice particles were more efficient than droplets in separating charge because of their rapid rates of growth which outweighed their reduced fall velocities. Sartor also showed that this mechanism would cause the electric field to build up exponentially, and calculated the rate of increase for various droplet separation efficiencies. The droplet separation efficiency is the fraction of droplets which do not coalesce after colliding. It was found that for a separation efficiency of 0.1 the electric field in a thundercloud would increase

1000- fold in about 10 minutes. In recent measurements on the charge separation between model ice crystals which do not touch, Latham, Mystrom and Sartor (1965 A) have shown that the charge transfer between separated cloud particles in an electric field is probably much more important for ice crystals than for water droplets, because appreciable quantities of charge can be transferred between ice crystals separated by distances comparable with their dimensions.

Sartor's theory of charge separation is a powerful one, but speculation on its relevance to thundercloud electrification must await further results on the interactions between water droplets and ice crystals in electric fields. These are needed if an accurate quantitative picture is to be obtained.

(h) Reiter's Theory.

Reiter (1965) has discovered a mechanism which, it is claimed, will separate charge in a thundercloud at a rate of  $15 \text{ C km}^{-3} \text{ min.}^{-1}$ . He has proposed this as a subsidiary charge separation mechanism, although the rate of charge production is 15 times as high as the value which Latham and Mason (1961 B) considered as being adequate. Reiter has shown that appreciable quantities of nitrate ions are produced in clouds, mainly by silent electrical discharges, and that the greater the degree of atmospheric instability, the greater the number of nitrate ions produced. Laboratory experiments showed that when ice particles grown by sublimation broke away from a

cold ice surface, they carried away 10-50 times as much charge when they were allowed to grow in an atmosphere containing nitrous gases as when the atmosphere was ordinary air. These results were applied to the thundercloud, and it was suggested that some atmospheric feedback process was operative, in which the charge separation mechanism was the fragmentation of crystal dendrites and needles and splinters from the surface of hailstones in a nitrous atmosphere. It was suggested that these charged particles could be segregated in some way which would increase the field and also the nitrate ion content, which would in turn increase the charge separated in the fragmentation processes.

A number of questions arise from this theory. Although it explains that the electrification is more intense in a thundercloud than in other types of cloud because the degree of atmospheric instability is greater, it does not explain why, once the charge segregation has begun in any small cloud, the process does not continue without limit until the field is large enough for a lightning discharge. It does not explain how the charges become segregated so as to enhance the field. Nor is any evidence given of how much splintering of ice particles occurs in thunderclouds. There is also the question of to what extent the laboratory results on splintering are comparable with atmospheric splintering processes. These are issues which warrant further investigation.

CHAPTER 2.

THE ELECTRIFICATION OF HAIL

1. INTRODUCTION.

In view of the importance attached to the role of precipitation, particularly solid precipitation, in many thunderstorm theories, many workers have been involved in estimating the magnitudes of the electrification of hail by the various processes described below. It will be seen that in some studies there have been large discrepancies between the results of different authorities, and it is the purpose of this thesis to investigate these discrepancies. In addition to the laboratory measurements it is desirable that the charges on natural hailstones in thunderclouds should also be measured in order to determine in a more direct manner the role of solid precipitation. Unfortunately, there are to date only a few measurements on the charge carried by hail.

2. THE ELECTRIFICATION PRODUCED ON MELTING.

The electrification produced on melting is important for ice crystals and snow particles as well as for hail particles. In spite of the great amount of work which has been done on this subject in recent years, there are basic questions still unanswered.

Dinger and Gunn (1946) showed that when a sample of pure ice was melted in a stream of air, the water retained a positive charge of  $1.25 \text{ e.s.u. gm}^{-1}$  of water melted. The amount of charge separated was very sensitive to the presence of impurities, small quantities of which neutralised the charging. The presence of dissolved gases was essential for any significant charge production. Dinger and Gunn concluded that electrification was caused by air bubbles, which were released from the melting ice, bursting at the water surface.

Matthews and Mason (1965) repeated the experiments of Dinger and Gunn, but did not detect any appreciable charging. Dinger (1964) suggested that this might be because the process was very sensitive to the presence of carbon dioxide, and large quantities of the gas were present during the Matthews and Mason experiments.

Kikuchi (1965) performed some experiments on the melting of natural snow crystals and pure ice samples containing varying quantities of air bubbles. It was shown that when the snow crystals melted the water droplets formed became positively charged. When an ice sample was melted it was shown that the amount of positive charge retained by the sample was proportional to the total volume of air bubbles over a very wide range. It was concluded that the bubbles were responsible for the observed charging.

The study of the melting of natural and artificial snow crystals by Magono and Kikuchi (1963, 1965) has established that these

particles became positively charged when they melted, and that the greater the dimensions and more complex the shape of a crystal, the higher the charge it retained. The production of charge was related to the eruption of air bubbles released from the melting ice. On average, a snow crystal melting to a droplet of diameter  $150 \mu$  acquired an average charge as high as  $2 \times 10^{-4}$  e.s.u. If this result is universally applicable to snow, then the process may well be a powerful generator of negative space charge in snow storms. These results were obtained predominantly for natural snow crystals. It might be of value for similar laboratory experiments, but with artificial snow crystals, to be performed. Then the effect of bubble concentration and impurities could be observed. The results would at least show whether results obtained from laboratory experiments on melting can be applied with reliability to the conditions in the atmosphere.

MacCreedy and Proudfit (1965) performed some laboratory experiments for comparison with their measurements in natural conditions. Ice cubes and ice spheres were melted in an air stream, and the sign and magnitude of the charge which was separated supported the results of Dinger and Gunn, except that it was considered that the charging was not as sensitive to the presence of impurities as was found by Dinger and Gunn. Naturally-formed hailstones were melted in the laboratory and were found to acquire positive charges of up to  $0.3 \text{ e.s.u. gm}^{-1}$ . It was observed that

the maximum rate of charging was towards the end of melting.

The field measurements of MacGready and Proudfit consisted of measuring the charges on hailstones inside and below thunderclouds which were entirely supercooled, and in which the cloud droplets in the region considered did not exceed 20 radius. It was found that at  $-5$  to  $-8^{\circ}$  C the hailstones had large positive charges, many of them approaching the limiting value which can be held before breakdown occurs (2 - 5 e.s.u.). Measurements indicated that when hailstones fell below the base of the cloud, their positive charges were reduced until they became zero at  $+5$  to  $10^{\circ}$  C. On falling further the hailstones became negatively charged, acquiring charges of similar magnitudes to the original positive charges. This negative charging was interpreted as being the result of the melting of the hailstones, although the sign of the charging was opposite to what would have been expected from the results of previous workers and from their own. Latham and Stow (1965<sup>C</sup>) showed that it was possible for the reduction of the mean positive charge at temperatures below  $0^{\circ}$  C to be explained in terms of the evaporation of the hailstone.

In summary, measurements on melting snow crystals have not caused the original conclusions of Dinger and Gunn to be modified significantly. Although it is difficult to compare quantitatively the results from melting pieces of ice with melting snow crystals, the qualitative picture remains the same. However, it is different

in the case of hail particles. The measurements of MacCready and Proudfit on individual hail particles falling below cloud bases have shown that although the charge on a melting hailstone is of the same order of magnitude as predicted by Dinger and Gunn, it is of the opposite sign. This result requires more substantiation before it can be accepted as being the general rule.

### 3. ELECTRIFICATION ASSOCIATED WITH TEMPERATURE GRADIENTS IN ICE.

#### (a) Investigations of the Temperature Gradient Effect.

Findeisen (1940) grew a very fine rimed deposit on an iced surface maintained at  $-60^{\circ}$  C. When fragments of ice broke away, the iced surface was left with a positive charge. In a later investigation (1943) it was shown that the ice fragments which broke off carried a negative charge. This was probably the first experimental evidence of a charge separation in ice which could be explained by the effects of temperature gradients in ice.

Reynolds Brook and Gourley (1957) stroked two ice-coated metal rods together asymmetrically, so that one rod was being rubbed over a smaller surface area than the other. It was observed that the former always acquired a negative charge, and the other rod acquired an equal and opposite charge. This was ascribed to the former rod being made warmer by the rubbing.

Brook (1959) made transient contacts between two ice specimens



at different temperatures, and observed that the colder ice specimen always acquired a positive charge, and the warmer a negative charge. It was also observed that when ice made from  $10^{-4}$  N sodium chloride was brought into contact with pure ice at the same temperature, the contaminated ice became negatively charged. Brook suggested that the conductivity of the ice depended on temperature and the concentration of impurity, and that charge was separated between two pieces of ice of different conductivity by proton diffusion and a pyroelectric effect.

Latham and Mason (1961 A) developed a theory of proton diffusion to explain the appearance of a potential difference across the ends of an ice specimen subjected to a steady temperature difference. They obtained the following expression for the potential difference:  $V = 1.36 \Delta T$  mV where  $\Delta T$  is the temperature difference between the ends. Experimental verification of this expression was very good, and the only departures from linearity could be explained by the variation of the conductivity of ice with temperature. The presence of impurities in the ice had a slight effect on the measured potential differences. The effect of sodium chloride was to reduce the potential difference and of hydrofluoric acid to increase it. It was also shown theoretically and experimentally that when transient contact was made between two ice specimens having different temperatures, the charge separated was time-dependent, the maximum separation being after a contact time of about 0.01 seconds.

There have been many publications in recent years which verify that a temperature gradient in an ice specimen causes a separation of charge. Perhaps the most unambiguous indication of this was by Latham (1964) in which an ice crystal was suspended on a fibre in a diffusion chamber and a separation of charge was observed without having the ice in contact with metallic or insulating surfaces other than the suspension, and thereby eliminating, as far as possible, sources of spurious effects.

(b) Collisions between Ice Crystals and Hailstones.

Reynolds Brook and Gowzley (1957) performed some experiments which enabled them to estimate the amount of charge acquired by a hailstone falling through a cloud of supercooled water droplets and ice crystals. The work was done in a large cold chamber measuring 3 x 4 x 9 ft. and operating at a temperature of  $-25^{\circ}$  C. The chamber contained a water vapour source which produced a cloud of supercooled droplets of about  $5\mu$  size. This cloud could be seeded by various methods, giving crystals of up to  $100\mu$  diameter. A rod was fixed to a rotating shaft. On each end of the rod was a 4 mm diameter ice-coated sphere connected to an electrometer. The spheres moved through the cloud at a velocity equivalent to the speed of fall of hailstones of similar size in the atmosphere. This speed was  $8 - 10$  m sec<sup>-1</sup>. Large positive and negative rates of charging of the simulated hailstones were observed. The relative proportions of

ice crystals and water droplets were varied, and it was observed that positive charging of the hailstone was associated with a high concentration of crystals compared with droplets, and vice versa for negative charging. When the cloud consisted of droplets only or crystals only there was little or no charging. When the cloud conditions were set to give positive charging, negative charging could be achieved either by heating the spheres with an infra-red lamp or by adding sodium chloride smoke to the cloud. Negative charging of the probe was explained as a temperature difference phenomenon in which the hailstone surface was made warmer because of the latent heat released by droplets freezing on it and which become charged negatively when colder ice crystals rebounded from it. By measuring a charging rate of 2 e.s.u.  $\text{sec}^{-1}$  for a crystal concentration of  $10^7 \text{ m}^{-3}$  an estimate of  $5 \times 10^{-4}$  e.s.u. for the charge separated per crystal collision was obtained. The estimate formed the basis for the thunderstorm theory which has been described.

Latham and Mason (1961B) measured the electrification of an iced probe by the passage of a stream of ice crystals in the absence of liquid water. The probe consisted of an insulated metal cylinder covered with a thin coating of ice and mounted on a copper rod. The surface temperature of the probe was raised by a small internal electric heater, and lowered by placing a cylinder containing solid carbon dioxide at various positions on the copper rod. This gave

temperatures down to about  $-30^{\circ}$  C. A stream of  $20 \mu$  size crystals at  $-20^{\circ}$  C was drawn past the probe for a fixed time, and the quantity of charge acquired by the probe was measured by placing the probe in an induction can attached to an electrometer. The results showed a linear relationship between the charge separated and the temperature difference between the ice crystals and the probe. For a temperature difference of  $5^{\circ}$  C the average charge separated per crystal collision was  $5 \times 10^{-9}$  e.s.u. which differs by a factor of  $10^5$  from the value found by Reynolds, Brook and Gourley. The probe ice was next contaminated with water containing  $3.6 \text{ mgm l}^{-1}$  of sodium chloride which is the concentration normally found in clouds. It was found that the effect on charging was equivalent to heating the probe by a further  $2^{\circ}$  C.

Magnus and Takahashi (1963) passed a stream of supercooled water droplets of approximate diameter  $5 \mu$  containing ice particles a few millimetres in diameter past an iced probe, the temperature of which could be varied, and observed how the charge acquired by the probe depended on riming by the droplets and collisions by the ice particles. Other parameters which were investigated were the temperature difference between the probe and the air stream, and the structure and ageing of the probe surface. On the whole their results agreed with the qualitative findings of Reynolds, Brook and Gourley. They considered that the most significant of their

discoveries was that the most important influence on the amount of charge separated by a rebounding ice particle was the state of the surface of the hailstone - an ice surface subjected to certain conditions of riming and ice particle bombardment acquired a fine structure, and this led to charging greater by factors of up to 6 than with a glazed ice surface. Two possible explanations of this phenomenon are that the charge enhancement is caused by the colliding ice particle, or alternatively that the ice particle sinks into the soft ice surface which enables charge transfer across a larger area of contact. Both of these explanations would seem to depend on the momentum of the impacting particle, so that for natural clouds, in which the ice crystals have been measured as being much smaller than in these experiments, it is possible that the effect of surface structure will not be so pronounced. No explanation was forthcoming at the time of the experiments of Latham and Mason to explain the very large discrepancy between their results and those of Reynolds Brook and Gourley, and the work for this thesis was begun in October 1963 with the intention of explaining this discrepancy. Latham (1965) has recently attempted to explain the differences between their results with reference to the results of Magono and Takahashi and also his own more recent results. A discussion of this paper is deferred until Chapter 5.

#### 4. COLLISIONS BETWEEN SUPERCOOLED WATER DROPLETS AND HAILSTONES.

A number of workers have measured the charge produced when supercooled water droplets encountered an iced surface, and there has been general agreement that the surface acquired a negative charge.

The exception to this are the results of Findeisen (1940) who found that when water droplets were sprayed on to a cold surface, the surface acquired a positive charge as soon as the droplets began to freeze. If the surface became smooth and glassy the positive charge was reduced to zero and became somewhat negative. Natural supercooled cloud droplets gave charging of the same magnitude as the spray droplets. Findeisen concluded that the electrification was caused by the quick freezing of water droplets, and that the faster the freezing the greater was the charging.

Kramer (1948) repeated Findeisen's work in great detail and showed that the rime deposit acquired a negative charge, the magnitude of which was proportional to the impact velocity of the droplets.

Meinhold (1951) deduced the rate of charging of an aircraft flying through supercooled cumulus congestus cloud by measuring the field strength at the surface of the aircraft. The aircraft acquired a large negative potential which was limited by spray discharging, and the corresponding rate of charging was  $5 \times 10^{-12} \text{ C cm}^{-2} \text{ sec}^{-1}$ . The disadvantage of this experiment was in not being able to measure the droplet sizes, but the electrical effects were

sufficiently strong to encourage other workers to perform laboratory experiments over a wide range of droplet sizes.

Weickmann and aufm Kampe (1950) sprayed supercooled water droplets on to an iced rod, and obtained a rate of charging which agreed well with Meinhold's value. Droplets were in the diameter range 5 to 100  $\mu$ . No precautions were taken to produce uncharged droplets, and the authors suggested that the results may have been affected by the electrification of the spray.

Reynolds, Brook and Gourley (1957) showed that when a simulated hailstone moved at 10 m sec<sup>-1</sup> through a cloud of supercooled water droplets condensed from the vapour, there was negligible charging. In this instance the droplet diameters were probably less than 5  $\mu$ .

More recently Latham and Mason (1961 B) measured the electrification associated with the growth of a simulated hail pellet by the accretion of supercooled water droplets. A spray of droplets was produced by an atomiser, and it was possible to select from this a narrow spectrum of droplets of the required size. The droplets were allowed to fall through a cold room in which they became supercooled, and were drawn past a simulated hailstone which was attached to an electrometer having a time constant of 200 sec. For droplets in the diameter range 40 to 100  $\mu$  impinging at velocities of 5 to 15 m sec<sup>-1</sup>, it was found that when droplets impinged on the probe they produced ice splinters, and imparted an appreciable negative charge to the probe, the amount of which was proportional to the number of splinters produced.

On average each droplet produced 12 splinters and caused a charge separation of  $4 \times 10^{-6}$  e.s.u. Latham and Mason showed that by applying their results to a typical thundercloud, this process would cause a charge separation of at least  $1 \text{ C km}^{-3} \text{ min}^{-1}$ . They concluded from this that the process was sufficiently powerful to be the principal charge generating mechanism in a thunderstorm.

These results have raised a number of questions, among them the question of whether the droplets were initially charged and what effect this would have had on the results. It has also been suggested that the droplets might have shattered in the air stream before encountering the probe, in which case the charge may have been produced by ice splinters colliding with the probe. There is also the question of whether significant electrical effects really are restricted to this particular spectrum of droplet sizes, or whether it only appeared to be so because of experimental limitations.

##### 5. ELECTRIFICATION BY EVAPORATION OF ICE.

When a specimen of ice evaporates in a current of dry air, its surface temperature is lower than its interior; thus there is a temperature gradient in the surface layer of the specimen. Applying the temperature gradient theory this would cause an ionic concentration gradient with the outer surface having a positive charge. When the outer surface is evaporated in the air stream, some positive charge



is removed and the specimen is left with a negative charge.

Latham and Stow (1965) measured the electric current produced when an iced copper sphere of diameter 3.4 cm was exposed to a stream of chilled nitrogen. The sphere was maintained at  $-20^{\circ}$  C and the temperature of the nitrogen stream was varied between  $0^{\circ}$  C and  $\pm 40^{\circ}$  C. It was found that for nitrogen temperatures between  $0^{\circ}$  C and  $-10^{\circ}$  C the sphere became charged positively and that for temperatures below  $-10^{\circ}$  C the sphere was always charged negatively. In a separate experiment the variation of the temperature gradient in the ice surface with the temperature difference between the nitrogen and the ice interior was found. Using these results it was shown that the electric current due to evaporation increased smoothly with the temperature gradient in the ice surface.

The maximum rate of charging of the ice sphere was found to be  $4 \times 10^{-4}$  e.s.u.  $\text{sec}^{-1}$ . For a 4 mm diameter hailstone the rate of charging would be approximately two orders of magnitude less than this. If hailstones were responsible for generating electricity in thunderstorms they must be charged at a rate of at least  $10^{-3}$  e.s.u.  $\text{sec}^{-1}$ , which is therefore much greater than the rate of charging caused by evaporation. The evaporation process, however, may be of importance in the production of positive space charge by cold dry winds blowing over the surface of snow, or by hailstones or snow crystals falling through cold dry air.

## 6. OTHER ELECTRIFICATION PROCESSES.

The Workman - Reynolds effect has already been described in Chapter 1. The suggested mechanism is that a wet hailstone develops a potential difference across the ice-water boundary because of the presence of contaminants and as it collects water droplets and grows beyond its critical size it throws off charged water droplets. It has been mentioned that this process is extremely sensitive to the presence of impurities, and because of this it is difficult to deduce its effect in the atmosphere from laboratory measurements. However, Latham and Mason (1961 B) were unable to detect any charging from the collisions of supercooled water droplets on a wet hailstone surface.

The Wilson process of selective ion capture (1929) very probably has a great influence on the charge carried on hailstones in regions where the polar conductivity of the air is very high, particularly in the region below the cloud where the space -charge density due to point discharge ions is very high.

## 7. COMPARISON OF FIELD MEASUREMENTS.

Field measurements of the charge on hail will only be of significance to thunderstorm electrification if the measurements are made in the right place under the right conditions. The few results which have been obtained differ from each other and this is probably because they were obtained under different conditions. Kuttner (1950)

made measurements inside thunderclouds on the Zugspitze. The charge carried down by hail was measured and found to be overwhelmingly positive. Moore (1965) reported that the polarity of the charge on falling hail collected at the ground varied from minute to minute, and was usually of the same polarity as the point discharge ions being created by the high potential gradient. MacCready and Proudfit (1965) made measurements of the charges on individual hailstones which differed from laboratory measurements. It will be recalled that they observed positive charges of a few e.s.u. at temperatures well below the freezing point, and these charges decreased as the freezing point was approached, becoming zero at +5 to +10° C. At temperatures warmer than this the particles became negatively charged. The positive charges observed by MacCready and Proudfit are not inconsistent with Kuttner's results, although the negative charges observed above the freezing point cannot be readily explained. The results of Moore can be explained by the Wilson process of ion capture, but whether the presence of ions had any influence on the results of MacCready and Proudfit cannot be judged since parameters such as space charge density and potential gradient were not included in the measurements.

Support for any thunderstorm theory in which precipitation is considered as the principal charge separation process must depend on reliable field measurements on the charges carried by precipitation, and if there are several charge separation processes at work, these must be separately determined and evaluated. It would seem that

such processes have different relative effects in different places, and from the point of view of thunderstorm electricity, the ground measurements may only be of significance in determining the net charge brought to the ground on hail and may be not at all related to the charge carried by hail which is situated well inside thunderclouds.

CHAPTER 3.

SOME THEORY CONCERNING THE ELECTRIFICATION OF ICE AND WATER.

1. INTRODUCTION.

Electrification of water and ice is achieved in several ways, and it is this fact which has led to the proposal of so many theories of cloud electrification.

It is the purpose of this chapter to explain the electrical properties of ice in terms of its structure, and for comparison, details will be given of the corresponding behaviour of water.

2. ELECTRIFICATION PROCESSES IN ICE AND WATER.

(a) Charge Separation in Ice.

The various mechanisms for separating electric charge when solids have been touched or rubbed together have been summarised by Henry (1953). Loeb (1958) has discussed many of them in greater detail. The details of most of them are of no direct relevance to the study of ice, as they are the result of electrolytic effects and contact potentials between dissimilar materials. Of all the mechanisms listed, the three most likely to cause electrification in ice are piezoelectric and pyroelectric effects, and processes involving ionic diffusion.

Piezoelectric effects are observed when externally applied stresses

cause crystals to become polarised. The most recently published measurements of piezoelectricity in ice appear to be those of Teichmann and Schmidt (1965), and they found the piezoelectric coefficients to be zero within the accuracy of measurement. Pyroelectric effects have been observed only in crystals which exhibit piezoelectricity, and is detected as a charge separation caused by local heating. It is uncertain whether a true pyroelectric effect exists in the absence of stress. Mason and Owston (1952) could not detect any pyroelectric effect in very large ice crystals.

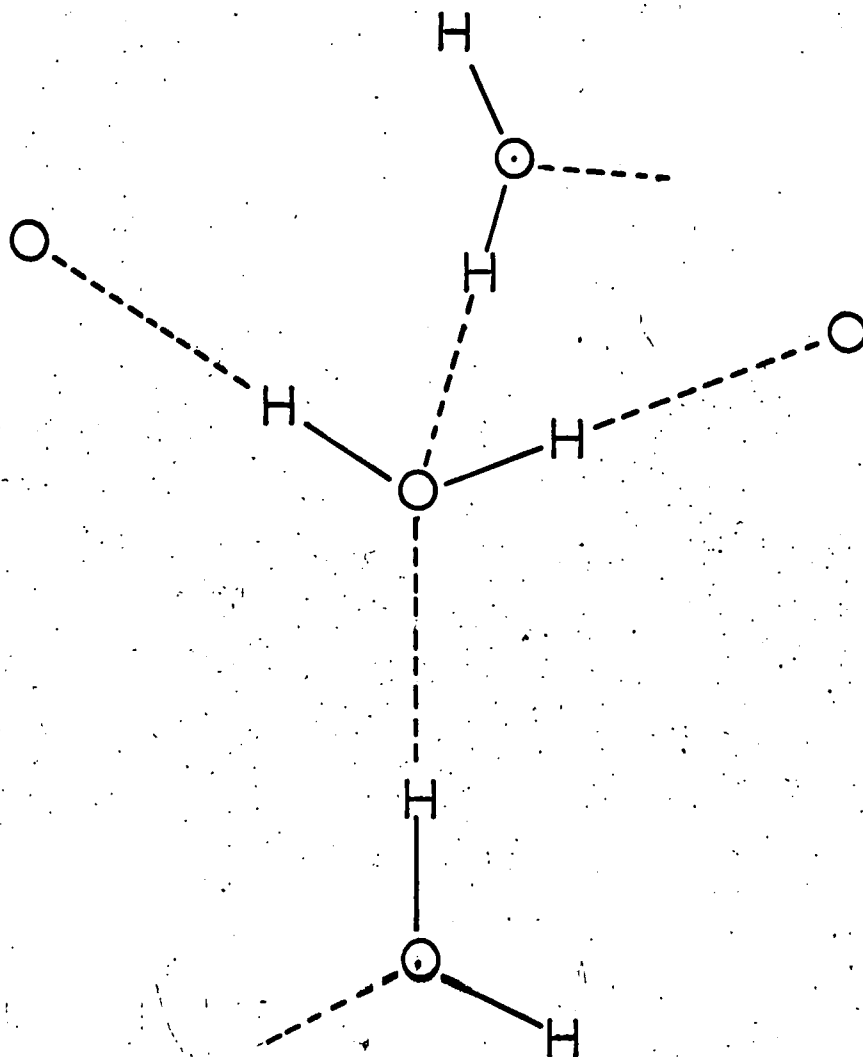
A temperature gradient effect was suggested by Henry to explain the result that when identical insulating materials were rubbed together asymmetrically they acquired equal and opposite charges. Since there were no free electron energy states to implement electronic charge transfer as in a metal, it was suggested that the temperature gradient produced by the rubbing caused the migration of charged particles down the gradient. Such a process has been shown to explain the electrification of ice. It depends upon there being a difference in electrical conductivity between the two samples, which can be achieved by asymmetric rubbing, direct heating, or the addition of impurities.

(b) Charge Separation in Water.

The principal ways of separating charge with liquids are spraying, splashing and bubbling. In contrast to ice, these phenomena are

———— Ionic Bond

----- Hydrogen Bond



O—H Bond Length = 1.00 Å

O-----H Bond Length = 1.76 Å

Fig.1 The Structure of Ice.

primarily the result of the presence of impurities in the liquid, and the existence of an electrical double layer at the liquid-air interface. A detailed account of the electrification in liquids has been given by Loeb (Static Electrification 1958).

### 3. THE STRUCTURE OF ICE AND WATER.

#### (a) The Structure of Ice.

Ice has crystal forms which depend on temperature and pressure. Under conditions normally found in the atmosphere the hexagonal type is formed, and it was for this that Bernal and Fowler (1933) proposed the following three rules:-

1. Hydrogen atoms lie at equilibrium positions along lines joining neighbouring oxygen atoms.
2. There is only one hydrogen atom on each such linkage, forming hydrogen bonds.
3. Each oxygen atom has two hydrogen atoms at some short separation, thus preserving the structure of water molecules.

The detail of the Bernal-Fowler model was modified by Pauling, (see Pauling, 1960). In order to explain the existence of a finite zero-point entropy it was necessary that hydrogen nuclei could move to the other equilibrium positions on the lines joining the oxygen atoms. This model is well supported by experimental evidence, X-ray and neutron diffraction work have shown that each oxygen atom is separated from neighbouring oxygen atoms by 2.76 Å and that the



hydrogen atoms lie on the lines joining oxygen atoms at a distance of about 1 Å from them. There are two possible positions on each bond for the hydrogen, and the time average structure consists of half of a hydrogen atom in each position. This is now the universally accepted picture of the ice structure. This is illustrated in Fig.1.

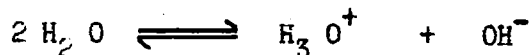
(b) The Structure of Water.

There has been little modification to the structural model originally proposed by Bernal and Fowler in 1933. They suggested that between 4° C and 200° C, liquid water has a tetrahedrally hydrogen-bonded structure with a lattice similar to the quartz form of silica and that below 4° C the lattice is similar to the tridymite form of silica. This is not a rigid structure because the hydrogen - bonding is a statistical process, and most of the molecules in liquid water are in a free unbonded state. The degree of hydrogen-bonding increases as the freezing-point is approached.

4. CHARGE TRANSPORT IN WATER AND ICE.

(a) Charge Transport in Water.

Since there are no free electrons in water it is necessary to look to the ions to explain the conductivity. Water molecules dissociate according to the reaction:-



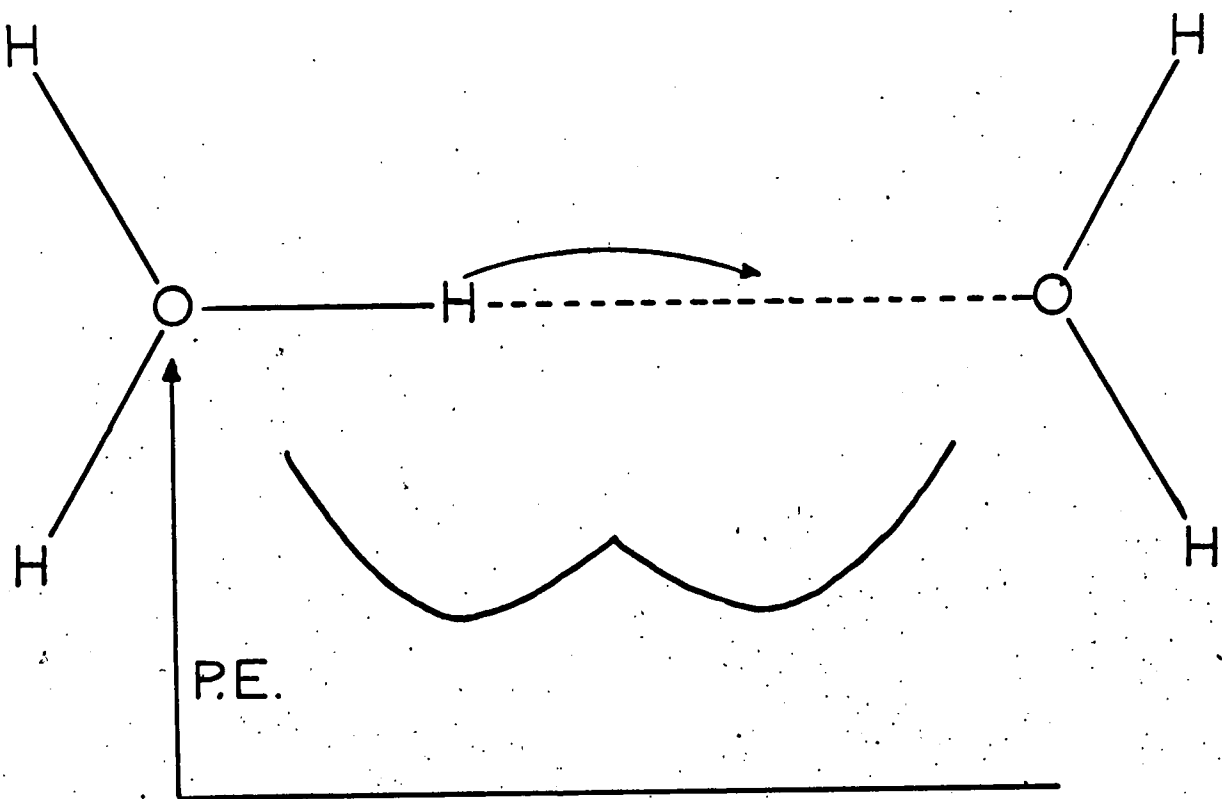


Fig. 2.1

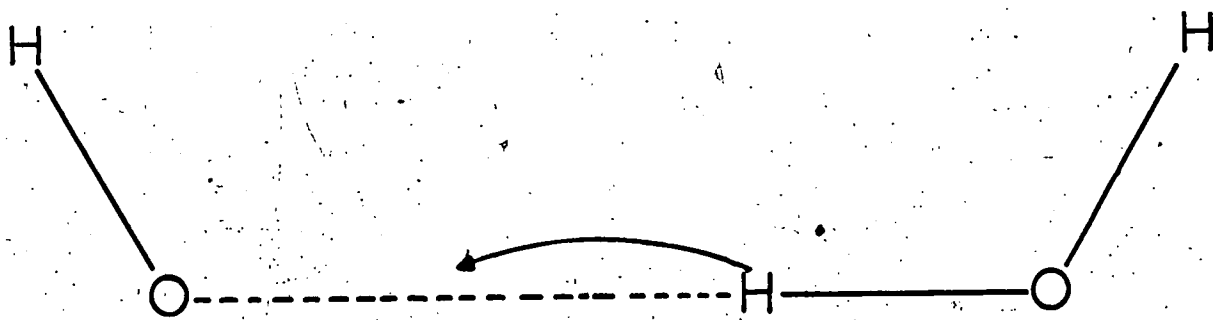


Fig. 2.2

Fig.2 Charge Transport in Water

The mobilities of these ion-states have been calculated:-

$$\text{H}_3\text{O}^+ = 36.2 \times 10^{-4} \text{ cm}^2 \text{ V}^{-1} \text{ sec}^{-1} .$$

$$\text{OH}^- = 19.8 \times 10^{-4} \text{ cm}^2 \text{ V}^{-1} \text{ sec}^{-1} .$$

which are high compared with  $7 - 8 \times 10^{-4} \text{ cm}^2 \text{ V}^{-1} \text{ sec}^{-1}$  for chlorine and ammonium ions, thus implying some special transport mechanism.

This is explained by the tunnelling of a proton through a potential energy barrier, becoming hydrogen-bonded to another water molecule.

Fig. 2.1 shows how a proton jumps from an  $\text{H}_3\text{O}^+$  ion to an  $\text{H}_2\text{O}$  molecule, leaving behind an  $\text{H}_2\text{O}$  molecule and forming an  $\text{H}_3\text{O}^+$  ion. Fig. 2.2 shows how a proton jumps from an  $\text{H}_2\text{O}$  molecule to an  $\text{OH}^-$  ion leaving behind an  $\text{OH}^-$  ion and forming an  $\text{H}_2\text{O}$  molecule. In this manner the ion-state passes very rapidly along a chain of molecules. The rate at which ion-states diffuse through the liquid is governed by the statistical probability of hydrogen-bond formation.

(b) Charge Transport in Ice.

When a specimen of ice is connected into a circuit and an electric field applied to it, it is found to have a measurable conductivity. The manner in which electric charge can diffuse through the lattice is explained by postulating two types of lattice defects. These are ion-states, by analogy with water, and lattice defects which were postulated by Bjerrum (1951) in order to allow ion-states to diffuse through the same molecule more than once.

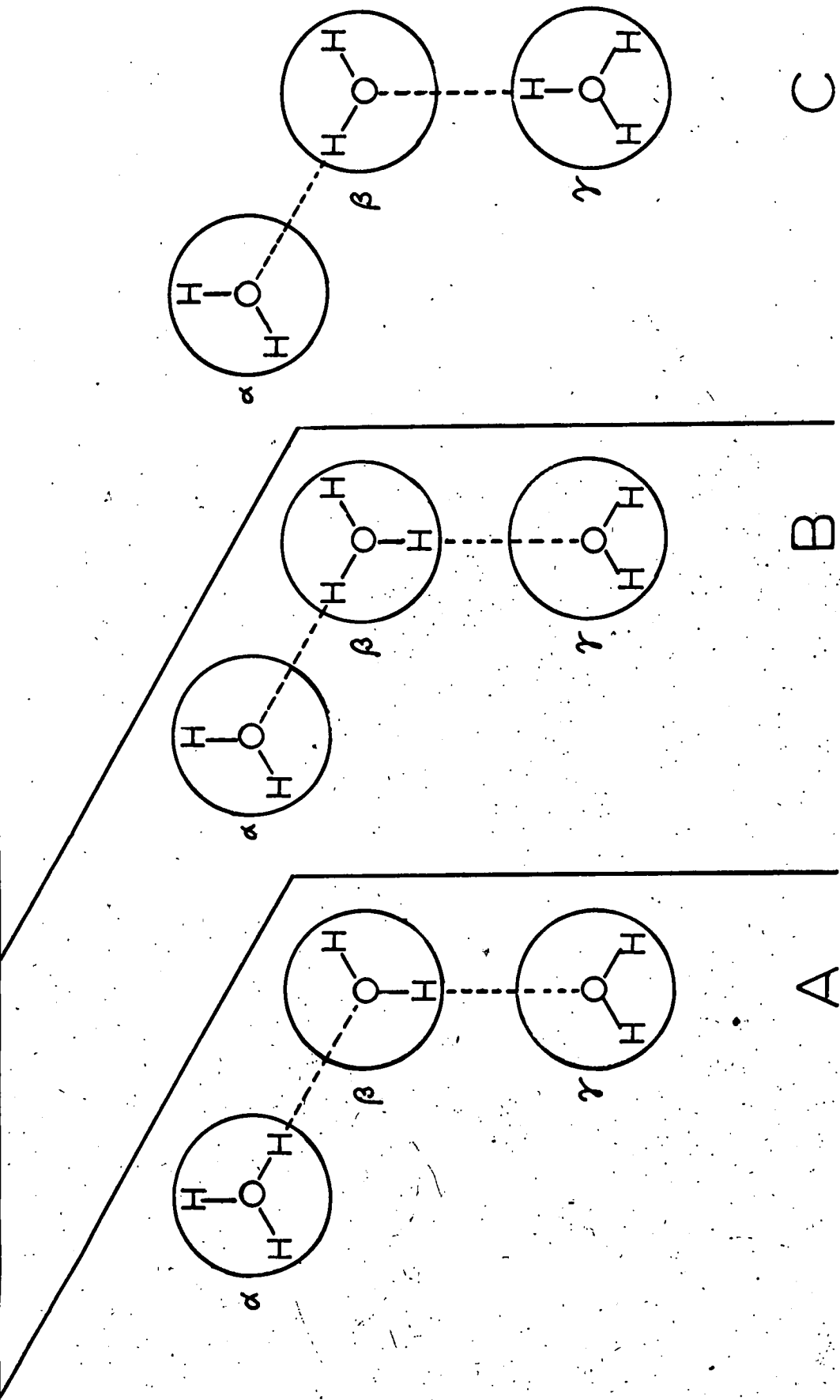


Fig. 3.1 The Diffusion of Ion-states.

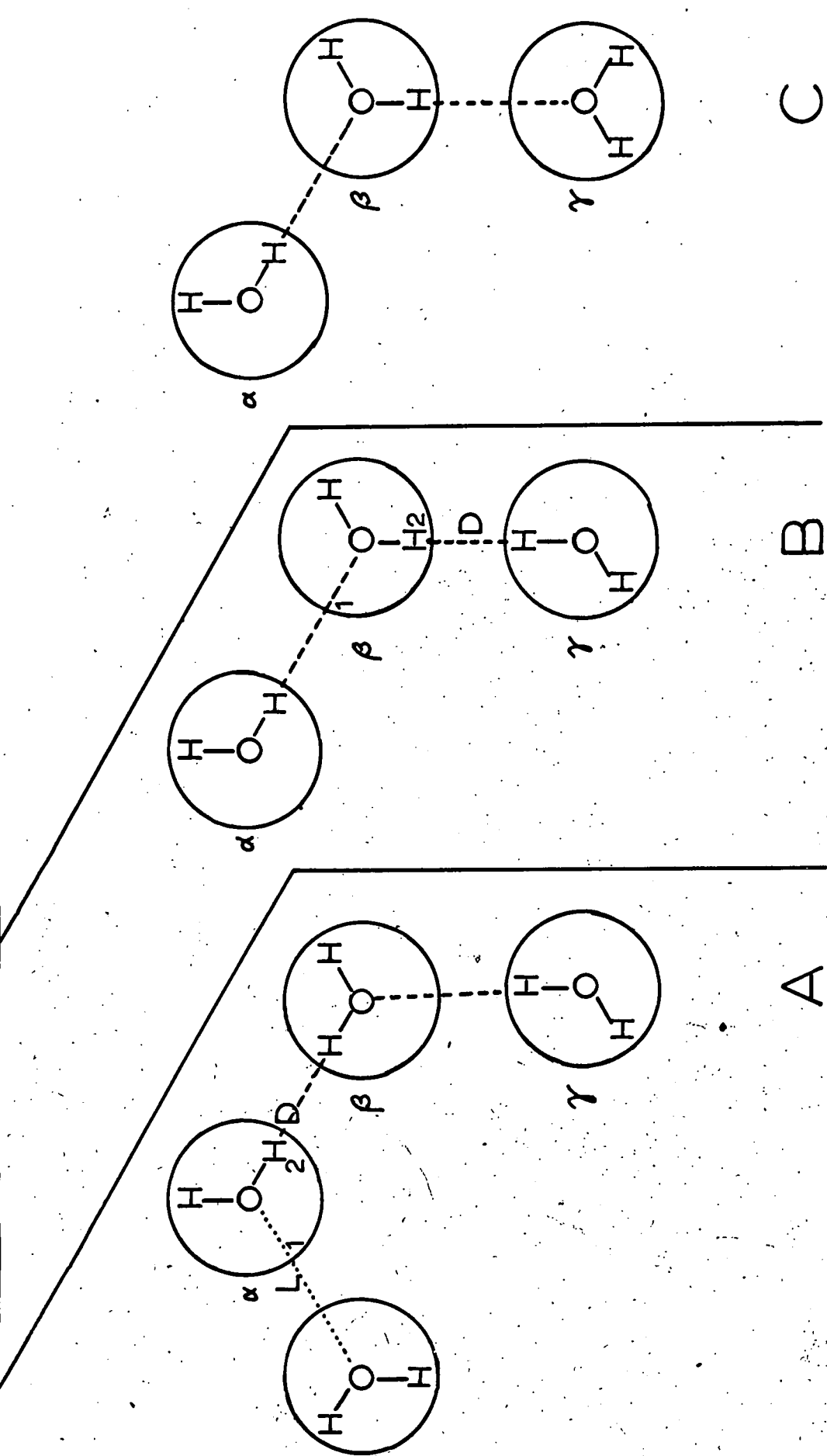


Fig. 3.2 The Generation and Diffusion of Bjerrum Defects.

The ion-states  $\text{H}_3\text{O}^+$  and  $\text{OH}^-$  are generated by the translational motion of a proton along a hydrogen bond to a neighbouring molecule, thus constituting a violation of the third Bernal-Fowler rule.

Fig 3.1 shows how diffusion through the lattice occurs. Proceeding from stage A to stage C, the  $\text{H}_3\text{O}^+$  ion-state in molecule  $\alpha$  of stage A has migrated to molecule  $\gamma$  of stage C. A similar process occurs for the  $\text{OH}^-$  ion-state. It will be observed that in the course of this diffusion molecule  $\beta$  has become oriented into a position such that no more ion-states from  $\alpha$  can diffuse through it. Thus if these ion-states were the only ones responsible for conduction, it would be expected that in the presence of an external electric field, the d.c. conductivity would vary with time as the molecules became oriented to inhibit diffusion. As no such variation has been observed, Bjerrum postulated a mechanism for reorienting the molecules. The molecules can be reoriented in various ways, but the one suggested by Bjerrum will be described here. It was suggested that lattice defects are generated by a thermally excited proton rotating about its oxygen atom to another equilibrium position on a neighbouring bond. Thus, referring to Fig 3.2, a rotation of the proton from position 1 to 2 has generated a doubly occupied bond (D - defect) and a vacant bond (L - defect). Calling normal bonds N, this can be expressed as the reversible reaction  $2\text{N} \rightleftharpoons \text{D} + \text{L}$ . It can be seen in Fig 3.2 that Bjerrum defects constitute a violation of the second Bernal-Fowler rule. In B and C of Fig 3.2 the D - defect has diffused through the chain by subsequent rotations of protons in molecules  $\beta$  and  $\gamma$  from positions 1

to 2. The L - defects diffuse by a similar process. In addition to the diffusion of the defects, molecule  $\beta$  has been reoriented to its original position as in Fig. 3.1 A which is favourable for the diffusion of a further ion-state from  $\alpha$  to  $\gamma$ . Since this molecular reorientation takes place in a time which is short compared with the rate of arrival of protons at  $\alpha$ , the diffusion process is governed by the rate of proton tunnelling along hydrogen bonds, which is very high and thus explains why the mobility of protons in ice is much higher than in water.

Table 1 gives a comparison between the two types of lattice defect. It can be seen that Bjerrum defects are much more numerous, but their mobility ratio is close to unity. The exact mobility ratios of both Bjerrum defects and ion-states have not yet been determined experimentally. The approximate value for the ion-states has been found by Eigen and de Maeyer (1958).

Table 1. Comparison of Bjerrum defects and ion-states for Pure Ice at  $-10^{\circ}$  C.

Energy of formation	$0.68 \pm 0.04$ eV	$1.2 \pm 0.1$ eV
Concentration of defects	$7 \times 10^{15}$ cm <sup>-3</sup>	$8 \times 10^{10}$ cm <sup>-3</sup>
Transition probability	$2 \times 10^{11}$ sec <sup>-1</sup>	$6 \times 10^{13}$ sec <sup>-1</sup>
Mobility (cm <sup>2</sup> V <sup>-1</sup> sec <sup>-1</sup> )	$\mu^{\pm} = 2 \times 10^{-4}$	$\mu^{\pm} = 7.5 \times 10^{-2}$
Mobility ratio	$\mu^{\pm}/\mu^{\mp} \approx 1$	$\mu^{\pm}/\mu^{\mp} = 10$ to 100
Activation energy of diffusion.	$0.235 \pm 0.01$ eV	0 (tunnelling)

## 5. THE TEMPERATURE GRADIENT THEORY FOR ICE.

The effect of temperature gradients in ice is similar to the Thomson thermoelectric effect in metals except that in ice the charge carriers are the lattice defects which diffuse under the influence of concentration, potential and temperature gradients. The theory of the thermoelectric properties of ice has been worked out by Latham and Mason (1961 A), and by Jaccard (1963, ~~1964~~) who used an approach which took into account properties of the crystal lattice and allowed for the fact that the effective charges transported by each defect were not unit charges. Jaccard's calculations included the effects of all four lattice defects, whereas Latham and Mason had assumed that the effects of the Bjerrum defects were equal and opposite and had considered that the ion-states were solely responsible for the thermoelectric effects. Jaccard derived an expression for the homogeneous thermoelectric power and by assuming a reasonable value of 1.2 for the mobility ratio of Bjerrum defects, showed that it agreed with Latham and Mason's value for the thermoelectric power. A part from the thermoelectric power and the surface density of charge under a uniform temperature gradient, the other quantity which is important in this study is the quantity of charge separated by transient contact between two pieces of ice. These quantities were deduced by Latham and Mason, and the physical principles are outlined below.

### (a) Uniform Temperature Gradient.

It is shown in Table 1 that the mobility of the  $H_3 O^+$  ion-state



is at least ten times greater than the mobilities of the other defects. Also the concentrations of  $H_3 O^+$  and  $OH^-$  rise quite rapidly with temperature, as is shown in the law of mass action equation:

$$C_+ C_- = \alpha \exp(-\phi / kT)$$

where  $\phi$  is the activation energy for dissociation and  $\alpha$  is the dissociation constant. When a temperature gradient is established across an ice specimen it produces concentration gradients of ion-states and Bjerrum defects. Since there is a tendency for the concentrations to become equalised, there will be an initial diffusion of all defects from the region of higher concentration and temperature. The  $H_3 O^+$  ion-states diffuse faster to the colder end, and thereby cause a separation of charge. This sets up an internal electric field which opposes the diffusion of more positive charge, and assists the diffusion of negative charge towards the colder end. Lattice defects are being generated continuously at the warmer end and are diffusing continuously to the colder end. The positive charge at the colder end builds up until a steady state is reached in which the internal field is sufficiently large to cause a current which is equal and opposite to the one caused by the concentration gradient. Thus a potential difference has been established across the specimen with no current flowing. Although the internal field is caused by a spatial distribution of charge, Latham and Mason considered that to a first approximation, the separated charges could be regarded as being entirely confined to the ends of the specimen. This gave a uniform internal field which could be

written as  $\frac{dV}{dx} = \frac{4 \pi \sigma}{\epsilon}$  where  $\sigma$  is the surface density

of charge and  $\epsilon$  is the static permittivity of ice. The expressions for the diffusion currents of the  $H_3 O^+$  and  $OH^-$  ion-states are:-

$$i_+ = -D_+ e \frac{dc_+}{dx} - \frac{1}{2} D_+ e c_+ \frac{dT}{dx} - e c_+ \mu_+ \frac{dV}{dx}$$

$$i_- = +D_- e \frac{dc_-}{dx} + \frac{1}{2} D_- e c_- \frac{dT}{dx} - e c_- \mu_- \frac{dV}{dx}$$

where  $\frac{dc}{dx}$  and  $\frac{dT}{dx}$  are the concentration and temperature gradients,

and  $D$  is the diffusion coefficient. Similar expressions for the diffusion currents of the Bjerrum defects could also have been included in the calculation, but as they have smaller and almost equal mobilities it was justifiable to leave them out. In the steady state  $i_+ + i_- = 0$ , and by rearranging the equations the following expression for  $\sigma$  was obtained:

$$\sigma = \frac{\epsilon k}{8 \pi e} \left( \frac{\mu_+/\mu_- - 1}{\mu_+/\mu_- + 1} \right) \left( \frac{\phi}{kT} + 1 \right) \frac{dT}{dx}$$

On substitution,  $\sigma = 4.95 \times 10^{-5} \frac{dT}{dx}$  e.s.u.  $cm^{-2}$

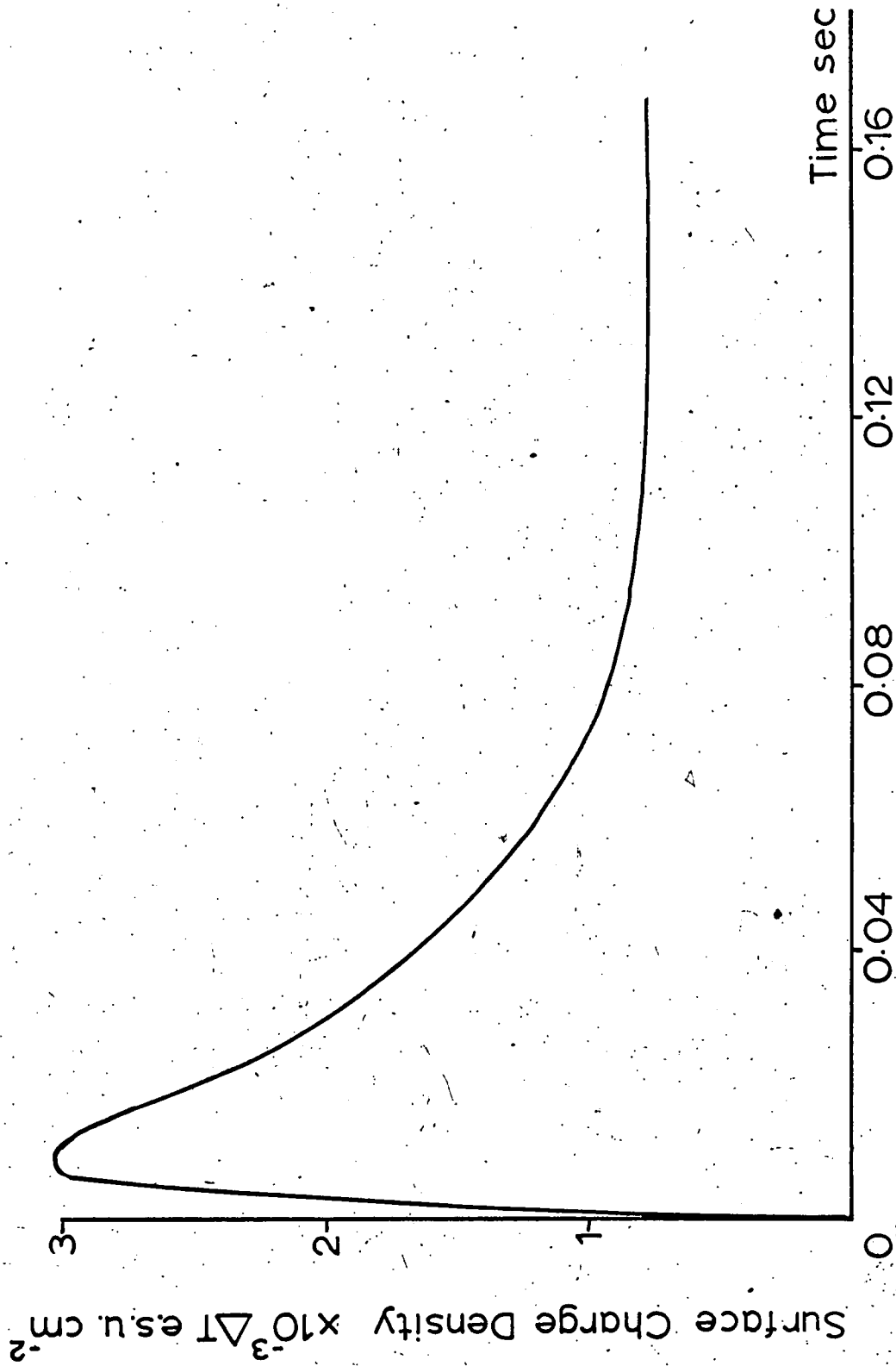


Fig. 4 The Charge Produced by the Separation of Two Pieces of Ice of initially Different Temperatures as a Function of their time of Contact.

(b) Transient Contacts.

When two pieces of ice at temperatures  $T_1$  and  $T_2$  are brought into contact, the temperature gradient after a time  $t$  at their plane of contact is  $(T_1 - T_2)$  where  $K$  is the thermal diffusivity of ice.

$$\frac{(T_1 - T_2)}{2(\pi Kt)^{\frac{1}{2}}}$$

This equation shows that immediately after contact the temperature gradient is very high and so the net current across the boundary is high. The rate at which charge separation occurs is governed by the rate of diffusion of charge against the increasing field. The temperature gradient is rapidly decreasing and soon its magnitude corresponds to the separated charge. At this point the charge separation has reached a maximum, and thereafter the charge separation decreases in accordance with the decreasing temperature gradient.

Latham and Mason used the same equations as before and by making certain assumptions, showed that the maximum charge was separated in a time  $8.5 \times 10^{-3}$  sec, and that the maximum surface density of charge separated was given by:

$$\sigma_{\text{max}} = 3.05 \times 10^{-3} (T_1 - T_2) \text{ e.s.u. cm}^{-2}$$

The deduced time variation of the charge separated is shown in Fig. 4.

CHAPTER 4.

MEASUREMENTS WITH A ROTATING PROBE.

Introduction.

The aim of the work described in this chapter was to investigate whether the magnitudes and general pattern of the charging observed by Reynolds Brook and Gourley (1957) could be reproduced.

Two simulated hailstones were rotated at  $10 \text{ m sec}^{-1}$  in a cloud which consisted first of supercooled water droplets only, and then of ice crystals together with supercooled water droplets. By varying the relative quantities of ice crystals and water droplets and their relative temperatures, a qualitative picture of the parameters affecting charging was built up.

By making certain modifications to the apparatus, quantitative results were obtained.

1. The Apparatus.

(a) The Refrigerator.

The work was performed using a refrigerator of internal dimensions 147 x 75 x 57 cm. A space measuring 59 x 39 x 57 cm. was partitioned off from this to enclose the compressor unit. Thus the partition formed a shelf at one end of the refrigerator (as shown in Fig. 12.) Access was gained to the refrigerator by three detachable hinged lids measuring 35 x 56 cm. placed on the top. The walls of the cold compartment were painted matt black so that cloud particles were observed against a dark background.

When the compressor was operating it caused the refrigerator to vibrate a great deal. In order to prevent the vibrations from increasing the noise level of the sensitive instruments, either directly or by piezoelectric effects in the cables, a bridge spanning the refrigerator was constructed from Handy Angle sections. Instruments placed on the bridge were then completely isolated from mechanical vibrations. Two brass plates, fitted with collars, were attached to one side of the bridge span. These held the vertical rods to which were to be attached the riming device and the thermocouple. In order to keep the refrigerator closed to the outside air, and yet enable instruments to be suspended in it from outside, half of one of the hinged lids was removed and replaced

SCALE: Actual Size

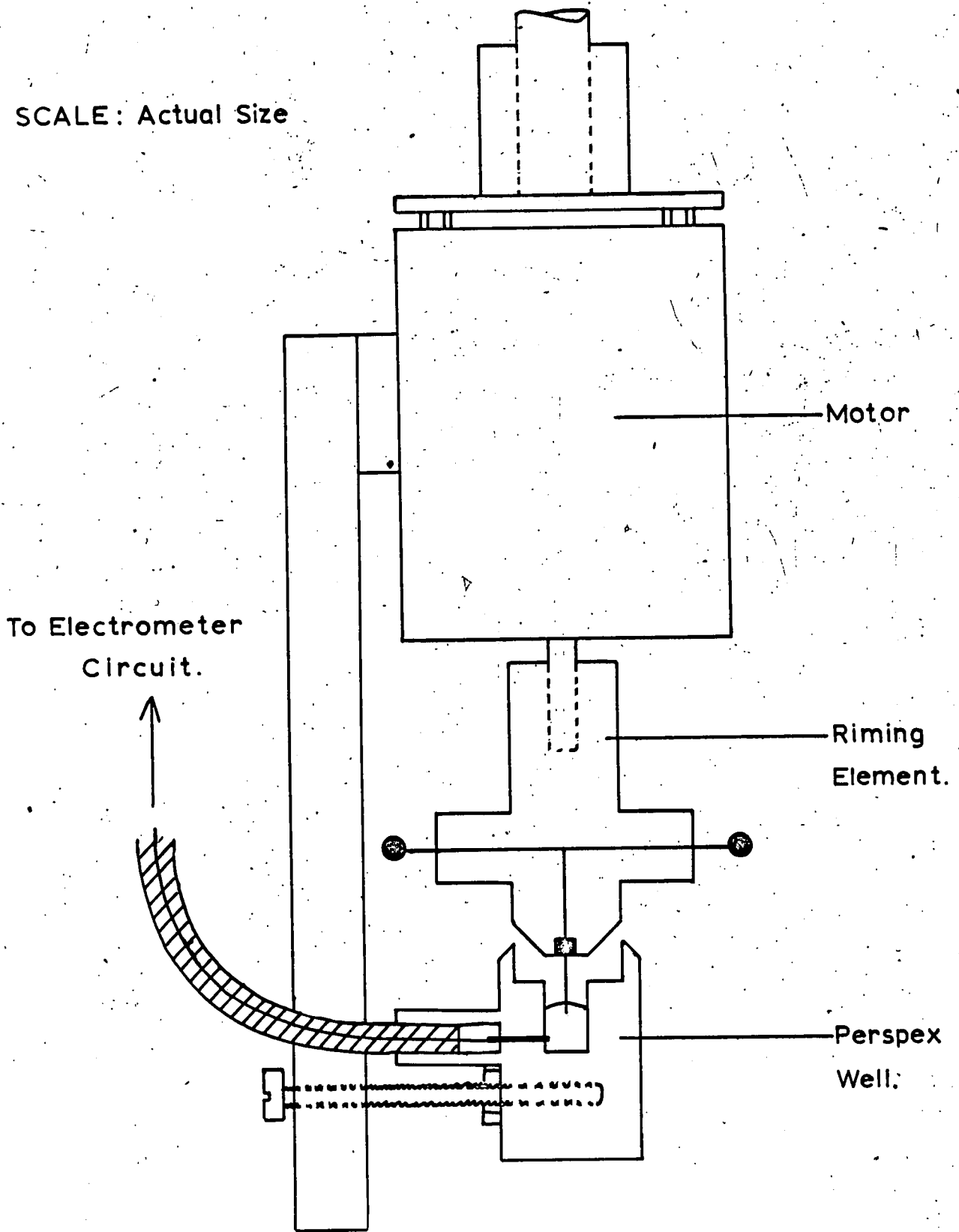


Fig.5 The Rotating Probe.

by a wooden frame which was divided into two halves. There were holes in one half through which the rods could pass, and the other half was a perspex window.

(b) The Rotating Probe.

The rotating probe is shown in Fig. 5. The riming element consisted of two 4 mm. diameter phosphor-bronze balls mounted at opposite ends of a 4.5 cm. long 12 mm. diameter perspex rod which was fixed perpendicularly through the end of a 5.5 cm. long 19 mm. diameter perspex rod. The balls were connected internally by thick copper wires to a brass pin sunk in the base of the larger rod. The latter was attached at its other end to a d.c. electric motor. The brass pin dipped into mercury contained in the specially shaped perspex cup. The purpose of the shape was to minimise the possibility of a conducting film forming on the perspex between the mercury and earth. The perspex cup was firmly fixed to a 12 mm. square cross-section bar attached to the motor housing. A collar was attached to the top of the motor housing to enable it to be joined to one of the vertical rods.

(c) The Electrical Circuits.

The temperature of the refrigerator, which could be controlled down to  $-20^{\circ}$  C., was measured by a thermocouple. This was made using lengths of 30 S.W.G. copper and eureka wire which were contained in p.v.c. sleeves. The warmer junction was fixed into a brass block



which was placed inside a small Thermos flask filled with distilled water and crushed ice, thereby maintaining a constant temperature of  $0^{\circ}$  C. A resistance box and Scalamp galvanometer were connected in series between the two junctions. The thermocouple was calibrated and the resistance box adjusted to give a sensitivity of  $1.5^{\circ}$  C cm.<sup>-1</sup>. The calibration was checked on subsequent occasions and readings were always found to be consistent to within  $\pm 0.1^{\circ}$  C.

It was of great importance to have a good earth connection. The earth point consisted of a 10 S.W.G. copper wire leading to a copper plate embedded in the ground. All instruments were earthed to this wire instead of to the mains earth. The steel bridge and the refrigerator casing were also earthed to it.

The electric motor, which was powered from a 24 v d.c. supply, was put in series with a small rheostat. The rotation of the probe was observed with a stroboscopic lamp, and the speed was adjusted by the rheostat until the balls, whose separation was 5 cm, had a tangential velocity of 10 m. sec.<sup>-1</sup> which, when the balls were coated with ice, was equal to the fall speed of hailstones of equal size in the atmosphere.

(d) Charge Measurement.

It was decided to measure the rate of charging of the probe, by allowing the charge acquired by it to leak away through a high

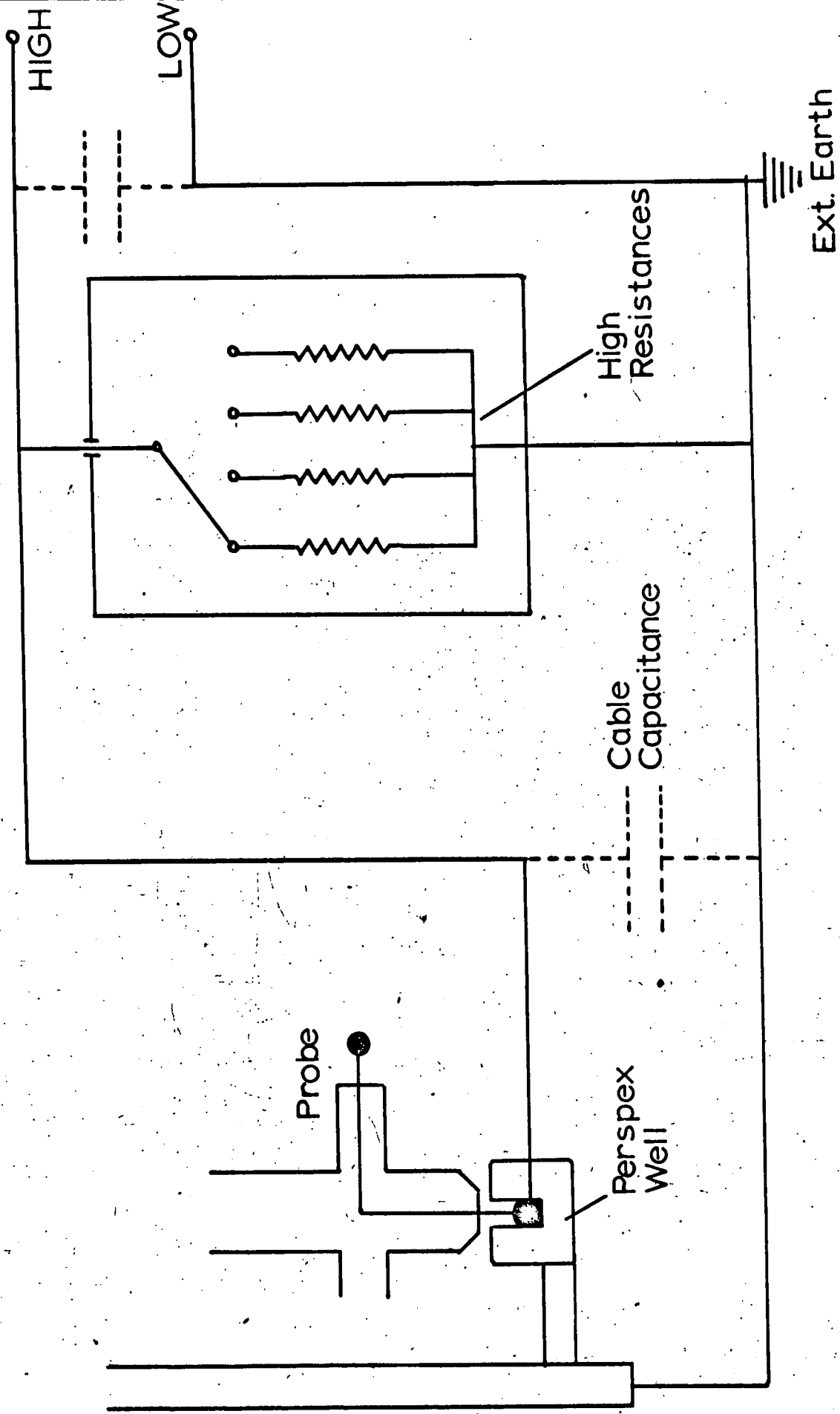


Fig.6 The Electrometer Circuit.

resistance, and to measure the potential difference across the resistance with an electrometer of very high resistance.

Electrical contact was made with the mercury through a brass bolt to which was soldered the inner conductor of a non-microphonic coaxial cable. The earthed outer conductor was connected to the motor casing. Four high resistances whose values ranged from  $10^{10}$  to  $10^{12}$  ohms were enclosed in a metal box which acted as an electrostatic screen. They were arranged such that any one could be connected across the electrometer input circuit while the rest were earthed.

The electrometer was a Vibron Model 33 B vibrating reed electrometer, which had five switched ranges, the minimum input voltage for a full scale deflection being 10 mV. The resistance to be used was connected between the High and Low terminals, the Low terminal also being connected to Earth. The inner conductor of the coaxial cable was connected via the resistance to High, and the outer was connected to Low. The arrangement is shown in Fig. 6.

When the apparatus was set up in its working position, the length of cable from the mercury well to the electrometer was approximately 2 m. It was seen that using the  $10^{10}$  ohm. resistance, the relaxation time of the electrometer readings was about 2 seconds, this being the time constant of the external circuit.

(e) Water Vapour Source

Water vapour was supplied from a pyrex beaker mounted in a

metal frame to which was attached a lid which could be operated from outside. The beaker was filled with hot water which was maintained near its boiling point by a small immersion heater consisting of a 12 ohm. coil of resistance wire enclosed in a glass tube, and being supplied with 20-30 V from a Variac transformer.

(f) Operation of the Rotating Probe.

When the probe was connected to the electrometer and held outside the refrigerator, it was observed that it was very sensitive to the motion of charged bodies near it, which caused large deflections. When the probe was placed inside the refrigerator, the refrigerator casing screened it very effectively from charged bodies outside the refrigerator. The maximum fluctuations of the needle were then  $\pm 0.1$  mV using the  $10^{10}$  ohm. resistance. When the probe was set in motion the fluctuations increased to  $\pm 0.3$  mV.

It was found to be necessary to keep the coaxial cable absolutely still to prevent the production of large spurious deflections. Non-microphonic cable is supposed to be better than ordinary cable in this respect, but no difference between the two was observed in practice.

After the riming device had been kept inside the refrigerator for a long time, a layer of black powder formed on the mercury surface. This caused the noise level to be increased by a factor of about two.

The only way to counter this effect was to replace the mercury regularly.

A larger noise level occurred when the riming element had not been centred accurately on the motor spindle, in which case the needle tip churned up the mercury to a greater extent.

An effect which sometimes, though infrequently, observed, was that when the probe had been rotating in a dense cloud of droplets and crystals, and had been switched off, there was a standing potential of a few millivolts. This was eliminated by removing the device from the refrigerator and allowing it to warm up to room temperature.

By observing the above precautions, the noise level was kept down to  $\pm 0.3$  mV. and it was to be demonstrated that the electrical effects associated with ice crystals were many orders of magnitude greater than the noise level.

#### Experimental Studies.

##### (2) Electrification Produced by Water Droplets Only.

###### Procedure.

The phosphor-bronze balls were coated with cold demineralised water of mean conductivity  $10^{-6}$  ohm<sup>-1</sup>, cm<sup>-1</sup>, and smooth shells of ice formed on them. The ice was 1/2 to 3/4 mm. thick.

The refrigerator was cooled down to  $-18^{\circ}$  C.

A cloud was formed in it by opening the lid on the vapour source for a specified length of time. It took a few seconds for the cloud to become appreciably supercooled. The cloud was viewed by a tungsten light and minute water droplets were visible to the naked eye.

The probe was set in motion and with the electrometer on its most sensitive range the deflection was noted at 30 second intervals. The results are shown in Table 2. After a number of readings had been taken the probe was stopped and inspected.

Results.

TABLE 2.

Results for the Accretion of Supercooled Water Droplets Only.

Time (sec)	0	30	60	90	120
Reading (mV)	-0.3	-0.2	+0.3	+0.3	+0.4

Upon inspecting the probe it was seen that each simulated hailstone had a covering of hard opaque ice on its forward face. This ice was formed by the impaction and freezing of water droplets.

Discussion.

The sizes of the cloud droplets were not measured directly here but were estimated by making a visual comparison with the sizes

of ice crystals whose diameters were measured at a later time.

The estimated diameter of the droplets was 3-5  $\mu$ .

It seemed that the droplets had frozen without splintering, because if splinters had been produced, they would have grown in the cloud at the expense of the water droplets and therefore they would have been observed. It also seemed unlikely that droplets of this size had splashed.

Since the rates of charging shown in Table 2 are exactly the same as the noise level of the instrument, it was not certain whether this riming process caused any charging at all, and that if the droplets had caused any separation of charge, then in view of the very high concentration of water droplets in the cloud, the mean charge separated per droplet must have been very small.

(3) Electrification Produced by Water Droplets and Ice Crystals Together.

Procedure.

The probe was set in motion and the cloud was seeded by dropping in small fragments of solid carbon dioxide which left behind them of minute ice crystals which grew very rapidly.

With the electrometer on its least sensitive range, which was 1000 mV, it was immediately apparent that there was very strong electrification of the probe, and often the needle went off-scale.

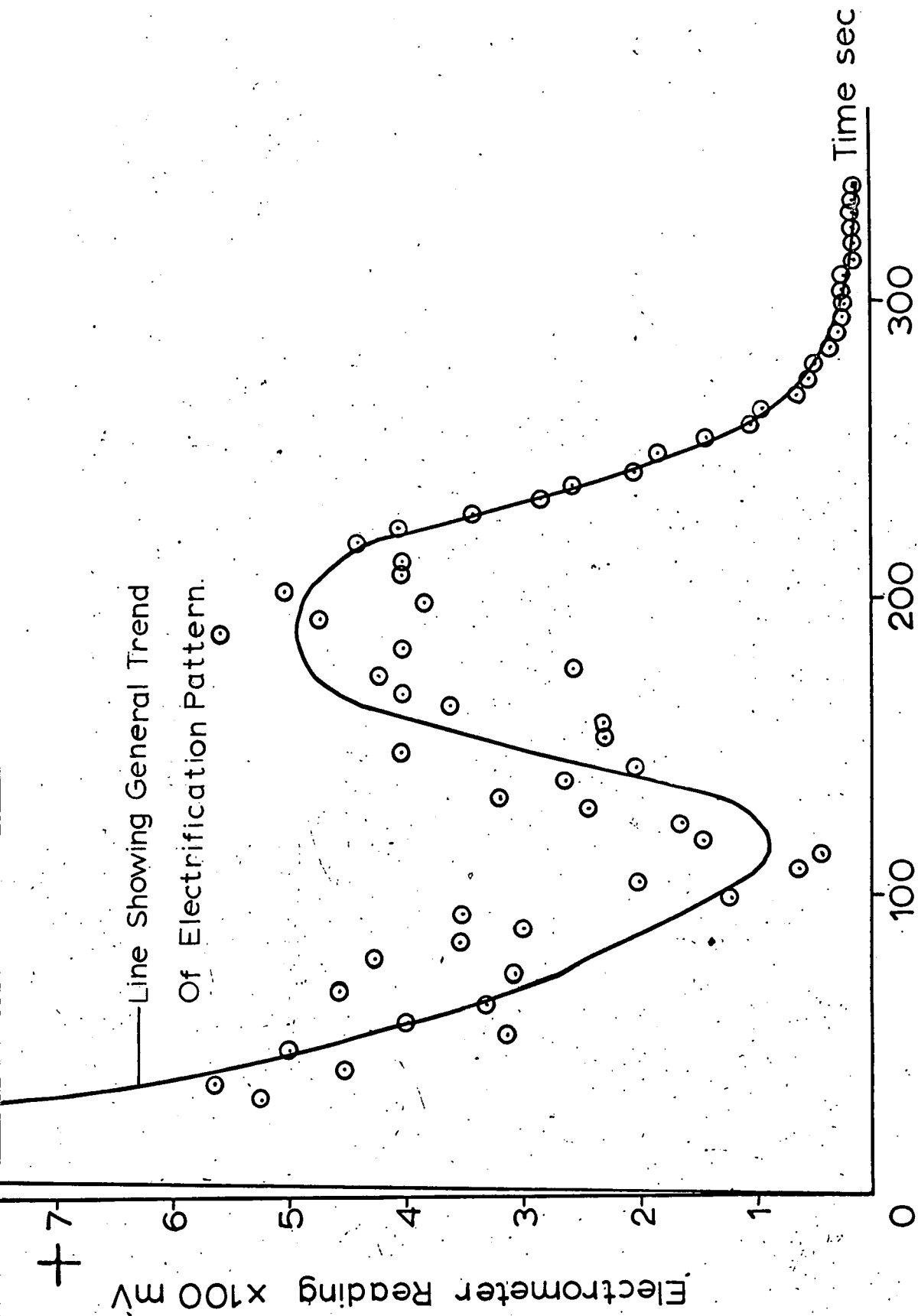


Fig.7 Variation of Charging with Time—1st Pattern.



Although the needle was fluctuating considerably, readings were taken every few seconds until it was seen that there were few crystals left. After repeating the procedure a few times, a characteristic charging pattern could be identified.

By altering the thermal condition of the cloud, different charging patterns were obtained.

(i) 1st Pattern.

The first series of readings was taken with water vapour being continuously supplied to the cloud. Considering the size of the refrigerator this meant that the degree of supercooling of the water droplets could not become very large, and that there was continuous mixing-in of warm freshly produced vapour with the colder supercooled water droplets.

Results.

Fig. 7 shows a typical charging record. It shows immediate very strong positive charging, which after a minute or so became reduced to a low value, followed later by a great enhancement of the positive charging to a value approaching the initial charging maximum. Then, after 4 - 5 minutes, the charging fell smoothly towards zero.

(ii) 2nd Pattern.

The water droplet concentration was much lower in the second method. A fixed amount of water vapour was formed in the refrigerator

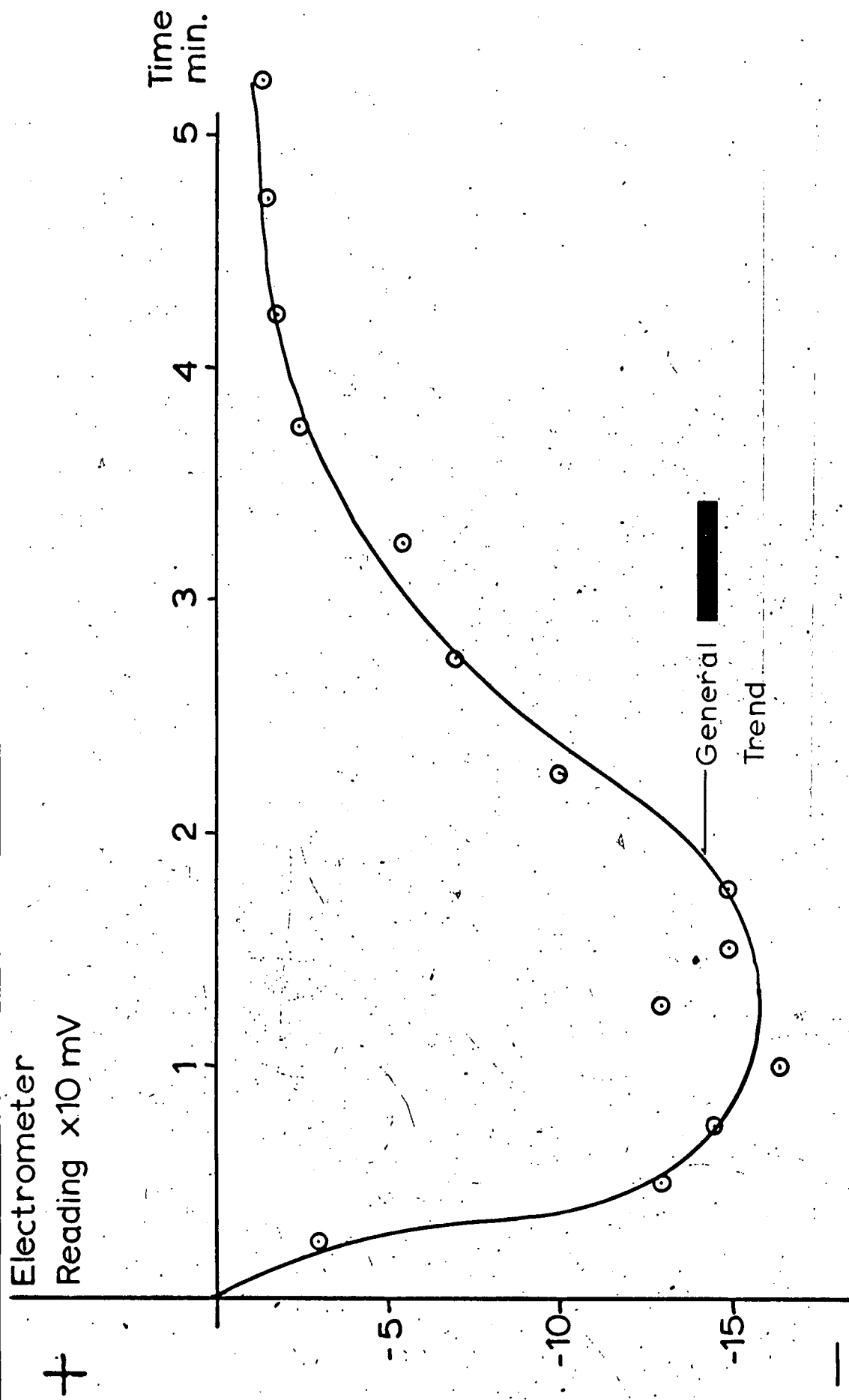


Fig.8 Variation of Charging with Time—2nd Pattern.

and allowed to supercool to a very low temperature ( $-18^{\circ}$  C). The cloud was nucleated, and thoroughly stirred before setting the probe in motion. The electrometer reading was taken every few seconds, and the procedure repeated to confirm that this was another characteristic charging pattern.

### Results.

The charging pattern which is shown in Fig. 8 contrasts strongly with the previous one. The rate of charging was less than before and the probe was charged negatively. Also there were less fluctuations than in the first case.

#### (iii) General Pattern.

The above two patterns represented extreme cases. In general the degree of supercooling was not as much as in the latter case, and consequently charging of both signs was observed.

The general pattern when a fixed amount of vapour was nucleated after being cooled for only a short time, was that there was an immediate strong positive charging of the probe, followed shortly by a more persistent, somewhat less intense negative charging which sometimes went positive again later, but generally remained negative, diminishing smoothly towards zero as the concentrations of both droplets and crystals became very low.

(iv) Further Observations.

The relative concentrations of droplets and crystals in the cloud were set to give negative charging of the probe. Further qualitative measurements were then made by introducing in turn a fixed volume of warm humid air, warm dry air, and cold air containing some supercooled water droplets into the vicinity of the probe, and the resultant effects that these had on the sign and magnitude of the charging were observed.

Warm humid air was formed by blowing air from a cylinder through a flask containing hot water at about 60° C. Cold air containing water droplets was formed by passing the warm humid air through a brass tube 1 m in length, 5 cm. in diameter placed on the floor of the refrigerator. The flow rate was low enough for the air to cool down to the temperature of the refrigerator air, but the concentration of water droplets present in the air flow was only small. Warm dry air was formed by blowing air from a cylinder through a hot glass tube.

It was difficult to put the results on a quantitative basis because of the difficulty of measuring small concentrations of water droplets and of estimating the local thermal effects of adding a stream of warm air to a volume of cold air. The most marked effects were noticed with warm humid air, and this was probably due to its greater heat capacity. The results are

summarised in Table below:-

TABLE 3.

The Effect on Charging of Adding Air in Various Conditions.

Before adding air, the probe was being charged negatively.

Type of Air	Resultant Effect.
Warm and humid	There was immediate strong positive charging, followed after a few seconds by negative charging more intense than the original negative charging by factors of up to about 5. This then fell to the original value.
Warm and dry	There was immediate positive charging, less intense than with humid air, which reverted slowly to the original negative charging without any enhancement of negative charging.
Cold and containing supercooled water droplets.	There was an enhancement of the negative charging by about 50% which reverted slowly to the former rate of charging.

(v) Other Observations.

A . Effect of Nucleating Agent.

There was the possibility that the electrification phenomena were caused by some contaminating effect of the small quantities of carbon dioxide which were introduced to seed the cloud. It was therefore desirable to observe the effect of using another nucleating agent. The compartment was refilled with fresh air. A cloud was formed and seeded by a metal rod which had been cooled in liquid nitrogen. Charge measurements were made.

It was seen that the charging pattern and the magnitude of the charging were the same as before, and it was concluded that the electrification phenomena did not appear to depend on the nature of the nucleating agent.

B. Effect of Infra-red Radiation.

An infra-red lamp was brought up close to the probe in an attempt to heat it relative to the cloud particles.

This procedure did not produce any detectable change in the readings.

It was concluded, however, that this result was not significant, since it was not known whether the probe was being heated by the lamp .

C. Effect of Refrigerator Temperature.

All the previous observations had been carried out when the refrigerator temperature was initially between  $-15$  and  $-20^{\circ}$  C.

Some further measurements were made with the refrigerator temperature initially at  $-8^{\circ}$  C., so that the temperature of a supercooled cloud was about  $-5^{\circ}$  C. The cloud was seeded and charge measurements were made.

It was seen that the electrification was considerably reduced and that the rate of charging was approximately an order of magnitude less than before. The general pattern of the charging was the same as before.

Summary of the Results.

It was demonstrated that when a cloud of supercooled water droplets was nucleated at  $-15^{\circ}$  C., so much positive and negative charging was produced that the electrometer needle sometimes went off-scale. This corresponded to a rate of charging of at least  $0.3 \text{ e.s.u. sec.}^{-1}$ . The charging was much less if the experiment was repeated at  $-5^{\circ}$  C.

Various characteristic charging patterns were obtained which depended on the relative concentrations of ice crystals and water droplets and also their respective temperatures.

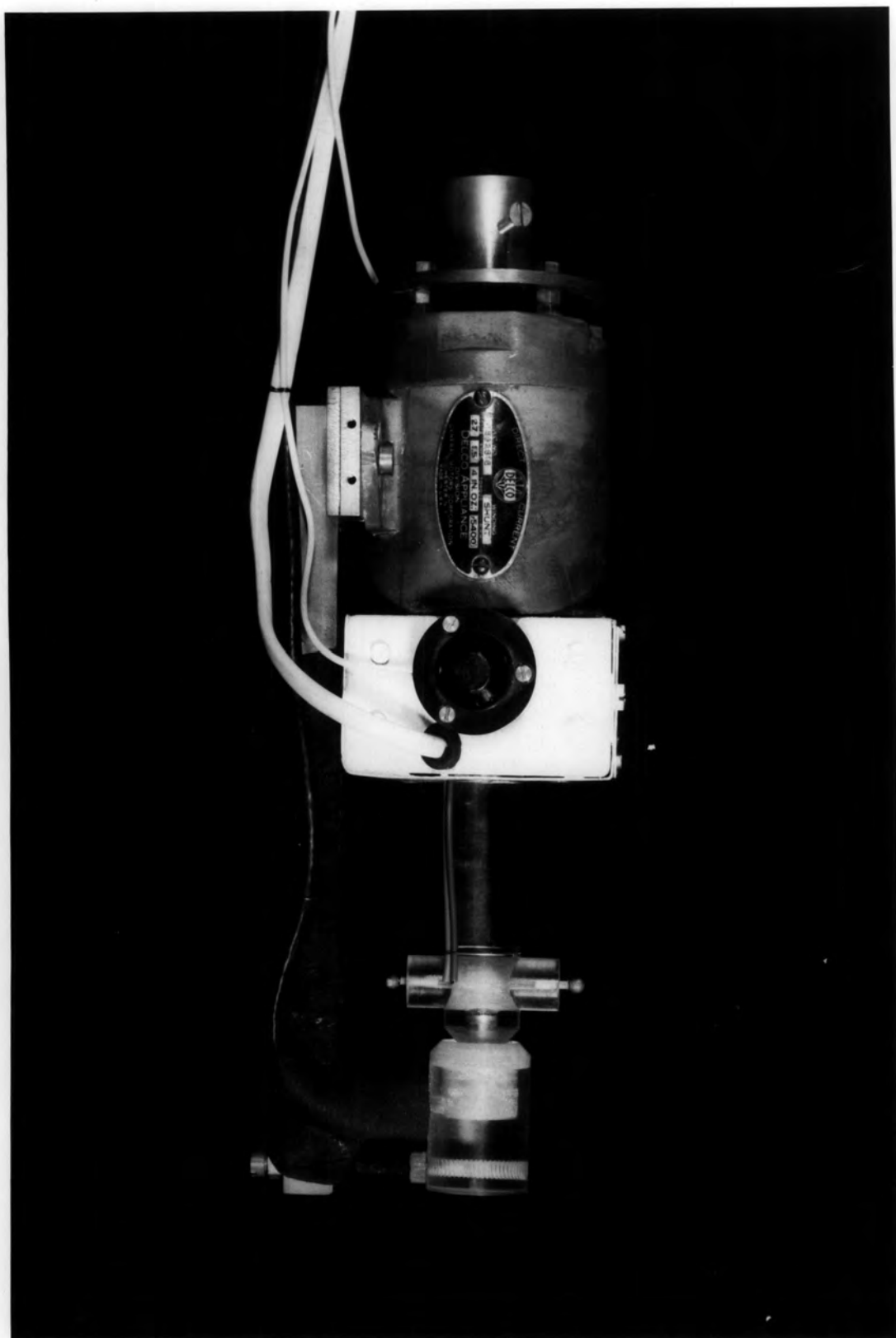


Fig. 9. The Rotating Probe for Charge and Temperature Measurement.



Positive charging of the probe was associated with high densities of warm water vapour and droplets compared with the concentrations of ice crystals, and negative charging was associated with low concentrations of cold water droplets. When the probe was being negatively charged it was shown that positive charging was caused when either warm moist air or warm dry air was introduced and that the negative charging was enhanced when cold moist air was introduced into the vicinity of the probes.

#### 4. Correlation of Rate of Charging with Temperature Difference.

##### Modifications to Apparatus.

The riming device was modified to enable the temperature of the probe to be measured. The modified form is shown in Fig. 9.

In this version only one of the phosphor-bronze balls was connected to the electrometer. A thermojunction was embedded in the other ball and the wires from this were connected to copper slip-rings positioned at the top of the perspex rotor. Contact was made between the slip-rings and the rest of the thermocouple circuit by carbon brushes. The slip-rings were surrounded by an aluminium box attached to the bottom of the motor housing.

In practice this proved to be a convenient method of measuring the temperature of a rotating body, except that in this case the thermocouple had a long response time. The thermocouple calibration remained constant throughout.

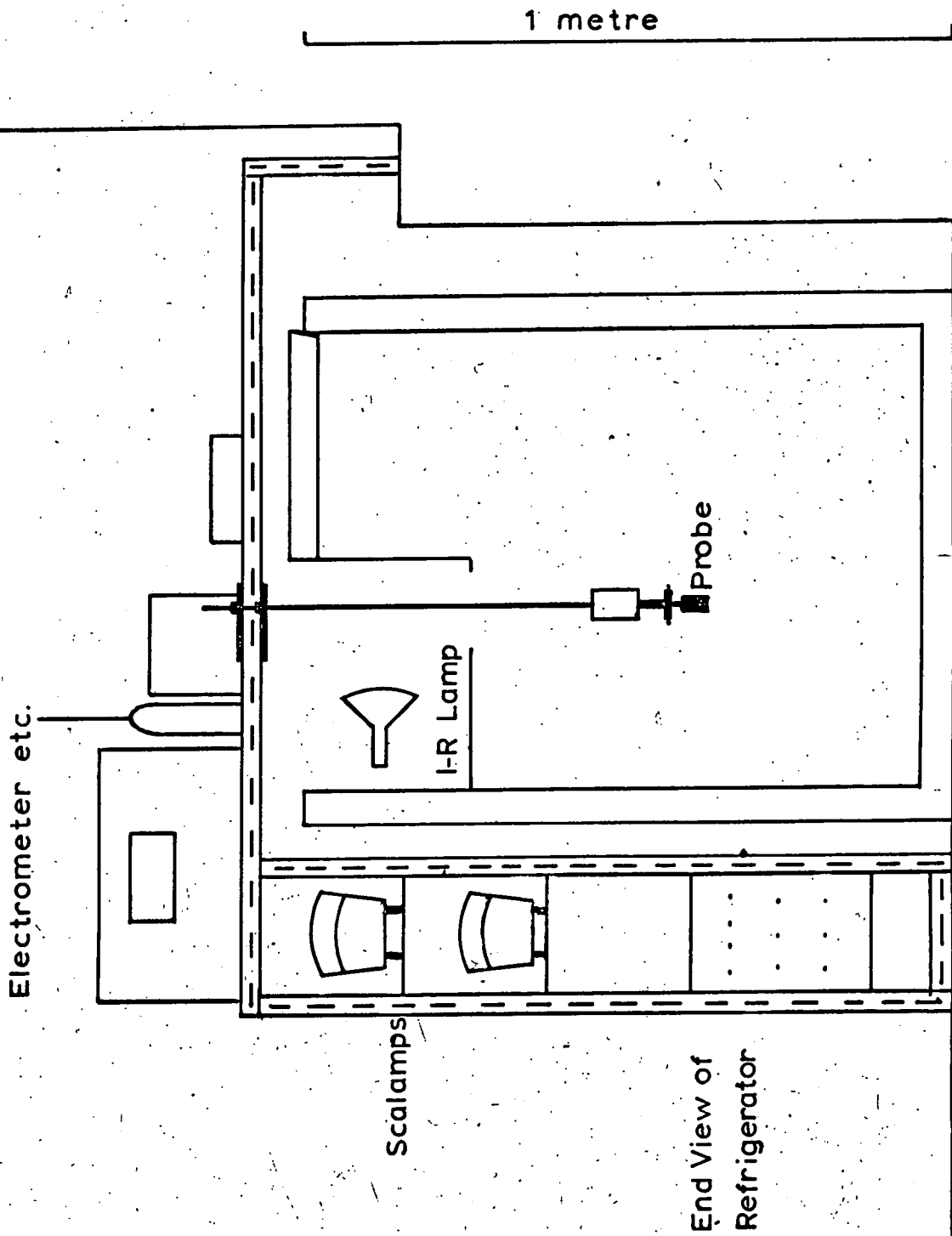


Fig.10 Experimental Arrangement for Chapter 4, Part 4.

It was observed that when the device had been kept in the refrigerator for a very long time, the thermocouple reading started fluctuating. This was caused by a non-conducting film forming on the slip-rings, and could only be eliminated by removing the device from the refrigerator and allowing it to warm up to room temperature.

The probe was to be pre-heated or pre-cooled before exposing it to the cloud of ice crystals. This was achieved by constructing a compartment measuring 28 x 28 x 35 cm., open to the air, into which the riming device could be raised through a trap-door. In this compartment the probe could be heated by the infra-red lamp, or cooled by placing it in a box containing a jacket of solid carbon dioxide. In this way the probe temperature could be varied between  $-5$  and  $-30^{\circ}$  C. The experimental arrangement is shown in Fig.10.

#### Experimental Procedure.

In the first set of readings the probe was preheated and in the second set it was precooled.

A cloud of crystals and water droplets was formed by allowing a fixed amount of vapour in the refrigerator to cool down to about  $-15^{\circ}$  C. After being nucleated the cloud was thoroughly stirred. After waiting for about a minute the water droplet concentration was relatively small, and the ice crystals had become large, although there were fewer of them than immediately after nucleation.

The temperatures of the refrigerator and the rotating probe were measured. The riming device was lowered quickly into the cloud and the initial deflection of the electrometer was noted. The motor was switched off, and a Formvar coated slide was placed on the floor of the refrigerator. The concentration of crystals in the cloud at that time was deduced from the number of crystals caught on the slide, making the assumption that all the crystals in the cloud would fall uniformly on to the floor of the refrigerator.

All the charge measurements were adjusted so that they referred to a standard crystal concentration and these values were plotted against the measured temperature differences. The results are shown in Tables 4 and 5, and are plotted in Fig. 11. The temperature difference was defined as positive when the probe was colder than the refrigerator air.

TABLE 4.

The Electrification of the Probe by Ice Crystals for Negative Temperature Difference.

Probe Temp. ° C.	Refrig. Temp. ° C.	Temp. Diff. ° C.	No. of crystals on 700 $\mu$ square N.	Electrometer Deflection (mV) V	Deflection referred to crystal cone* of $8 \times 10^8$ $m^{-3}$
-4.9	-15.0	-10.1	130	-600	- 920
-6.5	-16.1	-9.6	60	-200	- 670
-6.5	-14.4	-7.9	240	-400	- 330
-8.0	-14.3	-6.3	125	-200	- 125
-4.9	-15.9	-11.0	31	-110	- 710
-5.5	-16.2	-10.7	26	-100	- 770
-4.9	-15.9	-11.0	24	- 20	- 170
-6.2	-16.0	- 9.8	53	- 70	- 260
-5.8	-15.7	- 9.9	40	- 50	- 250
-7.4	-13.5	- 6.1	500	-150	- 60
-6.2	-14.1	- 7.9	170	-340	- 400
-7.4	-13.8	-6.4	130	-260	- 400
-6.2	-18.0	-11.8	140	-200	- 300
-4.0	-18.9	-14.9	100	-320	- 640
-5.2	-16.3	-11.1	110	-450	- 800

TABLE 4. (Continued)

Probe Temp. ° C.	Refrig. Temp. ° C.	Temp. Diff. ° C.	No. of crystals on 700 $\mu$ square N	Electro-meter Deflection(mV) V	Deflection referred to crystal cone <sup>n</sup> of $8 \times 10^8$ $m^{-3}$
-4.3	-17.7	-13.4	130	-600	- 920
-4.0	-18.1	-14.1	100	-600	-1200
-8.0	-20.2	-12.2	220	-300	- 270
-8.0	-21.0	-13.0	180	-900	-1000
-4.9	-20.2	-15.3	140	-600	- 500

TABLE 5.

The Electrification of the Probe by Ice Crystals for Positive Temperature Differences.

Probe Temp. ° C.	Refrig. Temp. ° C.	Temp. Diff. ° C.	No. of crystals on 700 $\mu$ square N	Electrometer Deflection (mV) V	Deflection referred to crystal cone <sup>n</sup> of $7 \times 10^8$ m <sup>-3</sup>
-15.3	-13.3	+2.0	100	+250	+500
-14.2	-11.7	+2.5	120	+100	+170
-17.3	-14.0	+3.3	200	+300	+300
-17.3	-12.7	+4.6	120	+150	+250
-19.0	-12.0	+7.0	140	+200	+300
-19.0	-13.8	+5.2	140	+100	+140
-24.5	-21.3	+3.2	180	+500	+550
-18.7	-11.7	+7.0	140	+420	+600
-17.0	-12.0	+5.0	180	+500	+550
-17.7	-14.1	+3.6	140	+300	+420

Crystal Conc.<sup>n</sup> =  $8 \times 10^8 \text{ m}^{-3}$       Temp. Diff.

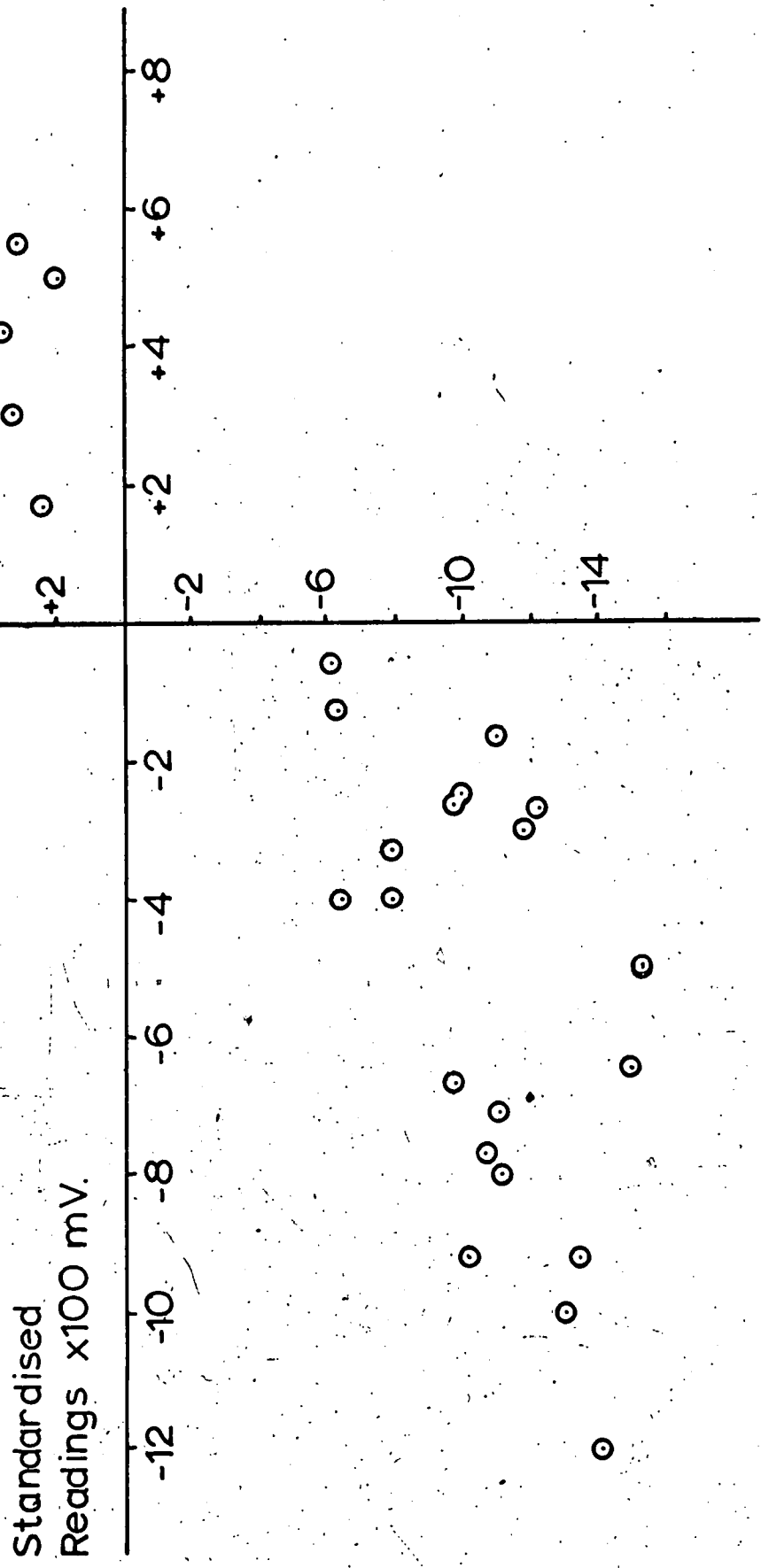


Fig.11 Variation of Charging with Measured Temperature Difference.



Discussion of Fig. 11.

One feature of the results stands out clearly in Fig 11; that when the iced probe was warmer than the ice crystals it always became charged negatively, and when it was colder than the crystals it always became charged positively. This is in agreement with the temperature gradient theory. However, in Fig. 11 the points are so widely scattered that the manner in which the charging varies with the temperature difference cannot be reasonably deduced. The two reasons for the large scatter are the error in the estimation of the temperature difference, and the error in the estimation of the crystal concentration.

It was stated that when the probe was lowered into the cloud, the initial rate of charging was measured. However it was noticed that the charging, whether negative or positive, was sustained for appreciable lengths of time, diminishing little over periods of the order of ten seconds. Since, after times of this order, any imposed temperature difference will have become very small, it may be surmised that the probe surface temperature approached the air temperature too rapidly for the measured rate of charging to be related to the initial temperature difference, and that in fact this rate of charging was related to a very small temperature difference.

The method of estimating crystal concentrations was to assume that all the crystals in the cloud would fall out and form a uniform layer on the floor of the refrigerator, so that a slide placed on

the floor would collect a number of crystals representative of the concentration in the cloud at the time when the slide was exposed. However, it took several minutes for all the crystals to fall out, and long before this the solvent on the slide had evaporated, so that many crystals fell on to the slide without making an impression. This leads to an underestimate of the crystal concentration and hence to an overestimate of the charge separated per crystal collision. This error may not be such a serious one, because the rate of fall-out was a maximum during the time that the slide was wet.

Calculation.

The crystal concentrations were calculated by counting the number of crystals  $N$  which fell on an area  $700 \mu$  square, and by multiplying this by the appropriate factor:-

$$\text{Volume of refrigerator} = 0.4 \text{ m}^3$$

$$\text{Floor area of refrigerator} = 0.7 \text{ m}^2$$

$$\text{Hence concentration of crystals} = \underline{3.5 N \times 10^6} \text{ m.}^{-3}$$

$$\text{Volume of air swept out by probe} = 200 \text{ cm.}^3 \text{ sec.}^{-1}$$

An electrometer reading of  $V$  millivolts corresponds to a rate of charging  $3 V \times 10^{-4} \text{ e.s.u. sec.}^{-1}$ , using the  $10^{10}$  ohm resistance.

Hence, the charge separated per crystal is  $4.2 V \times 10^{-7} \text{ e.s.u.}$

$\frac{-}{N}$

Referring to Fig. 1 $\frac{1}{4}$ , since the temperature difference may well have been grossly overestimated, there could be little value in relating the charge separated per crystal collision to some particular temperature difference.

Instead, the values of  $V/N$  were calculated for each reading in Tables 3 and 4, and the average was taken.

Result.

Average value of  $V/N$  is  $2.4 \pm 0.8$ .

Hence, the charge separated per crystal collision is  $(1.0 \pm 0.3)$   
 $\times 10^{-6}$  e.s.u.

5. SUMMARY

A. Explanations.

It was observed that when the iced probe was rotated in a cloud of ice crystals and supercooled water droplets a great deal of positive and negative charging was produced. It was concluded that the electrification of the simulated hailstones could be explained in terms of their collisions with rebounding ice crystals in the presence of supercooled water droplets. It was seen that there was negligible charging in the presence of water droplets only, and that the magnitude of the electrification caused by crystal collisions depended on the concentration of water droplets in the cloud.

The negative charging of the probe can be explained by the freezing of supercooled water droplets on the probe, and the subsequent warming of the probe surface relative to the air due to the release of latent heat by the freezing droplets. Applying the temperature gradient theory, when colder ice crystals touch the hailstone, protons migrate preferentially into them, and upon separation the crystals carry away positive charge.

The positive charging of the probe can be explained in a similar manner. When warm water vapour is introduced into a cloud of ice crystals it loses heat by condensation and cooling of the water droplets. Consequently the air becomes locally warmed, and so do the ice crystals floating in it. When these ice crystals collide with the probe it becomes positively charged as it is now the colder body.

It is considered that whether the probe becomes positively or negatively charged depends on whether the effect of heating the crystals relative to the probe is greater or less than the effects of heating the probe by the accretion of supercooled droplets.

When warm moist air is introduced into the cloud, the charging during the first phase is positive because the predominant effect is the warming of the crystals. In the middle phase the hailstone is being warmed by the accretion of water droplets, and the warmer crystals are now being cooled because of the dissipation of the

warmer air. This results in the electrification being reduced. In the final phase the crystals have completely cooled down again, but the probe is still being heated by accretion, and so it becomes negatively charged. The negative charging then persists unless some more warm water vapour is introduced. This reasoning was supported by the results shown in Table 3 in which the local addition of warm dry air would cause the crystals to become warmer than the probe, the addition of cold air containing a few droplets would raise the temperature of the probe relative to the crystals and the addition of warm moist air would first of all warm the crystals more than the probe and then after a time would warm the probe more than the crystals. It was also observed that with the warm moist air the changes in the electrification were more intense than with the other two types of air. This would be expected if the magnitude of the charging depended on the magnitude of the temperature difference, because the higher heat content of the warm moist air caused larger temperature differences than the other two types of air.

B. Comparison with the Results of Reynolds, Brook and Gourley

Reynolds et al observed that for negative charging of the probe, the cloud should contain a high concentration of water droplets relative to the concentration of crystals, and for positive charging of the probe, the water droplet concentration should be low. The results obtained in this laboratory showed that when the concentration

of water droplets was high the probe was charged positively and when there were fewer droplets it was charged negatively. Thus the two sets of results are apparently contradictory, although it may be possible to explain the differences in terms of the differences in experimental conditions. It may be recalled that the refrigerator used by Reynolds was much larger than the one used here, having a volume of approximately  $3 \text{ m}^3$  compared with  $0.4 \text{ m}^3$ . Also their refrigerator worked at a lower temperature,  $-25^\circ \text{ C}$ . compared with  $-15^\circ \text{ C}$ . It is considered that these differences would have some effect on the thermal condition of the cloud, because in the larger colder refrigerator, large concentrations of highly supercooled droplets could be produced in air at a temperature close to  $-25^\circ \text{ C}$ . whereas in the smaller refrigerator it was only possible to produce high concentrations of droplets which were only slightly supercooled in air which was only a few degrees below the freezing point. In the smaller refrigerator highly supercooled droplets could not be produced if there was a continuous supply of vapour, but only if a fixed quantity of water vapour was introduced and allowed to cool over periods of the order of minutes. Thus it is suggested that in the latter case, the positive charging in high concentrations of droplets was caused because the crystals had been warmed by the air to a greater extent than the probe had been warmed by the accretion of droplets. Although the probe was also warmed by the air, its initial temperature was lower, and because of its greater heat capacity

it would take longer to warm up than the crystals. In Reynolds' case there would have been no problem about the temperatures of the probe, droplets and crystals being initially different because of the greater cooling capacity of the refrigerator relative to the rate of supply of vapour, and consequently the interpretation was more straightforward, namely that the probe was warmed by the accretion of droplets, and was charged negatively by rebounding colder ice crystals.

The difference between the two sets of results for low droplet concentrations is more difficult to reconcile. Reynolds observed positive charging of the probe and did not apparently offer any explanation for this, other than the assertion that the probe was colder than the crystals. In this laboratory the probe was charged negatively in the presence of low concentrations of supercooled droplets, and this negative charging fell towards zero as the droplets became used up. However as the droplet concentration fell to zero, so did the crystal concentration, and so the two results may not be directly comparable. It may be that the positive charging observed by Reynolds was caused by the probe surface being cooled by evaporation in dry air containing an appreciable concentration of ice crystals.

So far, in this text, no mention has been made of the actual values of the droplet concentrations. This is because accurate measurements of droplet concentrations could not be made because of the small masses of liquid water involved and because the concentration did not remain constant long enough for any estimation to have much

significance. However it may reasonably be supposed that the range of droplet concentrations was similar to that measured by Reynolds, namely up to  $4 \text{ gm. m}^{-3}$ , since the droplets were of approximately the same size and the temperature and pressure were also approximately the same.

The quantity of charge separated per crystal collision was found in this laboratory to be  $10^{-6}$  e.s.u. This figure was derived from conditions in which the water droplet concentration was very low. Previous results, as shown in Table 3, indicated that if a greater concentration of water droplets had been added to the cloud, it would have increased this value by a factor of 5. This therefore gave a maximum value of  $5 \times 10^{-6}$  e.s.u., which is less than the value measured by Reynolds by a factor of 100.

One possible reason for the discrepancy may be in the estimation of the crystal concentrations, although in Reynolds' work, as in this laboratory, it was stated that the concentrations were measured in such a way as to give conservative estimates of the charge separated per crystal collision. The method by which crystal concentrations were measured in this laboratory has been described and it is considered that it causes an overestimate of the charge separated by a rebounding crystal by a factor of not more than 2 or 3. It would be of value to have more information about the technique used by Reynolds to measure concentrations.

Another reason may be that Reynolds' experiments were conducted



in a larger refrigerator working at a lower temperature, and giving ice crystals much lower temperatures than were possible in the refrigerator used in this laboratory. Also larger quantities of supercooled water droplets could be supplied continuously. It is suggested that these differences resulted in larger temperature differences which caused larger electrical effects. It is difficult, however, to estimate how much greater these electrical effects would be, as it is difficult to determine what the surface temperature of the probe would be when growing by the accretion of supercooled water droplets.

C. Comparison of the Results with the Temperature Gradient Theory.

The results in this laboratory have shown qualitative agreement with the temperature gradient theory of Latham and Mason, and the next step is to show whether there is quantitative agreement. In the following calculation assumptions are made which will be favourable to the theory. The mean diameter of the crystals (see Page. 119 ) was  $40 \mu$  and the contact area was taken to be one tenth of the *crystal area*. It was assumed that the temperature difference between the ice crystals and the probe ice was  $5^{\circ}$  C., and that the charge separated was the maximum charge i.e. corresponding to a time of contact of  $8.5 \times 10^{-3}$  sec. From Page 46, the maximum charge separated is given by the expression: 
$$\sigma_{max} = 3.05 \times 10^{-3} (T_1 - T_2) \text{ e.s.u. cm.}^{-2} .$$

Substituting the above values in this expression gives a charge

separation of  $2.5 \times 10^{-8}$  e.s.u. This is more than two orders of magnitude less than the measured value of  $5 \times 10^{-6}$  e.s.u.

This may partly be accounted for by the observations of Magono and Takahashi (see Page 27) that the charge separation was greatly enhanced when the probe surface had a fine structure, as it had in these experiments, whereas the temperature gradient theory applies to smooth ice surfaces. However, the charge enhancement observed by Magono and Takahashi was not greater than by a factor of 6, and if this factor were taken into account, together with the underestimate by a factor of 3 in the crystal concentration, the observed separation of charge would still be one order of magnitude greater than predicted by the theory. Also, calculations had been made on the assumption that the charge separation was a maximum, which was shown by theory to correspond to a time of contact of approximately  $10^{-2}$  sec. If this time of contact had been applicable in these experiments it would have meant that a crystal was in contact with the probe while the latter moved through a distance of 10 cm., which seemed to be an unreasonably high value, and it is suggested that a more likely estimate of the contact time was  $10^{-3}$  to  $10^{-4}$  sec. Thus, the charge separation expected from the theory would have been substantially less. Finally, it could not be said with any certainty whether the effective temperature difference was as high as  $5^{\circ}$  C.

#### D. Conclusion.

It was concluded that although the experiments had shown that

the sign of charging of simulated hailstones by ice crystals depended on the sign of the temperature difference between them, and that this was in qualitative agreement with the temperature gradient theory the experiments had shown that the charge separation of  $5 \times 10^{-6}$  e.s.u. per crystal collision was greater than could be explained by the temperature gradient theory. These results, however, were inadequate in certain respects. The electrical phenomena were observed only in the presence of supercooled water droplets, and it might be thought that the droplets could have produced additional effects due to freezing potentials. Also, when the probe was being precooled in solid carbon dioxide, the refrigerator received a large amount of gaseous carbon dioxide, and it might be thought that this had some influence on the electrical effects. Finally, from the point of view of attempting to correlate the rate of charging with the magnitude of the temperature difference, it was considered that no accurate measurements of the temperature differences actually involved were obtained.

With these inadequacies in mind, further experiments were performed. They are described in the next chapter.

CHAPTER 5.

MEASUREMENTS WITH A STATIONARY PROBE.

1. INTRODUCTION.

A stream of ice crystals was blown past a stationary iced probe, the temperature of the latter being varied, and the rate of charging of the probe was measured. The variation of the rate of charging with the sign and magnitude of the temperature difference, the presence of impurity ions in the ice on the probe, and the impact velocity of the ice crystals was determined.

2. THE APPARATUS.

(a) Production of Ice Crystals.

Ice crystals were produced by blowing moist air through a channelled, cubical box in which were immersed cylinders containing crushed solid carbon dioxide. The box which was constructed of tinned sheet, was approximately cubical, of side approximately 20 cm. The interior of the box was fitted with four vertical aluminium plates which made five vertical channels for the air to pass along before emerging from the box. Three brass tubes of internal diameter approximately 4 cm, length 18 cm and closed at their lower ends were attached to the detachable lid of the box and suspended in alternate channels. The air inlet to the box was through a 4 cm diameter brass tube approximately 80 cm long which was attached to the lid. A hole

was made in the lid and fitted with a rubber bung. The purpose of this was to divert the air stream. The air outlet tube was of 4 cm internal diameter and length approximately 1 m. It was fixed to the side of the box and sloped upwards in order to be accommodated in the restricted space of the refrigerator. The far end was bent into the horizontal position and tapered to form a tube of internal diameter 12 mm and length 5 cm. Two trap doors were constructed at this end of the tube in order to divert the air stream through a hole in the side of the tube.

A vacuum cleaner motor, encased in a brass cylinder, was used to extract air from outside the laboratory and to blow it through the apparatus. The motor speed and hence the extraction rate were controlled by a Variac transformer. After leaving the fan the air passed through a Cambridge ion filter and a water vapour source which consisted of a 2 l glass beaker fitted with a lid. The air, which already contained some water vapour was blown over the surface of water in the beaker thereby acquiring more water vapour. This moist air was passed via a flow-meter into the cubical box which was situated in the refrigerator. The brass cylinders contained tightly packed solid carbon dioxide, so the temperature of the air close to the cylinders was low enough to ensure that many nuclei would be formed. When moist air was blown past the first cylinder many very small ice crystals were formed, which proceeded to grow at the expense of the water vapour. The air containing growing crystals was forced past

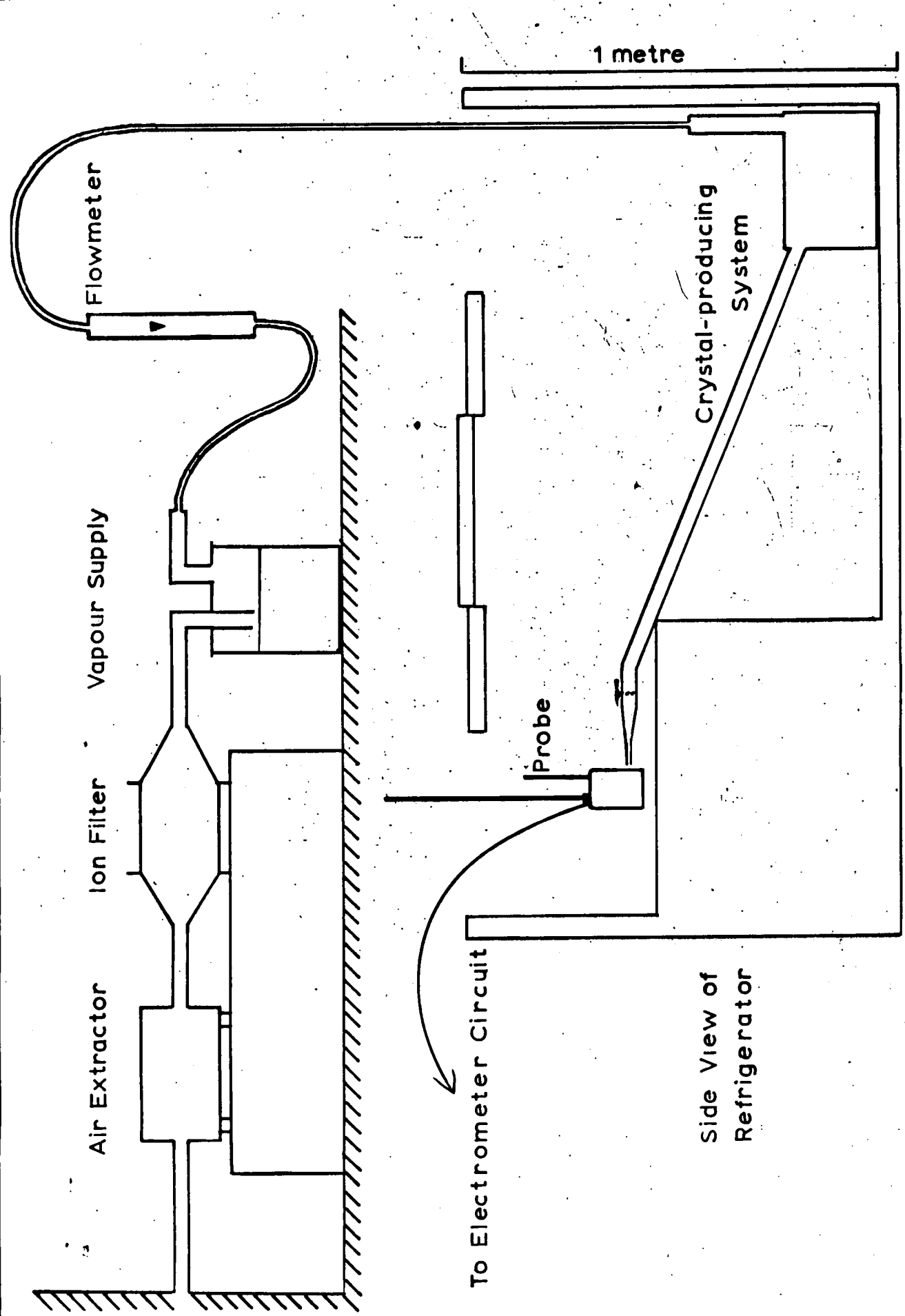


Fig.12 The Experimental Arrangement for Chapter 5.

□ Brass  
▨ Perspex

1 cm

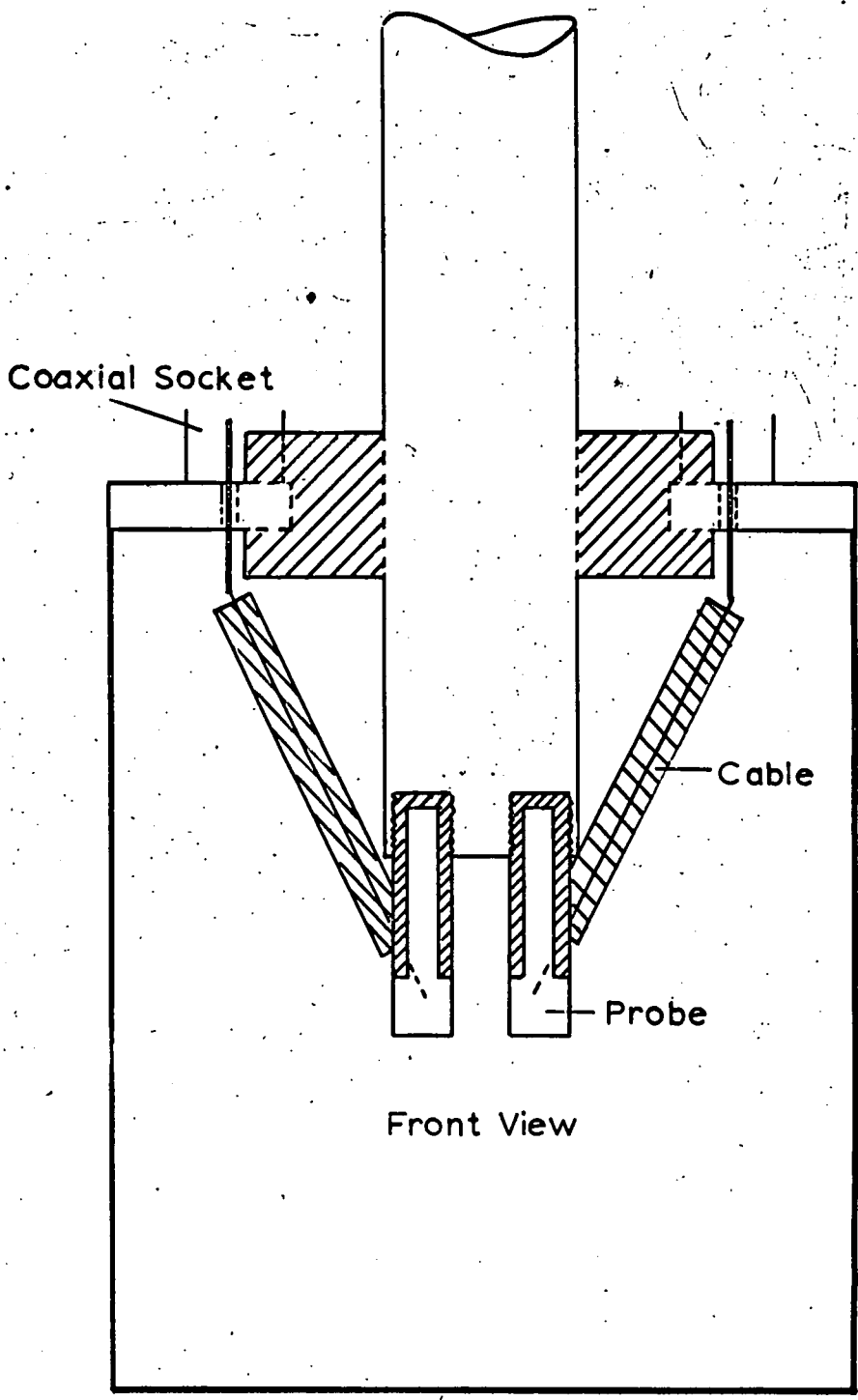


Fig.13 The Stationary Probes

the other two cylinders, and on passing out of the box it contained a great number of relatively large ice crystals. Formvar slides (see Appendix 1) showed that the crystals were prisms and hexagonal plates, and that they exhibited a great variation in size. A typical selection is shown in Fig. 21 in which the average size was estimated as  $20 \mu$ . By the time the air stream encountered the probe it had attained a temperature of about  $-20^{\circ}$  C. The arrangement of the apparatus is shown in Fig. 12.

(b) The Probe Unit.

Stationary probes were used because it was considered that their surface temperatures could be controlled and determined more readily. There were two probes which consisted of solid brass cylinders 4 mm in diameter for 4 mm of their length and 2 mm in diameter for the remaining length of 10 mm. Each 10 mm length fitted into a perspex sleeve of external diameter 4 mm and tapped at one end. The sleeves were screwed side by side into the end of a brass rod of diameter 12 mm and length 13 cm. This arrangement ensured optimum thermal contact between the rod and the probes, while maintaining electrical insulation. A brass plate 5.0 x 7.5 cm was fixed at right angles to the rod and thermally insulated from it. A brass collar and two sockets were joined to the plate. Short pieces of coaxial cable were soldered between the probes and the sockets. Aluminium sheet was bent to form an open-ended box around the probes, and this acted as an electrostatic screen. A diagram of the probe unit is shown in Fig. 13.



(c) The Operation of the Apparatus.

For most of the work only one probe was used. A smooth layer of ice was formed on it by dipping it alternately in liquid nitrogen and cold demineralised water, until the ice was approximately  $\frac{1}{2}$  mm thick. The probe unit was clamped to one of the adjustable rods attached to the Handy Angle bridge and the probe was connected to the electrometer circuit, in which the  $10^{10}$  ohm resistance was again incorporated. The probe screen and the crystal-producing apparatus were earthed. The probe was placed about 1 cm from the end of the tapered tube. Crushed solid carbon dioxide was packed tightly into the brass cylinders. The cylinders were closed with rubber bungs and the gaseous carbon dioxide was conducted by tubing out of the opposite side of the laboratory to which the fresh air was drawn in. The fan motor was switched on and a stream of crystals was blown past the probe. An electrometer deflection showed that the probe was being charged.

In the preliminary tests the fan was operated intermittently for several hours. It was noticed during this time that the sign and magnitude of the charging varied considerably. At first the probe was charged negatively but as time went on it became charged positively. The rate of charging increased somewhat when more solid carbon dioxide was added to the cylinders. This was because increasing the amount of solid carbon dioxide caused a greater number of crystals to be produced, as was shown by Formvar slides. It was also observed

as that time went on, not only were less crystals being produced, but that they were accompanied by a greater proportion of minute water droplets. Under conditions when a great number of crystals were being produced it was observed, by diverting the crystal stream into the illuminated refrigerator compartment, that the concentration of droplets associated with the crystals was generally extremely low. It was also sometimes noticed that erratic charging was produced when there was no solid carbon dioxide in the cylinders. This was unexpected because no crystals should have been produced. Formvar slides showed that the charging was caused by collisions of aggregates of very many small crystals with the probe. After these tests the crystal box was dismantled. It was seen that the brass cylinders were covered with a frost deposit a few millimetres thick. This deposit had undoubtedly reduced the efficiency of the system for producing ice crystals. The deposit was removed and the box reassembled. When the air stream was passed them, there was no electrometer deflection. The cylinders were refilled, and when crystals were blown past the probe, a negative electrometer deflection was observed. As time went on, the negative deflections became positive again, and in order to prevent this variation the procedure adopted was to dismantle the box and remove the frost deposit from the box at half-hourly intervals.

It was also noticed that there was poor reproducibility in the magnitudes of successive observations, and that the rate of charging decreased steadily with time. This effect was also seen to be caused by a reduction in the rate of production of ice crystals, and the

magnitude of the effect is shown by the results in Table 6.

TABLE 6.

Correspondence between Successive Readings when Precautions were  
Not Observed.

Time (min)	Rate of Charging (mV)
0	1000 +
1½	1000 +
3	820
4½	710
6	560
7½	450
9	380

Time (min)	Rate of Charging(mV)
10½	350
12	230
13½	190
15	130
16½	100
18	60

This effect was found to be due to poor thermal contact between the solid carbon dioxide and the cylinder walls, and was overcome by packing the coolant down tightly in the cylinders after each reading.

By taking the precautions mentioned above it was possible to obtain reproducible crystal concentrations in the air stream, as evidenced by Formvar slides and also by successive charge measurements. The charge measurements in Table 7 show the extent to which reproducibility could be achieved when the probe temperature

and the air stream temperature were kept constant.

TABLE 7

Correspondence between Successive Readings when Precautions were Observed.

Time (min)	Rate of Charging (mV)	Time (min)	Rate of Charging (mV)
0	250	15	620
1½	460	16½	610
3	550	18	630
4½	540	19½	620
6	550	21	540
7½	600	22½	390
9	690	24	500
10½	660	⋮	⋮
12	650	⋮	⋮
13½	650	30	670

(d) An Error in the Estimation of Flow Rate.

There were two conflicting requirements in the apparatus. They were that the ice crystal box needed to be quickly and readily dismantled for regular cleaning, and that the apparatus should be airtight.

The apparatus described above had the advantage that it could be taken apart quickly, but it was by no means air-tight. When the flow rate was set to give an air-speed of  $10 \text{ m sec}^{-1}$  at the end of the exit tube it was found that only a small fraction of the air issuing from the flow-meter emerged from the exit tube. This was because of leaks at the join between the box and its lid. In the earlier measurements the flow meter was removed and the motor speed was increased until it was considered that sufficient air was emerging from the exit tube. However, this air speed was not accurately known, and since it was discovered later that the rate of charging by the ice crystals depended upon their impact velocities it was clear that measurements taken with the apparatus in its present state, although they were of qualitative significance, had no quantitative value because the impact velocity was unknown.

In order to be able to measure the air speed accurately another box for producing ice crystals was constructed. This measured  $20 \times 28 \times 28 \text{ cm}$  and was constructed of brass plates, but otherwise it was physically the same as the first model. Great care was taken to ensure that it was airtight and all permanent joins were sealed with Araldite. The lid was secured by 32 bolts and made airtight with a rubber seal. The large number of screws meant that the half-hourly removal of the lid to clean the cylinders was tedious, but nevertheless it was done. This box is illustrated in Fig. 14. Also shown in the photograph are the sloping tube with its tapered end and on the



Fig. 14. The System for Producing Ice Crystals.

far right the probe. It can be seen that the sloping tube was joined along its length by another cross tube. The latter was incorporated for measurements on the variation of charging with impact velocity, but for purposes of earlier experiments this tube was kept closed. The box was tested at pressures of up to 1 atmosphere and was seen to be airtight. Thus the flow rate out of the tube could be measured accurately, and quantitative results could be obtained.

It was found in operation that this box was less efficient for the production of ice crystals than the first one and that appreciable numbers of crystals could only be produced for flow rates corresponding to crystal velocities of  $15 \text{ m sec}^{-1}$  or greater. Most of the results described in this chapter were taken using this more recent box, although the first measurements on the variation of charging with temperature difference were taken using the earlier model. It will be indicated in the text which model was used in a particular experiment by referring to them as Box I and Box II.

### 3. VARIATION OF CHARGING WITH TEMPERATURE DIFFERENCE.

#### (a) Procedure.

##### (1) Estimation of the Probe Temperature.

It was not possible to measure the temperature of the probe at the same time as measuring its rate of charging because of the electrical effects which would have been caused by having a thermocouple embedded in the ice. Instead the variation of the surface temperature with time

Surface Temp.  
of Probe °C

-28

-20

-12

-4

Time min.

16

14

12

10

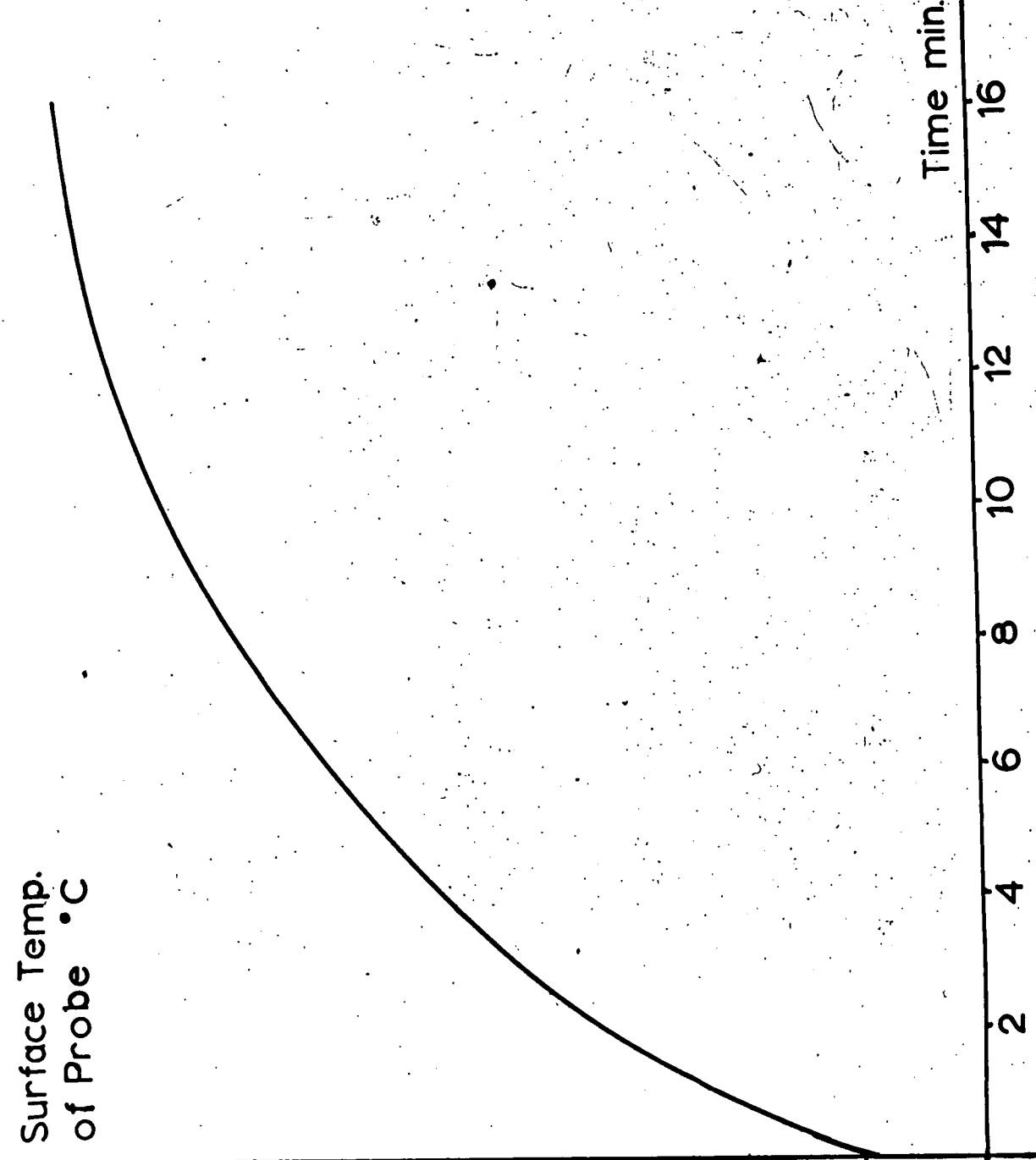
8

6

4

2

Fig.15 Variation of Probe Temperature with Time.





was determined independently. A fine thermocouple made from 40 S.W.G. wire was calibrated, and the cold junction embedded in the surface of the ice on the probe. The probe was always situated in a region where the air temperature was  $-9 \pm 1^{\circ}$  C. The probe was heated by fitting a 2 kg heated brass cylinder on to the 18 cm long brass rod. The temperature of the brass cylinder was  $100^{\circ}$  C, and it was kept on the rod for a specific length of time (1 minute) after which it was removed. It was observed that the surface of the probe became gradually warmer, until after 5 minutes it had reached a steady temperature of  $-3^{\circ}$  C. At this stage a hollow cylinder was put on to the rod and filled with finely crushed solid carbon dioxide. The surface temperature of the probe was then measured at 1 minute intervals. In order to ensure accurate comparison with experimental procedure, a stream of air containing ice crystals was blown past the probe for 5 seconds after each reading. After the lowest temperature had been attained, the probe was allowed to warm up. The whole procedure was repeated and six sets of readings were obtained. The average values of these are plotted on Fig. 15, and it can be seen that the values range from  $-3$  to  $-30^{\circ}$  C. The standard error on each point was  $\pm 0.3^{\circ}$  C. Thus by always adopting the same procedure for heating and cooling the probe, its surface temperature was always known prior to blowing a stream of ice crystals past it.

(ii) Measurement of the Rate of Charging.

The probe was warmed to  $-3^{\circ}$  C and the coolant was placed on the rod as described above. The following precautions were taken to ensure

that at the required moment a stream of ice crystals of uniform concentration and at a uniform temperature were blown past the probe. The trapdoor in the tube was closed and the trapdoor at the side of the tube was opened. The motor was switched on and the stream of crystals produced was diverted through the hole in the lid for a few seconds until the excessively cold air which had been standing in the box had been dispelled. Then the air stream was allowed to pass up the tube and out of the hole in the side of the tube. When there could be said to be a uniform concentration of ice crystals in the tube, one trapdoor was quickly closed and the other quickly opened, so that a uniform stream of ice crystals blew past the probe. The initial electrometer deflection was noted. The stream of crystals was blown past for about five seconds during which time the air stream temperature was taken from a thermocouple placed in the air stream. It was assumed that the temperature of the crystals was the same as the air stream temperature. The motor was switched off and the procedure was repeated at 1 minute intervals. From time to time, glass rods 4 mm in diameter and coated with viscous Formvar solution were held in the air stream. After a few readings had been taken the surface of the probe was inspected. Graphs were plotted of the measured rate of charging of the probe against the measured temperature. These were the semi-quantitative measurements and are shown in Figs. 16 and 17. Quantitative measurements were obtained for crystal impact velocities of  $20 \text{ m sec}^{-1}$ . For negative charging of the probe, the probe was kept at the temperature of its

environment, which was about  $-10^{\circ}$  C, and before crystals were blown past its surface temperature was measured with a fine thermocouple. The charging of the probe was then measured as before. For measurements of positive charging, the probe was cooled down to  $-31$  to  $-33^{\circ}$  C. The numbers of crystals colliding with the probe were determined by exposing Formvar-coated glass rods to the stream of ice crystals for measured times. These results are shown in Tables 8 and 9.

(iii) Precautions.

Since the air stream temperature was measured by a thermocouple permanently inserted into the tube it was necessary to show whether the presence of the thermocouple exerted any influence on the electrification measurements. It was concluded, from several readings, that the presence of the thermocouple made no detectable difference.

Since Latham and Stow (1965~~B~~) had shown that electrification was produced upon the evaporation of ice in an air stream it was necessary to show whether the electrical effects which had been observed were due to the cold air or to the ice crystals. After removing all ice deposits from the apparatus, dry air from a cylinder was blown through it and past the probe. Solid carbon dioxide was put in the brass tubes and in this way the dry air temperature was varied from about  $-10^{\circ}$  C to  $-25^{\circ}$  C. The electrometer was put on its most sensitive scale, the noise level being  $\pm 0.05$  mV. No deflection was observed when cold dry air was blown past the probe, and it was concluded that the electrical effects were caused by the ice crystals and not by evaporation.

(iv) Qualitative Results (Box I)

The results showed that when the probe was warmer than the ice crystals it was charged negatively, and as it was cooled down by the solid carbon dioxide it became charged positively. It was also shown that having obtained positive charging of the probe, the negative charging could be again obtained by warming it up. This showed that the sign of the charging of the probe could be controlled by adjusting its temperature and was not the result of some time-dependent effect in the stream of crystals or elsewhere. Although it could not be tested whether the crystals were at all charged before encountering the probe, the fact that the probe could be charged either negatively or positively showed that the charge imparted to the probe by the colliding crystals was not solely due to the crystals being initially charged.

Inspection of the probe after a few readings had been taken showed that some of the crystals had adhered to the probe, forming a very thin smooth white layer on the probe ice. Hosler and Hallgren (1960) measured the fraction of crystals which adhered to probes of similar size to this, and applying their results, it would be expected here that less than 10% of the impinging crystals adhered to the ice. Consequently the effect was not considered likely to affect quantitative estimates to an appreciable extent. However, the adhering crystals may be of significance in that they altered the surface structure of the probe which might give rise to the additional electric effects

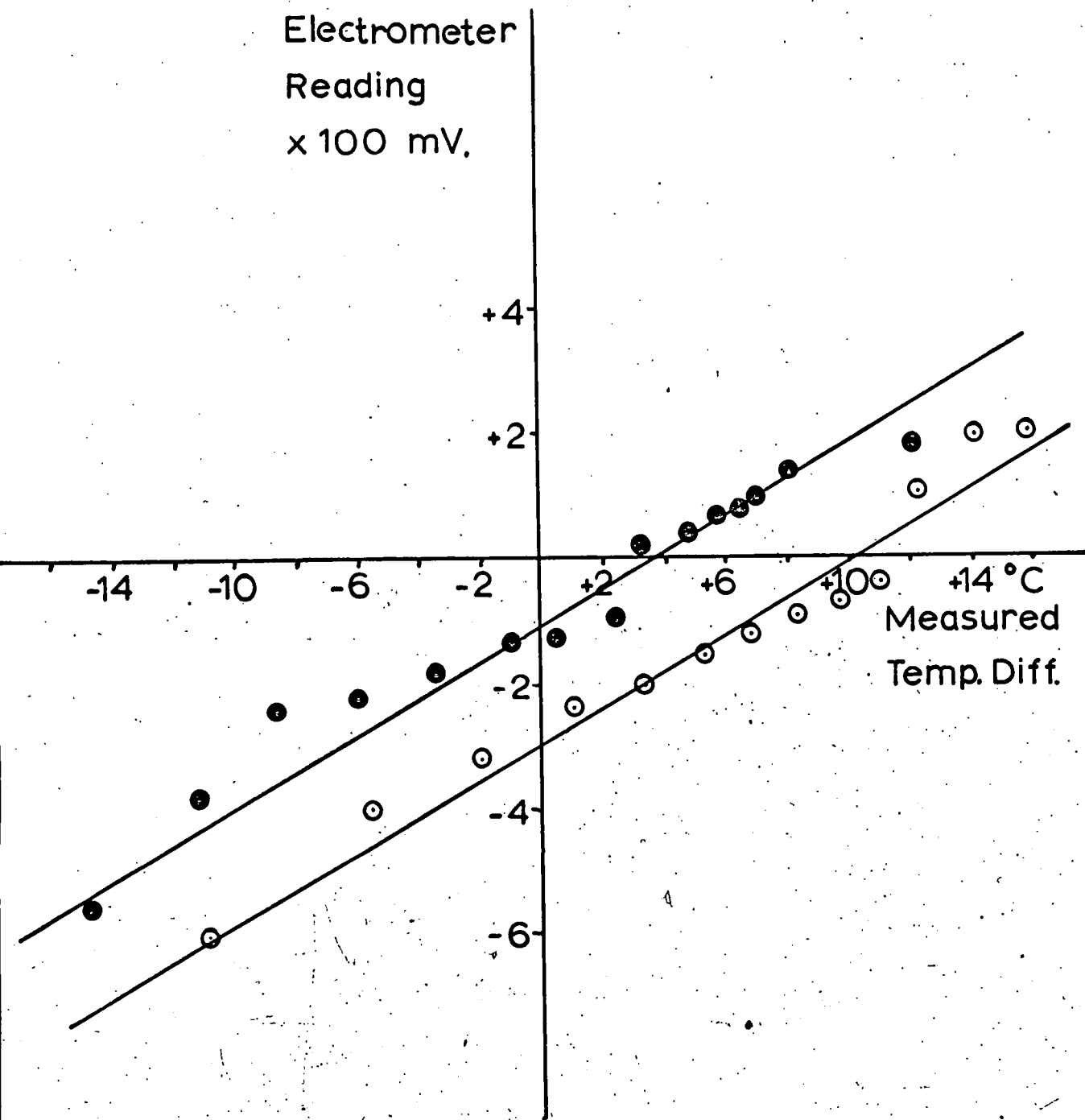


Fig.16 Preliminary Measurements on the Variation of Charging with Temperature Difference.

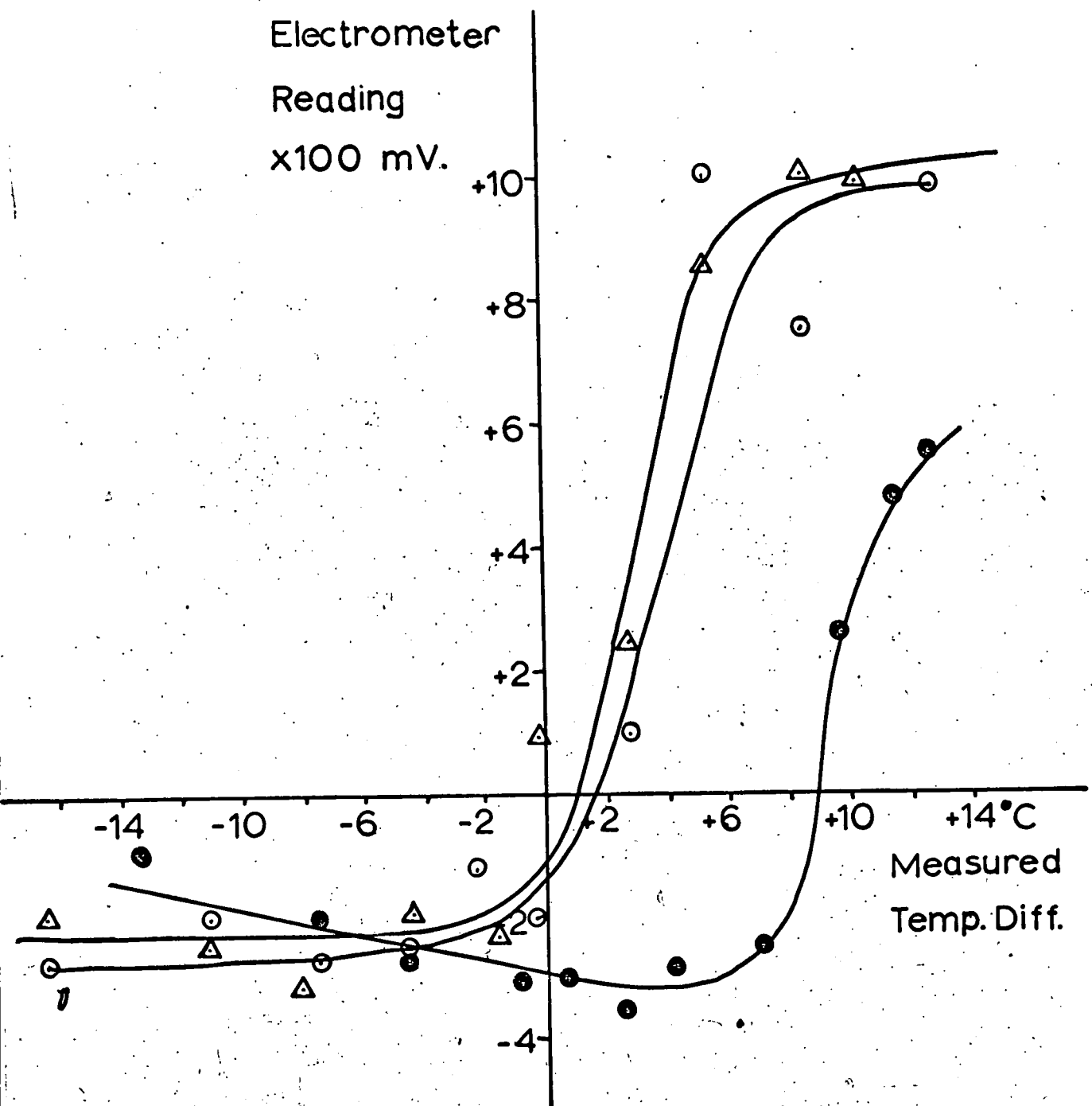


Fig.17 Variation of Charging with Temperature Difference when Further Precautions Taken.

observed by Magono and Takahashi (1963).

(v) Semi-quantitative Results (Box 1)

Two different sets of results were obtained because the first measurements were taken before it was realised that it was necessary to take steps to maintain a constant crystal concentration between successive readings. The first measurements to be taken indicated a linear variation of the rate of charging with the temperature difference, as can be seen in the two sets of results plotted on Fig. 16. The lines do not go through the origin but show a bias towards negative charging.

When precautions were taken to ensure constant crystal concentrations, the results were very different. Three sets of readings are shown in Fig. 17. These results show that starting with the probe warmer than the crystals the rate of negative charging remained fairly constant over a wide range of measured temperature differences and that the rate of charging of the probe suddenly changed from negative to positive, from one reading to the next. After the next one or two readings the rate of positive charging had become constant for successive measurements in the same manner as the negative charging, except that the magnitude of the positive charge separated was greater. The implication of these results is that when a stream of air at one temperature was directed at the probe at a different temperature, the surface of the probe approached the temperature of the air too rapidly for the observed electrification to be related to the initial temperature difference, and that the observed

rates of charging above correspond to small temperature differences.

It has already been explained that the results shown above were only semi-quantitative because the impact velocity of the crystals was not accurately known. Quantitative estimates are made in the following section.

(vi) Quantitative Results (Box II)

TABLE 8.

Measurements of the Negative Charging of the Probe by Ice Crystals.

Rate of Charging (mV)	Probe Temperature (°C)	Crystal Temperature (°C)	Temperature Difference (°C)	No. of Crystals Caught on 700 $\mu$ square.	Exposure Time (sec.)
- 8.5	- 8.4	-19.0	10.6	560	3.0
- 6.5	- 9.6	-19.8	10.2	700	3.5
-10.0	-14.6	-23.4	8.8	640	1.6
-28.0	-14.6	-25.2	10.6	800	1.0
-20.5	-12.6	-25.4	12.8	740	1.5
-12.5	-12.0	-26.3	14.3	640	2.3
- 5.0	-11.4	-23.5	12.1	700	3.0
-10.0	-12.3	-21.8	9.5	640	1.1
-18.0	- 8.7	-20.5	12.8	540	1.5
- 6.0	- 9.2	-20.1	10.9	380	2.9
- 4.0	-10.0	-13.4	3.4	400	3.5
- 6.0	-10.0	-21.0	11.0	260	2.0



TABLE 9.

Measurements of the Positive Charging of the Probe by Ice Crystals.

Rate of Charging (mV)	Crystal Temperature (° C)	Temperature Difference (° C)	No. of crystals caught on 700 $\mu$ square	Exposure time (sec).
+17.5	-26.8	6	1000	1.6
+36	-25.6	9	1500	1.5
+40	-20.4	12	880	1.0
+34	-22.8	10	400	1.3
+30	-20.4	12	580	2.0
+28	-21.8	11	1500	1.5
+ 6	-21.6	11	1200	2.2

The temperature of the probe was maintained constant between -31 and -33° C. The calculation was performed as follows:

The number of crystals encountering the probe every second is  $\frac{A}{a} \cdot \frac{N}{t}$  where A is the area of the probe and N is the

number of crystals which fell on a sampling area a in time t.

This causes a charge separation of  $3V \times 10^{-4}$  e.s.u.  $\text{sec}^{-1}$  where V is the electrometer deflection in millivolts.

Hence the average charge separated per crystal collision is  $3 V \times 10^{-4} \frac{a}{A} \cdot \frac{t}{N}$  e.s.u.

Substituting the results of Table 8 in this expression gives the mean charge separated per crystal collision to be  $(2.2 \pm 0.3) \times 10^{-7}$  e.s.u. The results of Table 9 give the estimate as  $(3.0 \pm 0.8) \times 10^{-7}$  e.s.u.

The average result is therefore that when ice crystals of mean diameter  $20 \mu$  collide with a simulated hailstone at  $20 \text{ m sec}^{-1}$ , the mean charge separated per crystal collision was  $(2.5 \pm 0.5) \times 10^{-7}$  e.s.u. The corresponding measured temperature difference was approximately  $10^\circ \text{ C}$ .

(vii) Summary.

It was shown that the electrification of the probe was caused by collisions with ice crystals and not by the passage of cold air. It should be mentioned here that it has not been proved that the charging was solely due to ice crystals rebounding from the probe; there may be other processes which cause a separation of charge and which depend upon the presence of ice crystals, for example the tearing-off of ice crystals which have adhered to the surface. It was also shown that whether the probe became charged positively or negatively by the ice crystals was determined solely by the surface temperature of the probe. The first results apparently showed that the magnitude of the charge separated varied linearly with temperature, but when greater care was taken over the experimental technique, it was shown in Fig. 17 that the magnitude of the charging was independent of the measured temperature difference and that the changeover from

charging of one sign to the other occurred rapidly. This implied that only a small temperature difference was operative while these measurements were being made, and this was substantiated by the results of Table 10 in which a stream of ice crystals was blown past the probe for 100 seconds, and the electrometer deflection was noted every 10 seconds. These results

TABLE 10.

Variation of the Negative Charging of the Probe with Time.

Time (sec)	0	10	20	30	40	50	60	70	80	90	100
Rate of	10	9	9	9	12	14	12	11	12	14	
Charging (mV)	15	9	9	9	8	8	8	12	11	13	15

could similarly have been obtained for positive charging of the probe. They show that the rate of charging after 100 seconds when the temperature difference must have been very small was approximately the same as the initial rate of charging.

The mean charge separated per crystal collision was found to be  $2.5 \times 10^{-7}$  e.s.u. and although the initial temperature difference was measured as being about  $10^{\circ}$  C, it appears that the actual effective value may have been much less. The charge estimate is greater than that of Latham and Mason by a factor of 50, and the significance of this is discussed at the end of this chapter.

#### 4. VARIATION OF CHARGING WITH IMPACT VELOCITY.

##### (a) Introduction.

A method was devised whereby the velocities of the ice crystals were increased without increasing the rate at which they collided with the stationary probe. The principle was to cool air from a cylinder, mix it with the air stream containing ice crystals and to blow the mixture past the probe. The velocity of the ice crystals was increased simply by increasing the supply of dry air.

##### (b) Experimental.

###### (i) Modifications to Apparatus.

A 4 cm internal diameter brass tube, 60 cm in length was welded to the side of the main tube, and attached by a 25 mm diameter rubber pipe to another brass tube of 5 cm internal diameter and 90 cm long, which lay on the floor of the refrigerator. This latter tube was connected via a flow-meter to a cylinder of dry air.

###### (ii) Procedure.

It was first of all shown that after dry air from the cylinder had passed through the tubes and reached the main tube it had attained the temperature of the refrigerator, which was about 4° C warmer than the crystals. This showed that the temperature of the crystals was not greatly affected by mixing in the dry air. In the first set of readings the smooth iced probe was maintained at the same temperature as its surroundings i.e. -9° C. A stream of ice crystals was blown past

the probe at  $20 \text{ m sec}^{-1}$  and the first reading was taken when no dry air was mixed with the air stream containing crystals. After the electrometer deflection had been noted the dry air supply was turned on and adjusted until its flow-rate was equivalent to an air velocity of  $10 \text{ m sec}^{-1}$  at the exit tube. The deflection corresponding to this impact velocity of  $30 \text{ m sec}^{-1}$  was taken, and the procedure was repeated with dry air velocities of 20 and  $40 \text{ m sec}^{-1}$ , thus giving crystal impact velocities of up to  $60 \text{ m sec}^{-1}$ . In the second set of readings, the probe was cooled down to about  $-30^\circ \text{ C}$ . When crystals were blown past the probe positive charging of the probe was recorded. Readings were taken as above for impact velocities in the range 20 to  $60 \text{ m sec}^{-1}$ . Each set of readings was taken as quickly as possible, and a complete set of four readings could be taken in 5 to 10 sec. Several sets were taken and are shown in Tables 11 and 12.

(iii) Results.

TABLE 11.

Enhancement of the Negative Charging of the Probe by increasing the Impact Velocity of the Ice Crystals.

Impact velocity ( $\text{m sec}^{-1}$ )	20	30	40	60
Rate of charging of probe (mV)	18	50	150	380
	20	95	170	300
	15	50	90	160
	10	40	100	150
	11	35	85	170
	5	16	24	40
	3.5	15	35	30
	0.4	1.4	2.9	7.0

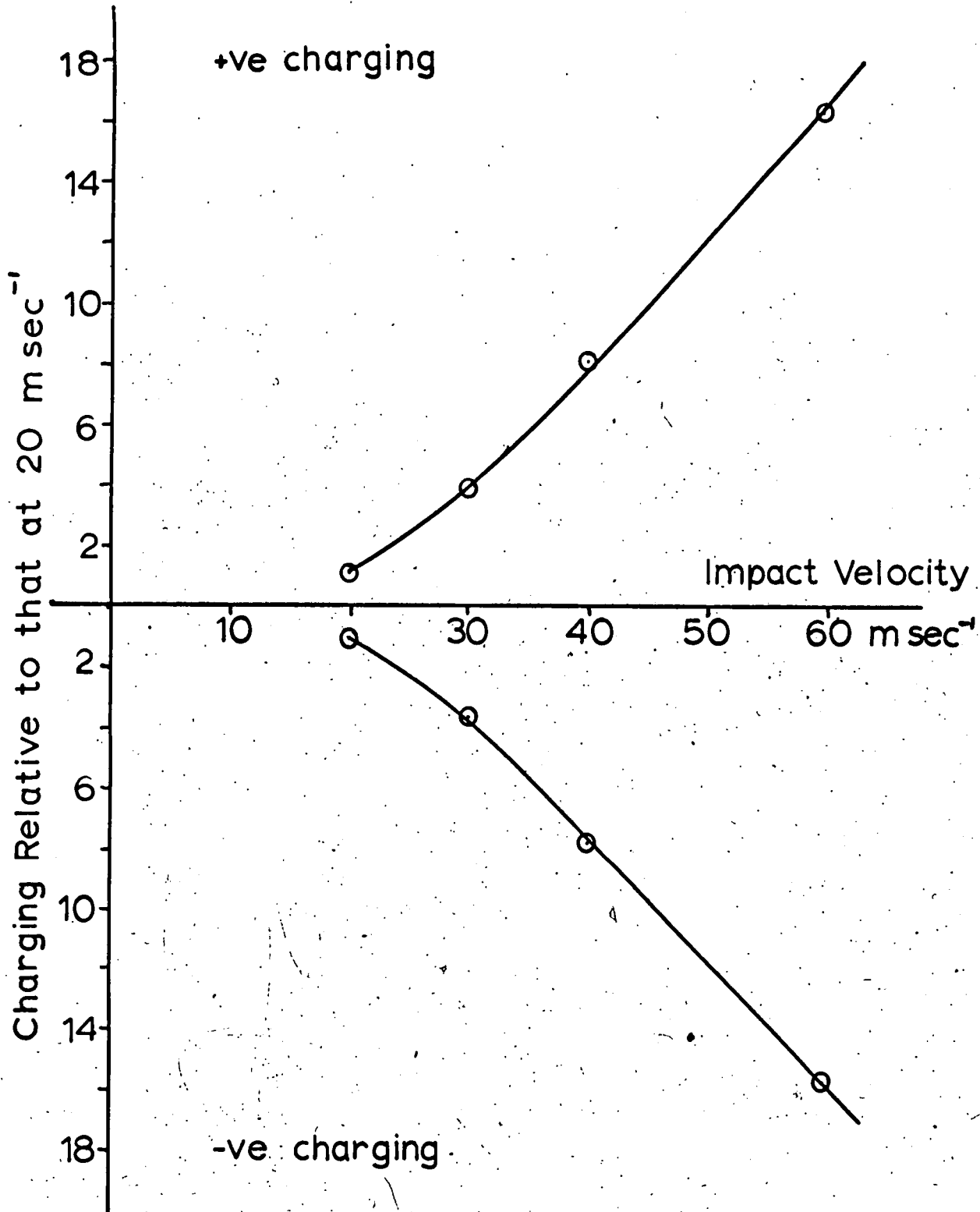


Fig.18 Variation of Charging with Impact Velocity.

TABLE 12.

Enhancement of the Positive Charging of the Probe by increasing  
the Impact Velocity of the Ice Crystals.

Impact velocity (m sec <sup>-1</sup> )	20	30	40	60
	30	130	280	700
	20	60	130	320
Rate of charging	10	60	150	340
of probe (mV)	8	55	120	220
	60	140	280	400
	120	340	550	840
	130	350	600	1000
	120	300	580	920

For each set of readings in Tables 11 and 12, each reading was expressed as a ratio relative to the rate of charging at 20 m sec<sup>-1</sup>. The averages of these ratios are given below in Table 13, and are plotted in Fig.18.

TABLE 13.

The Enhancement of the Charging of the Probe relative to an Impact  
Velocity of 20 m sec<sup>-1</sup>.

Impact Velocity (m sec <sup>-1</sup> )	20	30	40	60
Averages for Positive Charging	1.0	3.8	8.0	16.2
Averages for Negative Charging.	1.0	3.6	7.8	15.7

(iv) Discussion.

The results have shown that when the probe was being charged negatively by ice crystals, increasing their impact velocity increased the rate of negative charging, and similarly the positive charging of the probe was enhanced by increasing the impact velocity of the ice crystals. There was a very marked dependence of charging on impact velocity, and it can be seen that increasing the impact velocity from 20 to 60 m sec<sup>-1</sup> caused the rate of charging to increase by a factor of 10. Table 13 shows that there is a remarkable correspondence between the average values for charging of both signs, which is better than would have been expected from Tables 11 and 12. These results are an extension of the work of Latham and Stow (1965 B) and Latham and Miller (1965). Latham and Stow showed that when ice specimens impacted at 17.5 cm sec<sup>-1</sup> the charge separated was about three times higher than would have been expected from the temperature gradient theory. Latham and Miller measured the electrification of an ice sphere by ice crystals in the velocity 4 to 20 m sec<sup>-1</sup>, and showed that between 10 m sec<sup>-1</sup> and 20 m sec<sup>-1</sup> the average charge separated per crystal collision increased by a factor of about 5. The present results indicate that between 30 m sec<sup>-1</sup> and 60 m sec<sup>-1</sup> the average charge separated increases by a factor of 4.2, which is quite close to the value of Latham and Miller, although rather different from the factor of 2.5 derived from the results of Latham and Stow for an increase in velocity from 10 to 20 cm sec<sup>-1</sup>. The results for crystal impact velocities in the range 20 to 60 m sec<sup>-1</sup> may not have



very much significance in themselves to atmospheric problems but they have served to substantiate the results of other workers and have also indicated that the magnitude of the charge separated is not explicable solely in terms of the temperature gradient theory.

## 5. EFFECT OF CONTAMINANTS ON ELECTRIFICATION.

### (a) Introduction.

In order to determine whether there was any difference in the electrification produced by crystals impacting on a probe coated with pure ice and a probe coated with contaminated ice, two probes were exposed simultaneously to the same stream of crystals. One probe was coated with the pure water and the other with various dilute solutions. The solutions used were sodium chloride in concentrations of 10 and 100  $\text{mgm l}^{-1}$ , and  $10^{-3}$  N and  $10^{-4}$  N nitric acid.

### (b) Preparation of the Ice Surface.

The contaminated ice layer was formed by putting a small amount of the solution on to the probe and dipping it into liquid nitrogen. This procedure was repeated until the probe was uniformly coated. It was necessary that the solution should be frozen on to the probe rapidly because slow freezing would have resulted in a higher concentration of impurity in the outer ice layer. Charging measurements were then made by two different methods.



(c) First Method.

(1) Procedure.

In the first method the electrification of both probes was measured on the same electrometer. Some sets of readings were taken with the probe initially at  $-9^{\circ}$  C, which was the temperature of the surrounding air, and others were taken with the probe initially  $-30^{\circ}$  C. Crystals were blown past the probe for a few seconds each minute. The probes were connected alternately to the electrometer for two-minute periods, readings being taken at one-minute intervals. The results which are shown in Tables 14 and 15 are for a solution containing  $100 \text{ mgm l}^{-1}$  of sodium chloride. The readings in Table 16 were taken when both probes were coated with pure ice, and show the correlation between successive readings. The reason why successive readings for the same probe are different is that the precautions mentioned in 2(c) for maintaining constant crystal concentrations were not observed here.

(ii) Results.

TABLE 14.

The Positive Charging of the Pure and Impure Ice Probes.

Time (min)	0	1	2	3	4	5	6	7	8	9
Reading for Impure Ice (mV)	40			18	16			8		
Reading for Pure Ice (mV)		50	36			18	13			
Impure Ice	45			22	14			8		
Pure Ice		31	25			15.5	9			
Impure Ice	9			5.5	5			3.5	2.5	
Pure Ice		11.5	7			5.5	6.5			3.5
Impure Ice	24			20	19			15		
Pure Ice		29	26			18	18			
Impure Ice	32			27	26			14	13	
Pure Ice		40	30			25	18			13
Impure Ice	48			34	24			15	9	
Pure Ice		58	36			32	16			8

TABLE 15.

The Negative Charging of the Pure and Impure Ice Probes.

Time (min)	0	1	2	3	4	5	6	7	8
Reading for Impure Ice (mV)	16			14.5	7.5			5	
Reading for Pure Ice (mV)		13	7			4.5	2.5		
Impure Ice	50			12	8			10	
Pure Ice		25	9			6	3		

TABLE 16.

The Correlation of Two Identically Coated Probes.

Time (min)	0	1	2	3	4	5	6	7	8	9	10	11
Probe 1 (mV)	18.5	16.5			17.5	15.0			11.5	10.0		
Probe 2 (mV)			18.0	16.0			15.5	13.0			10.5	9.0

(iii) Discussion.

Although the results were very erratic it can be seen in general that the presence of  $100 \text{ } \mu\text{gm } \ell^{-1}$  of sodium chloride in the ice reduces the charging of the probe when the probe is colder than the crystals

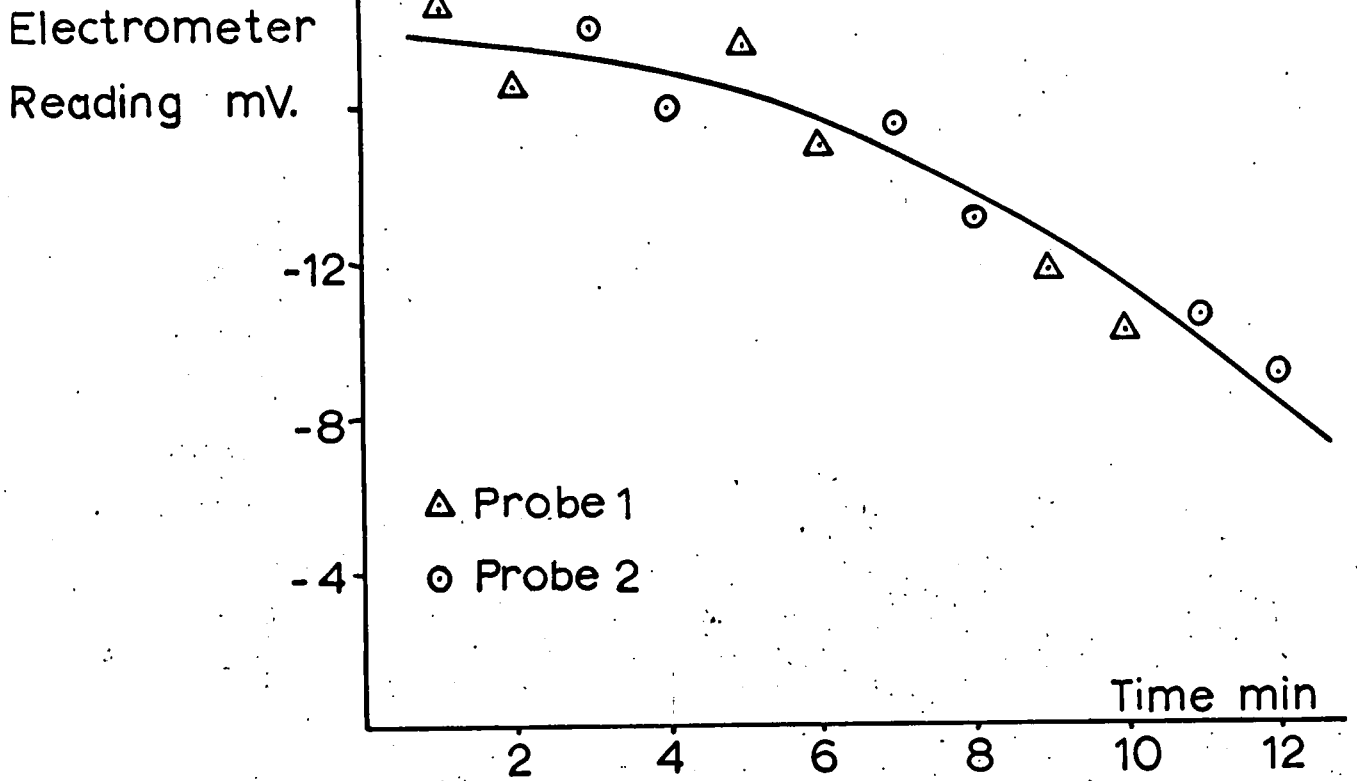


Fig.19.1 Correlation of Identical Probes.

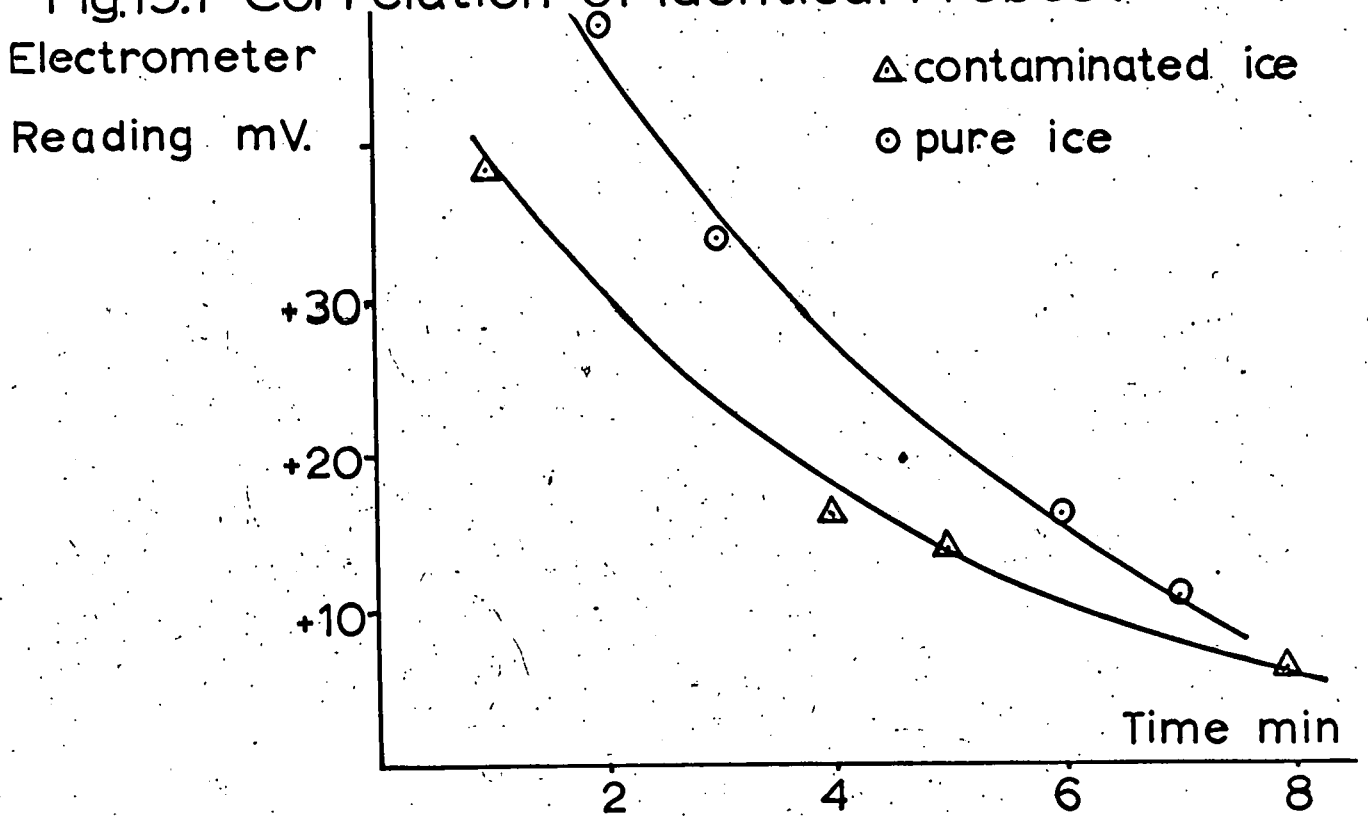


Fig.19.2 Comparison of Pure and Impure Iced Probes.

and that it increases the charging when the probe is warmer than the crystals. This conclusion was supported by graphical comparison with the observed correlation of the successive deflections of both probes contaminated with pure ice. The results of Table 16 were plotted in Fig. 19.1, and the first set of readings in Table 14 were plotted in Fig. 19.2. Fig 19.1 shows that even with identical ice surfaces the readings show quite a large scatter. However if the readings obtained from one probe were systematically different from the readings of the other probe, it would have been possible to draw one curve through each set of readings for each probe, thereby producing two separate curves. It was not possible to draw two curves through the distribution of points shown in Fig. 19.1 and so only one was drawn. This indicated that no difference could be detected in the magnitude of the electrification of each probe. Fig. 19.2 is a different matter. It shows that a single smooth curve cannot be drawn through all the points and that the distribution favours the construction of two smooth curves showing a systematic difference in the magnitude of the electrification of each probe. It was therefore concluded from Fig. 19.2 that when the probe was colder than the crystals the rate of positive charging of the probe was reduced by the presence of sodium chloride in a concentration of 100 mgm  $l^{-1}$ . It can also be seen from Table 15 that when the probe was warmer than the crystals, the rate of negative charging of the probe was increased by the presence of sodium chloride.

(d) Second Method.

(i) Procedure.

In the second method each probe was attached to a separate electrometer and readings were recorded simultaneously as it was thought that this would show the differences in the rates of charging of the probes in a more definite manner. Although both electrometers had nominally the same resistances in parallel, one had a tolerance of 1% and the other of 20% , and they showed different readings for the same input voltage. In order to eliminate this difference and also the possibility of the probes having different surface areas, the connections of the probes to the electrometers were interchanged after a number of readings had been taken. The results are shown in Tables 17 and 18.

(ii) Results.

TABLE 17.

Simultaneous Measurements of the Negative Charging of the Ice Probes.

Time (min)	0	1	2	3
Impure Probe Reading (mV)	10	28	11	16
Pure Probe Reading (mV)	10	20	8	12
As above but with the connections to the electrometers interchanged.	4	5	6	7
	50	19	8	10
	25	9	6	3

TABLE 18

Simultaneous Measurements of the Positive Charging of the Ice Probes

Time (min).	0	1	2	3
Impure Probe Reading (mV)	8	3	2	2
Pure Probe Reading (mV)	16	3	6	4.5
As above but with the connections to the electrometers interchanged	4	5	6	
	4	2	1.5	
	12	4	3.5	

In each of the above pairs of measurements, the reading for the impure probe I was divided by the reading for the pure probe P.

The average value of the ratio  $I/P$  was evaluated for both Table 17 and Table 18.

For negative charging the average value of  $I/P$  was  $\underline{1.64 \pm 0.26}$

For positive charging the average value of  $I/P$  was  $\underline{0.44 \pm 0.06}$

(iii) Discussion.

The results of simultaneous measurements have shown that when a probe was warmer than the ice crystals the rate of negative charging was increased by about 60% when sodium chloride in a concentration of 100 mgm  $l^{-1}$  was present, and the rate of positive charging was reduced by about the same amount.



One undesirable factor was that during each set of readings both probes became coated with a thin layer of ice crystals. The layer of ice crystals was very thin, but the resultant effect must have been to reduce any effect of impurity. To what extent the presence of the layer of crystals masks the impurity effect cannot be estimated, but it can be said that sodium chloride in a concentration of  $100 \text{ mgm } \ell^{-1}$  did not have any dominating effect on the charge separated or this would have been apparent at the beginning of each set of results when the probe ice was not coated with crystals.

(e) Results for other Solutions.

The experimental procedures described above were repeated for solutions containing  $10 \text{ mgm } \ell^{-1}$  of sodium chloride and  $10^{-3}$  and  $10^{-4}$  N solutions of nitric acid.

The results showed that for these solutions no effect of impurity on charging could be detected with any certainty.

(f) General Summary.

Perhaps the most significant conclusion from these results is that the electrification of hailstones by ice crystals is not dominated by the presence of impurities, and that even quite large concentrations of impurity are not sufficient to alter the sign of the charging resulting from the sign of the temperature difference. It was shown that sodium chloride in a concentration of  $100 \text{ mgm } \ell^{-1}$  affected the magnitude of the charging by about 60%, and that the effect of sodium

chloride in a concentration of  $10 \text{ mgm}^{-1}$  could not be detected. Since the concentration of sodium chloride normally found in clouds is  $3.6 \text{ mgm}^{-1}$  it was concluded that the presence of this concentration of impurity would have a negligible influence on the possible charge transfer between ice particles in the atmosphere. The purpose of working with nitric acid was to investigate the observations of Reiter (1965) that the effect of the presence of nitrate ions on electrification was far greater than temperature gradient effects. However, it was later realised in the course of these experiments that experiments in which ice was contaminated with nitric acid were not comparable with Reiter's experiments in which only the nitrate ions were present in the ice. Finally, it was concluded that the experimental techniques described above were not suitable for making accurate quantitative measurements, and that if the effect of contaminants on charge transfer were to be investigated further, other techniques involving contacts between larger ice specimens should be adopted.

6. A DISCUSSION OF THE RESULTS OF REYNOLDS BROOK AND COURLEY,

LATHAM AND MASON, AND THE PRESENT RESULTS.

(a) A Comparison between the Present Results and those of Latham and Mason.

Latham and Mason showed that the sign of the charge separated by ice crystals rebounding from an artificial hailstone could be explained in terms of the temperature gradient theory, and that the magnitude of the charge varied linearly with the measured temperature

difference. The magnitude of the mean charge separated per crystal was found to be  $5 \times 10^{-9}$  e.s.u. for a measured temperature difference of  $5^{\circ}$  C. They also showed that the charge separated per crystal was the same for crystal impact velocities in the range 1 to  $30 \text{ m sec}^{-1}$ , and also that contaminating the probe ice with sodium chloride in a concentration of  $3.6 \text{ mgm l}^{-1}$  had the same effect as heating the probe by a further  $2^{\circ}$  C. The present work was designed to repeat the experiments of Latham and Masen, although there were differences in experimental detail. The results were not the same. It was shown in the present studies that although the charge separation could be explained in terms of the temperature gradient theory, the magnitude of the charge did not vary linearly with the measured temperature difference in spite of very careful precautions. The results illustrated in Fig. 17 indicated that the charge measurements were related to only a small temperature difference, instead of the initially measured temperature difference, and this conclusion was substantiated by the results in Table 10. The value derived for the mean charge separated per crystal collision was  $2.5 \times 10^{-7}$  e.s.u. for a measured temperature difference of about  $10^{\circ}$  C and a crystal impact velocity of  $20 \text{ m sec}^{-1}$ . It was shown that the mean charge separated varied with the impact velocity, and that the charge separated at velocities of  $60 \text{ m sec}^{-1}$  was about 16 times higher than at  $20 \text{ m sec}^{-1}$ . The effect of sodium chloride in a concentration of  $100 \text{ mgm l}^{-1}$  in the probe ice was to cause the negative charging to be enhanced by about 60%, and the positive charging to be reduced by about 60%.

There was no detectable difference for concentrations of  $10 \text{ mgm } \ell^{-1}$  or less.

It may be possible to explain some of the differences by the differences in the probes used in the experiments. The probe used by Latham and Mason consisted of an insulated hollow metal cylinder with a  $\frac{1}{2}$  mm coating of ice. The size of the probe was not specified but judging from Figure 1 in the 1961 B paper, its diameter would seem to be much larger than 5 mm. A small electric heater was situated inside the probe. The probe used in the present experiments consisted of an insulated solid brass cylinder of diameter 4 mm, the temperature of which was varied by conduction along a 12 mm diameter brass rod. Other types of probe had been tried including a 5 mm diameter hollow probe containing an internal heater. Some measurements on the variation of charging with temperature difference had been made using this probe, and it had been concluded from these that the internal heater was not a satisfactory way of maintaining a constant temperature difference between the probe surface and an air stream. The reason for this arises from the fact that the interior of the probe is unventilated, whereas the probe surface is highly ventilated by the air stream. The effect of ventilation is to increase the rate of heat transfer at the surface by a factor which is a function of the Reynolds number of the probe in the air stream. Consequently, to maintain the surface of the probe at a significantly higher temperature than the air stream, the air inside the probe would have to be raised to a high enough

temperature to compensate for the conduction of heat from the ventilated surface. This would mean, however, that the surface temperature of the probe could not be measured, because a thermocouple would be influenced both by the surface temperature and also by the air stream, and if the air stream were turned off, the probe would heat up sufficiently for the ice to melt. It was concluded that the only way a probe containing an internal heater could be operated was to supply the heater with a very small current, so that in the absence of an air stream a steady surface temperature could be achieved and measured. However, upon blowing cold air past the probe, the heat contained in the probe would be rapidly conducted away, and could not be replaced at a sufficiently high rate by the heater. Latham and Mason measured the charge acquired by the probe after drawing crystals past it for 30 seconds, and it would seem that a hollow probe, which was only being heated at a relatively low rate, would approach the air temperature very rapidly and the average temperature difference over the 30 seconds would be very small. It was therefore concluded that a solid brass probe which was heated by conduction from a relatively large mass of brass and which had a greater heat content than the hollow probe, was a more satisfactory means of maintaining a temperature difference between the probe and the air stream. However, even in spite of this, the results shown in Fig. 17 indicated that the surface temperature of the probe varied too rapidly in the presence of an air stream for the measured rate of charging to be related to the measured temperature difference. However the average effective

temperature may have been higher here than in the earlier experiments.

Apart from the construction of the probe, the size of the probe used by Latham and Mason appeared to be larger than the one used in these experiments. Also, the air stream was drawn past the probe in the earlier experiments, whereas here, the air was blown at the probe. It seems likely that these two effects would cause the probe used by Latham and Mason to have a smaller collection efficiency for ice crystals than the one used here, although it cannot be estimated here how small this would be. There is perhaps some evidence for the smaller collection efficiency in that Latham and Mason considered that the structure of their probe was the same throughout, and only observed that crystals adhered to the probe near to the freezing point. In the present experiments, a smooth iced probe soon became coated with ice crystals at all temperatures. This thin layer of crystals may have altered the surface structure of the ice in such a manner as to cause an enhancement of the charging, as was observed by Magono and Takahashi (1963). The fact that Latham and Mason did not detect any difference in the mean charge separated per crystal in the velocity range 1 to 30 m sec<sup>-1</sup> may have been due to the difficulty in obtaining accurate Formvar replicas of the numbers of crystals at the higher velocities and also to the collection efficiency of the probe becoming smaller at the higher velocities.

Latham and Mason showed a greater dependence of the magnitude of the charging on contamination than was shown here. This may

have been because in the present case the effect of impurities was masked by the thin surface layer of crystals. Latham and Mason showed that the presence of sodium chloride in a concentration normally found in clouds had an electrical effect equivalent to heating the probe by  $2^{\circ}$  C, whereas it was concluded in the present experiments that the effect of such small quantities of contaminant could not be detected.

In the above discussion an attempt has been made to describe some of the differences between the present work and that of Latham and Mason, in an attempt to reconcile the difference in the estimates for the separation of charge. To summarise, the differences which are considered to account for the value of Latham and Mason being less by a factor of 50 than the value obtained here are the size, surface structure and method of heating of the probe, and the method of causing crystal impacts. Unfortunately, only one of these, the effect of surface structure, can be evaluated quantitatively, and from the results of Magonc and Takahashi, this would account for a factor of 6. Numerical estimates cannot be made of the other quantities because of insufficient information, and it can be only suggested that their combined effect is to account for the remaining factor of 8.

(b) The Results of Reynolds, Brook and Gourley, Latham and Mason,  
and the Present Results.

The estimate of the average charge separated per crystal collision was found by Reynolds Brook and Gourley to be  $5 \times 10^{-4}$  e.s.u. Similar

experiments to theirs were performed in this laboratory, and it was shown that the mean charge separated by the rebounding of ice crystals from a pre-cooled or preheated probe was  $10^{-6}$  e.s.u. when the water droplet, concentration was very low. This value could be augmented to  $5 \times 10^{-6}$  e.s.u. when supercooled water droplets were present, under which condition it was not necessary to pre-heat or pre-cool the probe.

Latham and Mason estimated that the charge separated was  $5 \times 10^{-9}$  e.s.u., whereas the estimate made in this laboratory was  $2.5 \times 10^{-7}$  e.s.u. This value of  $2.5 \times 10^{-7}$  e.s.u. corresponds quite well with the value of  $10^{-6}$  e.s.u. from the previous experiment, bearing in mind that although the impact velocity of crystals in the earlier experiments was half of that in the later experiments, the mean diameter of the crystals was twice as large in the earlier work. It is considered that the values of  $2.5 \times 10^{-7}$  and  $10^{-6}$  e.s.u. were derived from experimental conditions where only very small temperature differences were operative, and it is also considered that this is a part of the explanation of the low values found by Latham and Mason. The complementary part of the explanation has been given in 6 (a).

The advantage of the technique of Reynolds Brook and Courley was that there was continuous heating of the surface of the probe by the freezing of supercooled water droplets, whereas in the case of Latham and Mason the rate of supply of heat must have been small in comparison with the rate of conduction of heat away from the probe surface. It can be said that in the experiments of Reynolds et al



the maximum possible temperature difference between the probe and the crystals was about  $20^{\circ}$  C, but it is a difficult matter to deduce the order of magnitude of the temperature difference which was operative in the experiments of Latham and Mason. It would be unwise to speculate on whether the order of magnitude of the effective temperature difference was 1,  $10^{-1}$  or  $10^{-2}$  ° C.

Returning to the results obtained in this laboratory, a number of factors have been suggested to reconcile the value of Latham and Mason with the value of  $2.5 \times 10^{-7}$  e.s.u. found here. This value corresponds quite well with the value of  $10^{-6}$  e.s.u. found by another method. This value was augmented to  $5 \times 10^{-6}$  e.s.u. when supercooled water droplets were present. Thus, the experimental results in this laboratory gave results which were two orders of magnitude smaller than the estimate of Reynolds, Brook and Gourley. It has been suggested in Chapter 4, that the estimate obtained in this laboratory might have been enhanced if supercooled water droplets could have been supplied to the probe at a greater rate. It was also mentioned that errors in the estimation of crystal concentrations might also be significant.

In conclusion, it has been possible to reconcile the results of Latham and Mason with the results obtained in this laboratory, which were two orders of magnitude less than those of Reynolds, Brook and Gourley. Any attempt to produce closer correspondence than this with these results would be based on speculation. As was concluded at the end of Chapter 4, the results have shown that the sign of the

charge separated by the collisions between ice particles can be explained qualitatively in terms of the temperature gradient theory, but the actual magnitude of the charge separated is much higher.

#### APPENDIX 1.

##### Formvar Slide Technique.

Samples of crystals were obtained using a method originated by Schaefer (1946). Crystal concentrations, forms and sizes were observed by forming permanent plastic replicas of them on microscope slides and viewing the slides under a microscope. A Formvar solution was made up by adding a small quantity of a synthetic plastic resin called polyvinyl formal to ethylene dichloride in a bottle, and shaking vigorously until the solute had dissolved. It was necessary for the ethylene dichloride to be completely anhydrous, otherwise glutinous streaks formed when the liquid was cooled. The bottle of liquid was stored stoppered in the refrigerator. When some replicas were to be made, some Formvar solution was poured into a beaker and a few clean microscope slides were immersed in it and left for a few minutes. Slides were taken out of the beaker and crystals in the cloud fell on to them and became completely immersed in the solution. The slides were left in the refrigerator until the solvent had completely evaporated, leaving a hard plastic film bearing a permanent impression of the ice crystals. Slides were then removed, and,

after allowing the condensation to evaporate, they were examined under the microscope. The most useful magnification was found to be 150 X.

In order to obtain satisfactory results, it was necessary to observe the following precautions:-

1. The concentration of the solution was quite critical. It was found that for small crystals such as were formed here that the ideal concentration was 0.2% by weight of the resin in the solvent. Concentrations weaker than this tended not to wet the glass in a uniform film, and the plastic films which formed at higher concentrations were too thick.
2. The temperature of the solution was also very important. If it were too low a uniform film could not form. Solutions were kept at the raised end of the refrigerator compartment at about  $-8^{\circ}$  C.
3. Care was taken to prevent dust and ice particles from falling into the solution because these caused a glutinous suspension to form. Also the liquid collected preferentially around dust particles on a slide.
4. The solution standing in the beaker evaporated quite quickly and was replaced every two or three days to ensure that the correct concentration of solution was maintained.

Kobayashi's (1955) technique of replica production was tried. This consisted of allowing crystals to land on a slide already covered

with a hard plastic film. The slide was placed close to the surface of some cold ethylene dichloride in a beaker, and some of the vapour condensed on the slide, dissolving the plastic film. The crystals became immersed in this solution, which was then allowed to evaporate, leaving behind impressions of all the crystals which had fallen on to the slide. Although this method would have given more accurate quantitative results, it was found to be more difficult to apply than the more direct method. Consequently the latter was adopted.

In later work when it was necessary to sample crystals moving in an air blast, the above precautions did not have to be followed so carefully. For crystals moving at  $10 \text{ m sec}^{-1}$  the ideal concentration of the Formvar solution was found to be in the range 2 - 5%.

Slides were photographed using a Cooke microscope fitted <sup>with</sup> reflex housing for quarter-plate photography. Using Ilford K-40 panchromatic plate, and cutting down the illumination with the green filter, the correct exposure was 15 seconds. Some results are shown in Figs. 20 and 21.

#### Appearance and Sizes of Crystals.

Of the crystals formed from a supercooled cloud in the refrigerator, the majority were imperfectly formed hexagonal plates and they varied infinitely in detail. There were also some prisms which were smaller. Fig. 20 shows a typical selection. Crystals with diameters up to  $100 \mu$  were observed, and the mean size was about  $40 \mu$ . On occasion

very unusual symmetrical plates which did not have a hexagonal shape were formed.

Fig 21 shows the size and type of crystals which were produced in the box cooled with cylinders of solid carbon dioxide. Since the impressions left on the glass sampling rods were not suitable for photography, a coated microscope slide was passed quickly through the stream of crystals, producing the illustrated pattern. It can be seen that there is a considerable variation in sizes and also that there is a greater proportion of prismatic crystals, some almost square in cross-section. It was difficult to assess the average size but this was estimated as  $20 \mu$ .

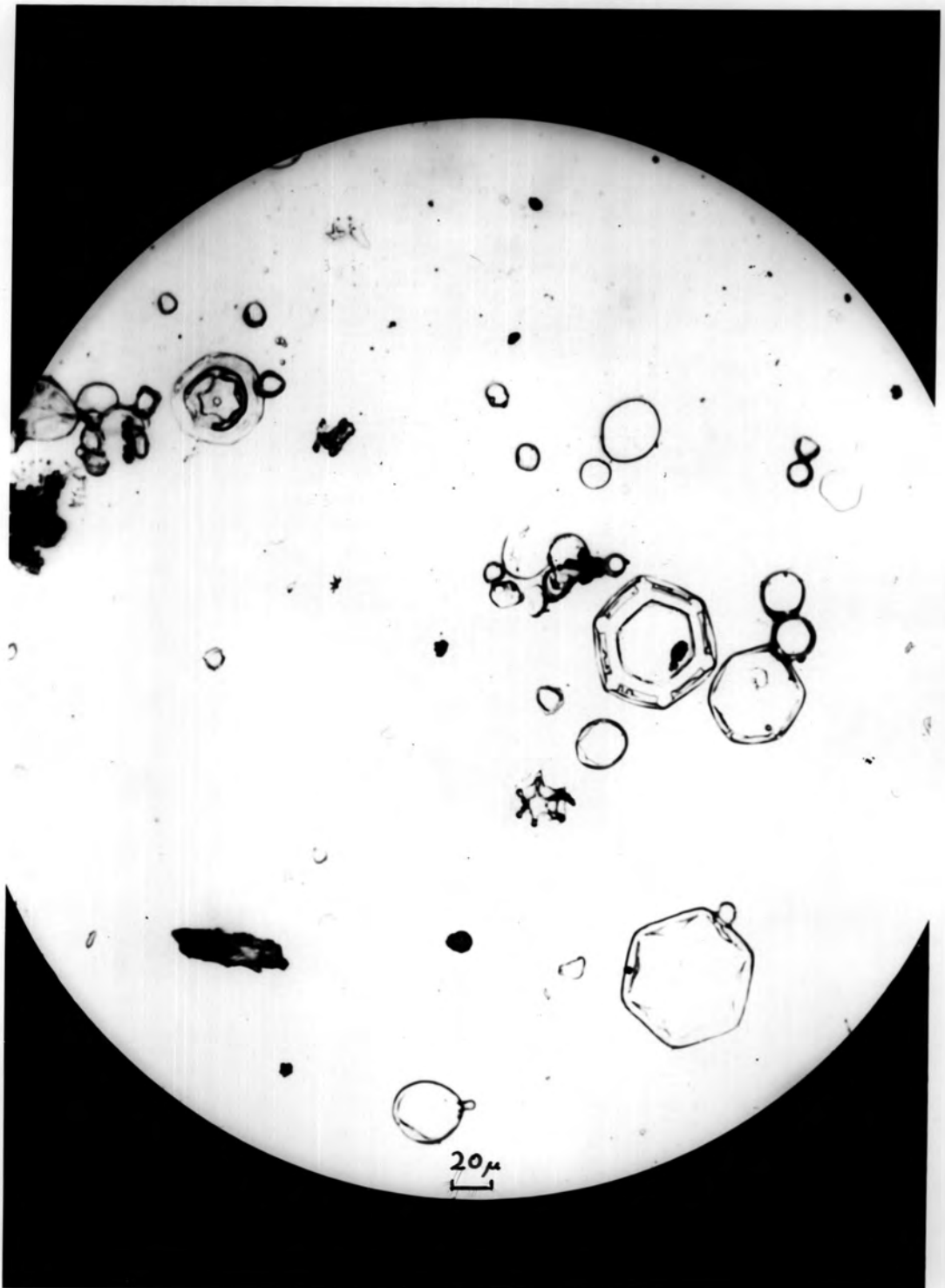


Fig. 20. Examples of Crystals Formed by Seeding a Cloud  
in the Refrigerator.

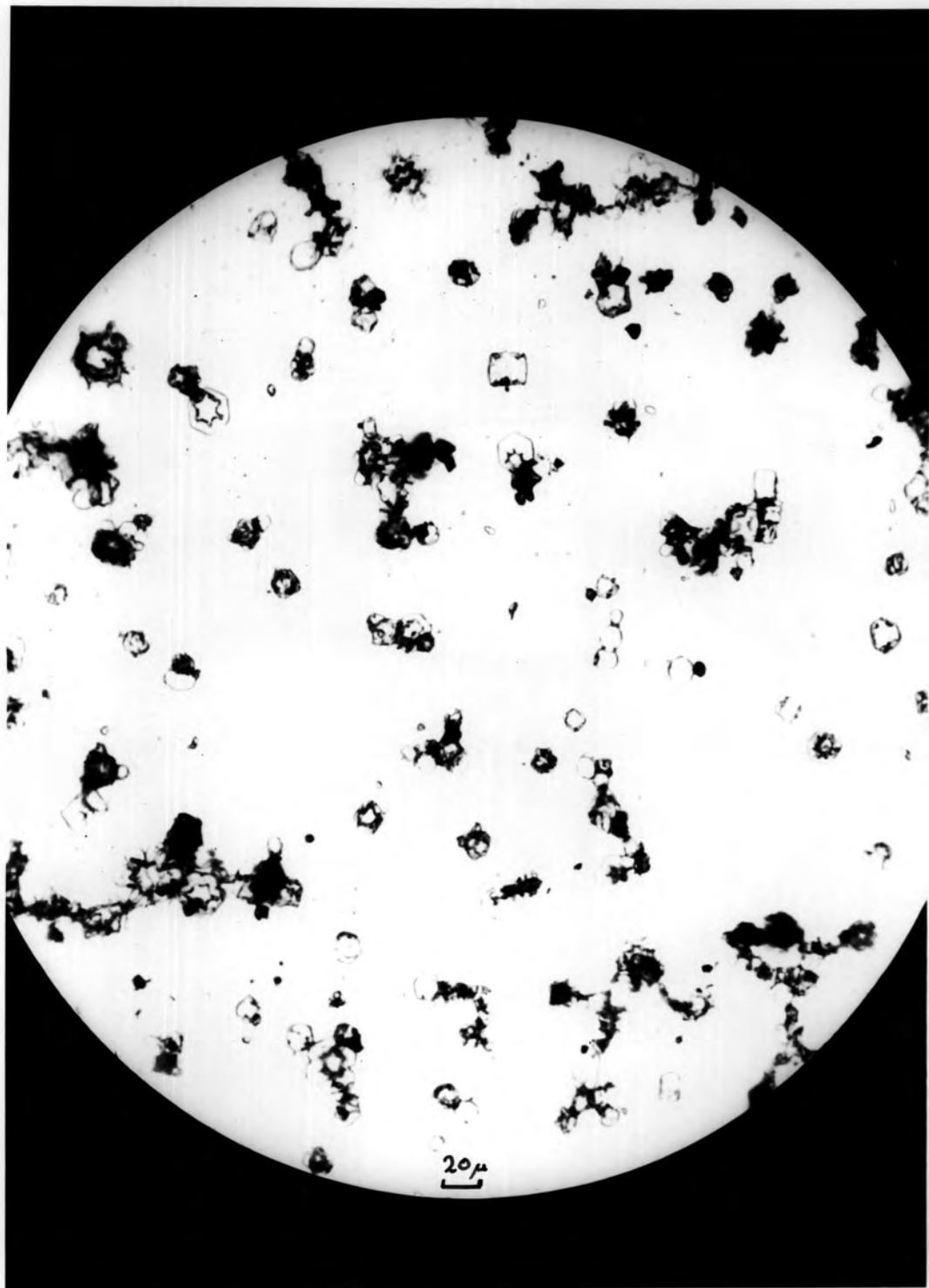


Fig. 21. Examples of Crystals Formed in the Cold Box.

## CHAPTER 6.

### APPARATUS FOR PRODUCING UNIFORMLY SIZED SUPERCOOLED WATER DROPLETS.

#### 1. INTRODUCTION.

Uniformly sized water droplets in the diameter range 50-500  $\mu$  were produced by a vibrating needle device. The droplets, which were ejected horizontally, passed through stabilising tunnels, after which they entered a vertical tube closed at the lower end. There was a temperature inversion of the air in the tube which caused the falling droplets to be cooled.

#### 2. THE VIBRATING NEEDLE DEVICE.

##### (a) Introduction.

This instrument is illustrated in Fig. 22 and Fig. 23. The principle of operation is the same as the model described by Jayaratne, Mason and Woods (1963), from which it differs only in details. Uniformly sized water droplets were produced by exciting a resonance in a fine bore hypodermic needle through which water was being forced. This was achieved by attaching a steel diaphragm to the needle and causing it to vibrate by bring near to it an electromagnet connected to an a.c. supply of the required frequency.

##### (b) Construction Details.

An ordinary glass hypodermic syringe without the plunger was used. A brass tube was welded to the screw cap to enable rubber tubing to be attached. The needle used was of the finest bore



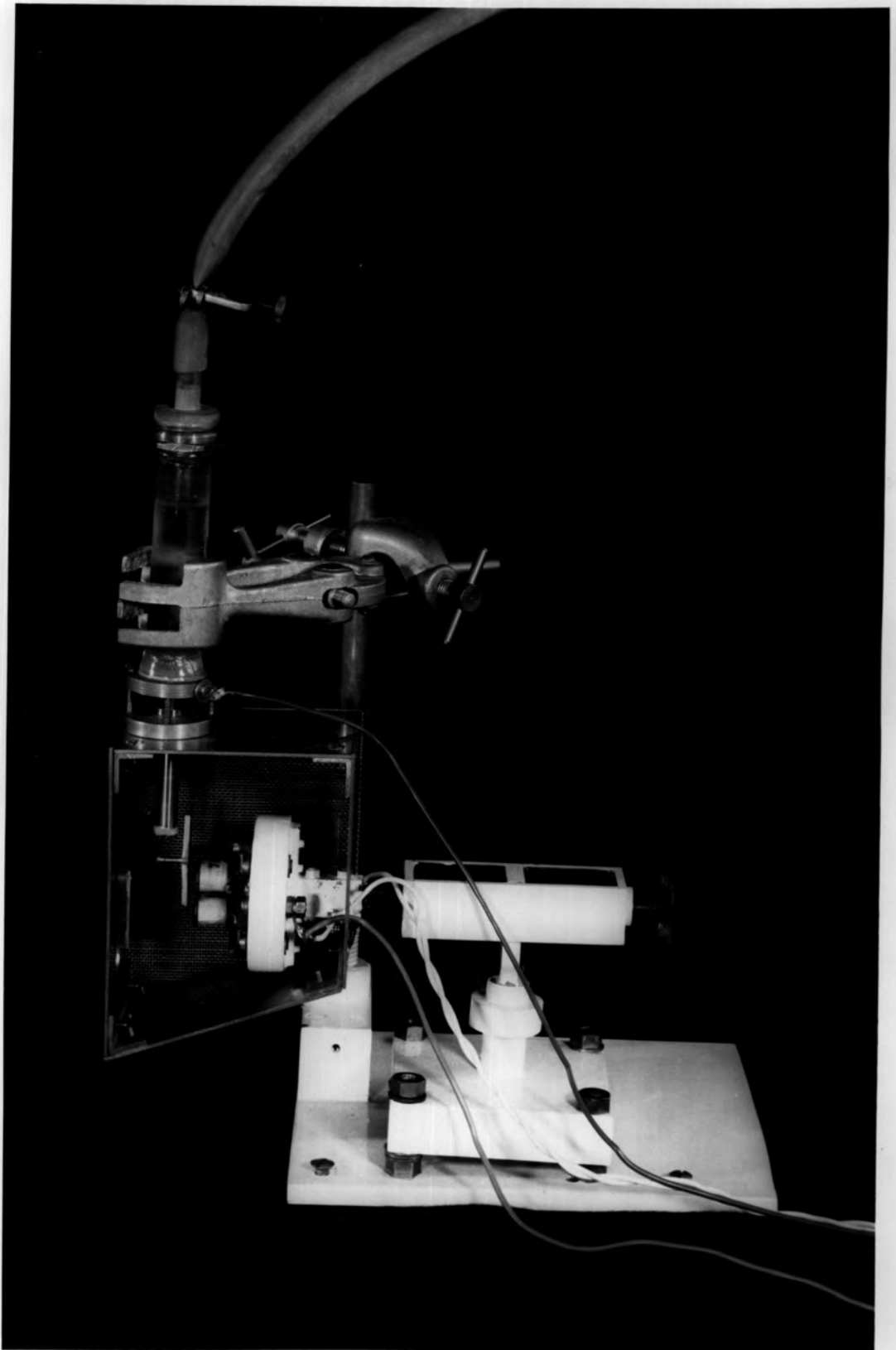


Fig. 22. The Vibrating Needle Device.

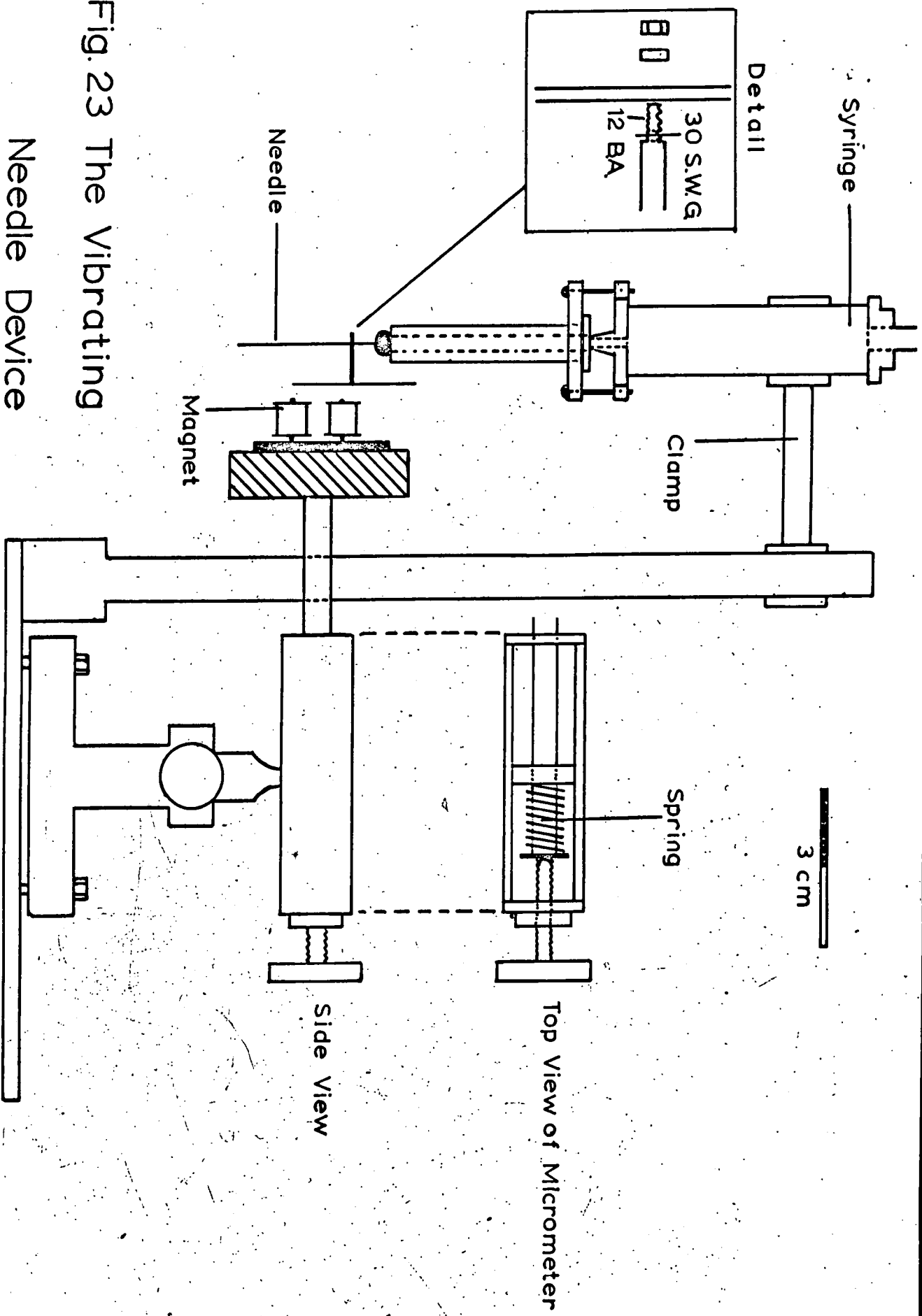


Fig. 23 The Vibrating

Needle Device

available, being 30 S.W.G. 140  $\mu$  diameter bore and 4 cm long. The needle mount was of the Luer type. It was turned down and cemented into a stainless steel tube which was fastened to the bottom of the syringe by a system of collars and 3 cm bolts. This extension gave more room for the attachment of a diaphragm and ensured that the needle could not be forced off by the pressure head. As the diaphragm had to be as light as possible it was made from razor blade steel ground into rectangular shape measuring 3 x 35 mm. It was reinforced with strips of wood and a cylindrical brass cantilever was cemented to the centre, perpendicular to the plane of the diaphragm. The cantilever was 1.5 mm in diameter and of length 11 mm. A 12 B.A. thread was made on the end and a 30 S.W.G. hole was drilled through the end of the cantilever, perpendicular to its length. The hypodermic needle fitted through this hole and the cantilever was tightened on to the needle by a washer and 12 B.A. nut. Details of the fitting are shown in the inset of Fig. 23.

The electromagnet was formerly part of a telephone earpiece. It was attached to the end of a horizontal bar incorporated in a fixed frame. The bar could be moved backwards and forwards by a micrometer screw, but could neither twist about its own axis nor rotate about the vertical. This micrometer device was mounted on a rod having a key-way, which fitted into a socket mounted on the base-plate. This enabled it to be clamped at various heights relative to the base-plate without rotation. This arrangement permitted the necessary degree of movement of the electromagnet relative to the diaphragm. The coils of the

electromagnet had a resistance of 14 ohms and were therefore energised from the low impedance output terminals of an audio oscillator.

The needle and electromagnet were surrounded by an earthed brass cage which, when viewed from the side, was trapezium-shaped for purposes of drainage. The cage was attached to the hypodermic syringe. The sides of the cage were of wire gauze and easily detachable. The purpose of the cage was to screen the needle from external charged bodies which otherwise could have exerted some electrical influence on the needle and caused the droplets to receive spurious charges. Water droplets passed out through a hole in the front panel. There was also a hole in the rear panel which allowed the electromagnet to be moved freely to and fro.

A 12 mm diameter brass rod was fastened perpendicularly to the base plate and the hypodermic syringe was clamped to this and adjusted until the components were in their correct positions. The components of the device were placed as close as possible to the base plate to minimise flexing effects which would have caused a variation in the magnet-diaphragm separation and hence a variation in the amplitude of oscillation of the needle.

(c) Operation of the Vibrating Needle Device.

Before operating the device all glassware and tubing was thoroughly cleaned in an aqueous solution containing 5% hydrogen fluoride, 33% nitric acid and 2% Teepol and then rinsed several times in tap-water and finally in demineralised water. The syringe was then filled

with demineralised water and connected to a large aspirator half filled with the same. The demineralised water had an average conductivity of  $10^{-6}$  ohm<sup>-1</sup> cm<sup>-1</sup>. For the preliminary tests the aspirator was connected to a compressed air supply which gave pressure heads of up to 3 atmospheres. In order to establish the optimum operating conditions of the device a number of tests and consequent adjustments were made. In the first series no water was being passed through the needle.

The electromagnet was connected to the 5 ohm output of an Advance J2B audio oscillator. With the diaphragm approximately 3 to 4 mm from the electromagnet, 5 to 10 volts were applied to the coils and the frequency altered. For particular frequencies the needle tip was caused to oscillate through amplitudes of several mm. The results of the first series of tests are summarised below:

(i) The needle tip oscillated in a straight line provided the cantilever was firmly fixed.

(ii) The resonance was very sharp. Oscillations were completely damped when the frequency was altered by 10 c/s.

(iii) The fundamental resonant frequency of the unloaded needle was 160 c/s. When the needle was loaded with a diaphragm this resonant frequency became somewhat less, decreasing as the mass of the diaphragm increased. However, resonances could be excited at higher frequencies provided the diaphragm was not too massive. The circular diaphragm supplied as part of the earpiece weighed

about 4 gm, and using this, resonances above 100 c/s could not be obtained. The rectangular diaphragm, which has already been described, was constructed so as to be as light as possible. It weighed 540 mgm and worked successfully at frequencies of up to 300 c/s.

(iv) In order to obtain the maximum amplitude of oscillation for a given applied voltage, the vertical position of the electromagnet relative to the diaphragm had to be critically adjusted. The maximum amplitude was obtained when the electromagnet was in the position shown in Fig. 23 .

(v) Resonances were excited in the frequency range 200 to 300 c/s. depending on the position of the point of support of the cantilever on the needle. Contrary to expectation, it was found that the nearer the cantilever was fixed to the needle mount, the lower was the resonant frequency. The lower limit of frequency was about 200 c/s. On fixing the cantilever further away from the mount, the frequency increased, but the system became more compliant and the diaphragm tended to stick to the magnet. The upper limit of frequency was about 300 c/s. A working frequency of  $250 \pm 5$  c/s was decided upon.

In the next series of tests water was forced through the device under various heads of pressure. The break-up of the liquid thread at the needle tip was observed with a stroboscopic lamp. The following observations were noted:

(vi) The resonant frequency increased slightly as the flow rate was increased.

(vii) By critical adjustment of the flow rate and the amplitude of oscillation, single stable streams of uniformly sized droplets of diameters up to  $350 \mu$  could be obtained. More generally, however, several streams of droplets were produced. Their sizes were in the diameter range 50 to  $300 \mu$ . The smallest droplets could not be obtained as stable streams, but occurred as a shower of several unstable streams. Stable streams of droplets down to  $100 \mu$  diameter could be readily selected. Sometimes the smallest droplets did form in stable streams, but these could not be produced at will.

(viii) In order to determine the optimum working pressure, pressures of up to 3 atmospheres were applied. It was found that flow-rates were too high at high pressures and too many streams of droplets were produced. A mercury manometer was inserted in the air line and it was found that the optimum pressure head was 20 to 25 cm of mercury.

(ix) The droplet trajectories were very sensitive to mechanical vibrations of the apparatus and to draughts. From the point of view of vibrations it was seen to be desirable to have the apparatus installed on a rigid support in a ground-floor room. The effect of draughts was eliminated by suitable screening. When these disturbances were eliminated, the positions of the droplets could be completely "frozen" in space in the stroboscopic light for considerable times.

(d) Attempts to Produce Smaller Droplets.

The first method which was tried to produce smaller droplets

was to dip the needle tip in molten wax and to clear the bore with a fine wire. The wax should have reduced adhesion between the needle and the water and this might have caused the production of smaller water droplets. However, this was not observed in practice, and on the few occasions that this method was tried it actually seemed that the wax inhibited the production of small droplets.

The second method was the one used successfully by Jayaratne, Woods and Mason in which a short length of very fine bore steel tubing was inserted into the end of the needle. This was tried in this laboratory with short lengths of steel tubing of internal diameter 50  $\mu$ . This was not successful because of the difficulty of cutting off a short length of tubing without closing the end. It was considered to be an impossible task using conventional workshop tools and the matter was not pursued any further, because of time limitations.

(e) Suggestions for Further Development of the Device.

Smaller droplets could be produced either by increasing the resonant frequency of the needle or by reducing its bore. It might be possible to increase the resonant frequency by putting a wide bore hypodermic needle around the 30 S.W.G. needle.

It would be worth investigating the effect on droplet sizes produced by inserting small lengths of very fine tubing, which may have to be prepared by a commercial company. It should be noted here that if even smaller bores are going to be used, extra precautions will have to be taken to keep the water free of dust particles. It



would also be desirable not to use rubber tubing, as it was observed that small particles sometimes detached themselves and assisted in the blocking of the needle bore.

The effect of the length of the cantilever on the resonant frequency has not been investigated.

Finally, it might be possible to increase the efficiency of the electromagnet by using only one of the coils and by replacing the magnetic iron core by a soft iron core. This might result in a larger amplitude of vibration for a given applied voltage.

### 3. THE OTHER APPARATUS.

#### (a) General Design.

The requirements of the apparatus were that it caused droplets to become supercooled and to impinge on an ice-coated probe at relative velocities of the order of  $10 \text{ m sec}^{-1}$ . Such impact velocities could be achieved either by drawing the droplets past the probe in a stream of air or by allowing droplets falling at their terminal velocities to strike a rotating probe. The first method did not seem to be practicable in this laboratory because of the limited supply of cold air and because of the relatively long thermal relaxation times of the droplets. Consequently it was decided to use a rotating probe and to cool the droplets by causing them to fall into a vertical tube closed at the lower end and standing in the refrigerator. There was a temperature inversion of the air in the tube which caused cooling, and the air in the tube could be cooled further by surrounding the tube with methylated

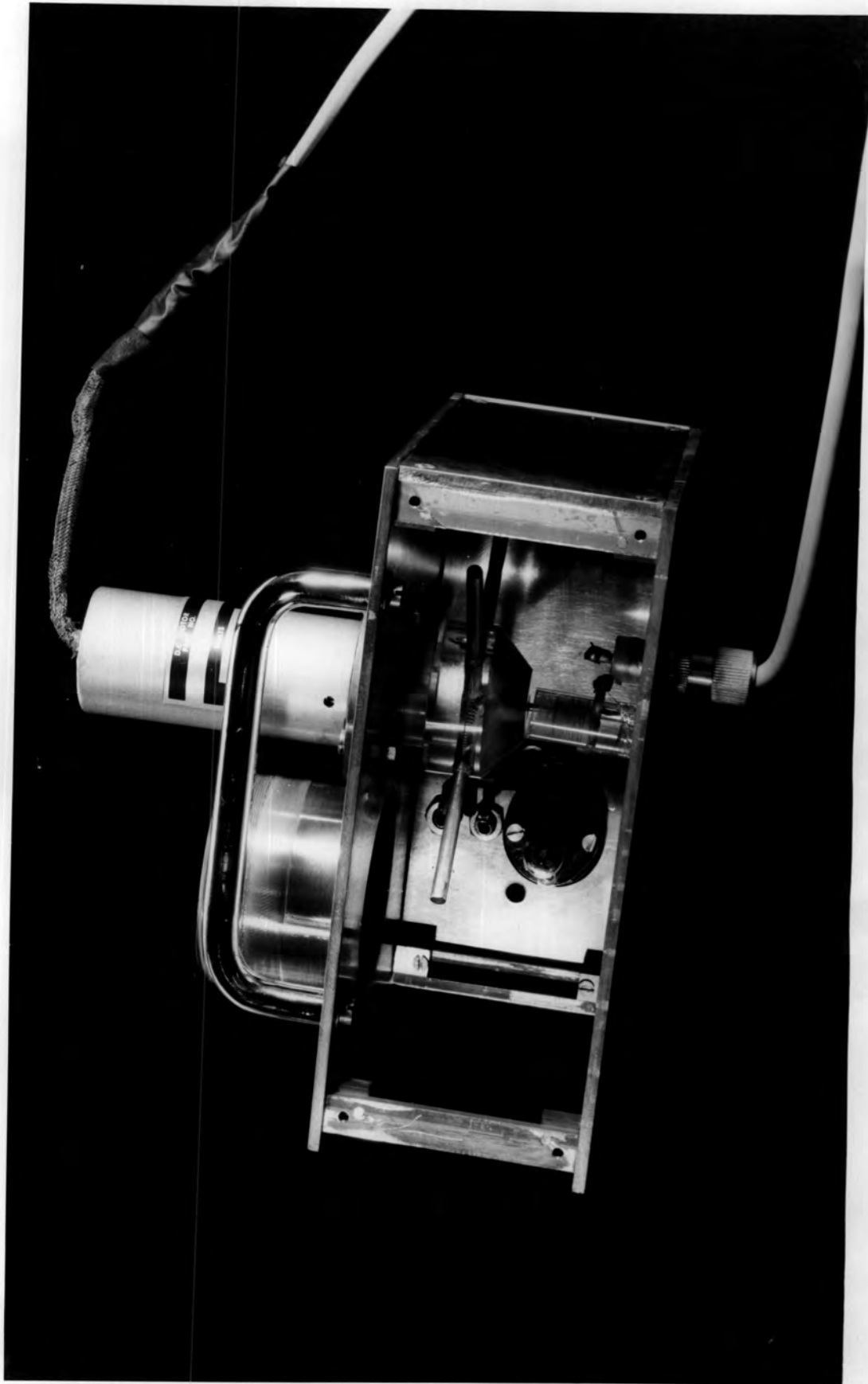


Fig. 24.

The Rotating Probe in its Casing.

spirits chilled with solid carbon dioxide.

(b) The Main Tube.

The main tube consisted of concentric brass tubes of internal diameters 5.7 and 7.7 cm, and 125 cm long. They were welded together at both ends. The tube was lagged and covered with polythene sheet. At the top end was welded an inlet pipe for the refrigerated liquid, and holes for the escaping gas. At the bottom end was welded a short length of brass tubing with a few turns of an internal coarse pitch thread. The tube was held in the vertical position inside the refrigerator by Handy Angle supports which were arranged so as to prevent vibrations of the refrigerator being transmitted to the tube, and also to allow the tube to be removed frequently and still be replaced in the same vertical position.

(c) The Probe.

(1) Construction.

Fig. 24 shows the probe in its brass casing but with two of the panels removed. The probe consisted of four brass rods of 4 mm diameter and length 3.8 cm joined at right angles to a perspex rotor which was attached to a small d.c. motor. The overall diameter of the probe was 11.4 cm. The rods were electrically connected to a vertical pin at the base of the rotor. The pin dipped into a mercury well which was connected to the electrometer circuit. The electrometer circuit was the same as described in Chapter 4. The probe was enclosed in a brass case of overall dimensions 13 x 16 x 7 cm. A

small illumination source was included in the case. The purpose of this was to illuminate the compartment so that the progress of falling droplets could be observed. There was a hole in the top of the case through which droplets fell, and the hole was so positioned that when the probe rotated, the ends of the rods traversed a diameter of the hole. A 4 cm length of brass tube was welded to the top of the casing. Around the top of the tube were two or three turns of a coarse pitch thread which enabled the brass case to be easily screwed on to or unscrewed from the main tube. A handle was provided on the case in order to facilitate this operation.

(ii) Operation.

The probe case was screwed on to the main tube which was earthed. The probe was set in motion and the fluctuation level of the electrometer when on its most sensitive range was observed. The noise level varied from one occasion to the next but was generally  $\pm 0.2$  to  $0.4$  mV. The noise level was greatest at very low temperatures which were obtained when the coolant was used, and sometimes became as high as  $\pm 1$  mV.

The velocity of rotation of the probe was altered by adjusting resistances which were in series with the motor. The speed quoted in the calculations was the speed of the probe tip. Speeds in the range  $5$  to  $20 \text{ m sec}^{-1}$  were used.

(d) The Rest of the Apparatus.

The rest of the apparatus was built on to the top of a cupboard of convenient height, and was thereby situated about  $2\frac{1}{2}$  m above the

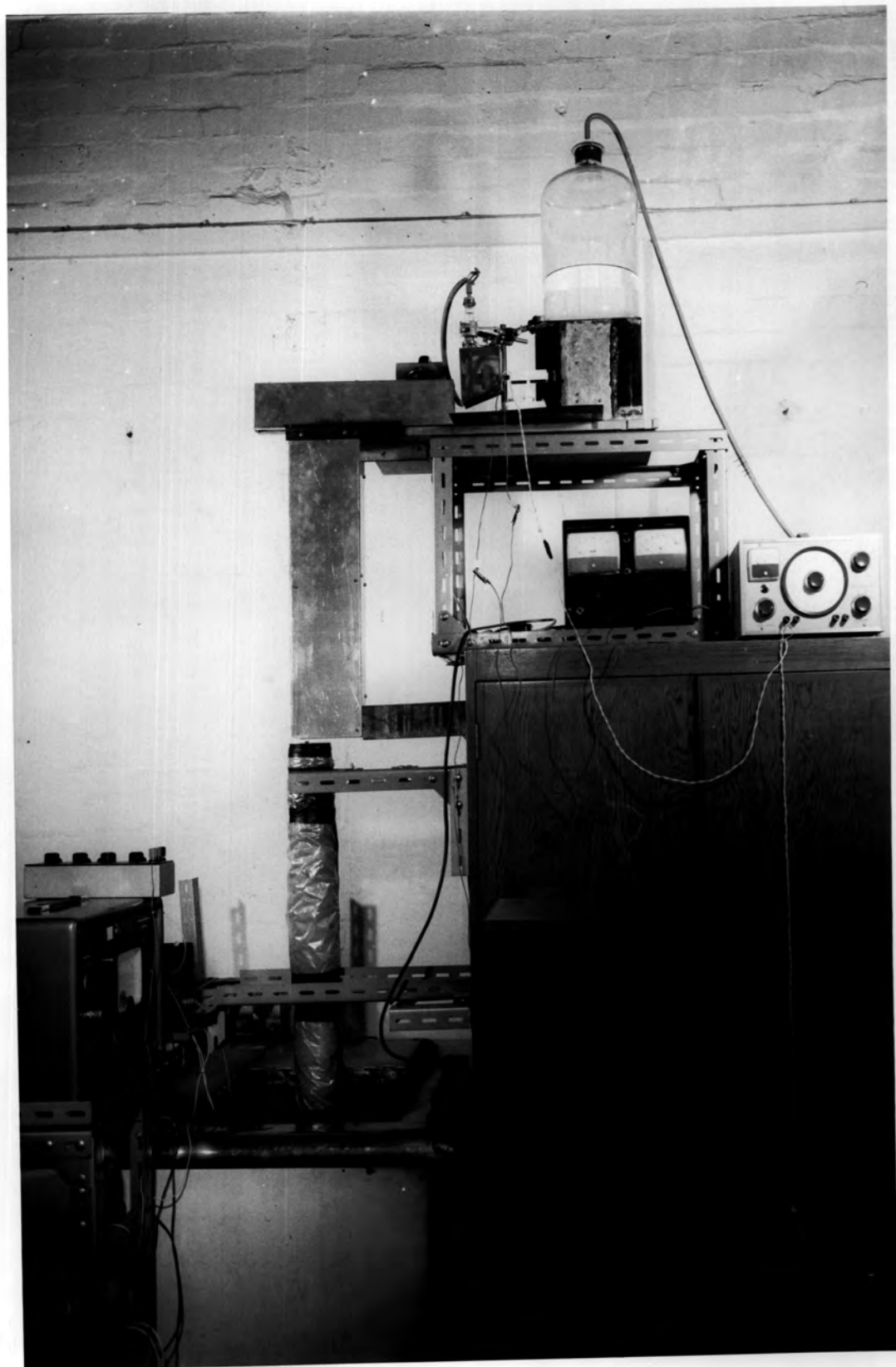


Fig. 25.

General View of the Apparatus.

floor. The vibrating needle device, a water reservoir and a stroboscopic lamp were built on to a separate platform overhanging the refrigerator. Also on the cupboard were the audio frequency oscillator and a variable d.c. supply which was used to apply potentials to the needle.

It has been stated that the droplet trajectories were severely affected by slight draughts, so in order to prevent this, a tunnel in the shape of an inverted L was built on to the platform and placed above the main tube. Thus as soon as the droplets were produced they entered a region in which the air was relatively undisturbed. The dimensions of the vertical section of the tunnel were 6 x 14 x 60 cm, and the clearance between it and the top of the tube was about 1 cm. The horizontal section of the L was adjustable in length to cater for droplets of different sizes and trajectories. There were small holes in the top through which the falling droplets could be observed. For the smallest droplets this section was removed, and the droplets were shielded by a smaller aluminium screen.

A general view of the apparatus is shown in Fig. 25

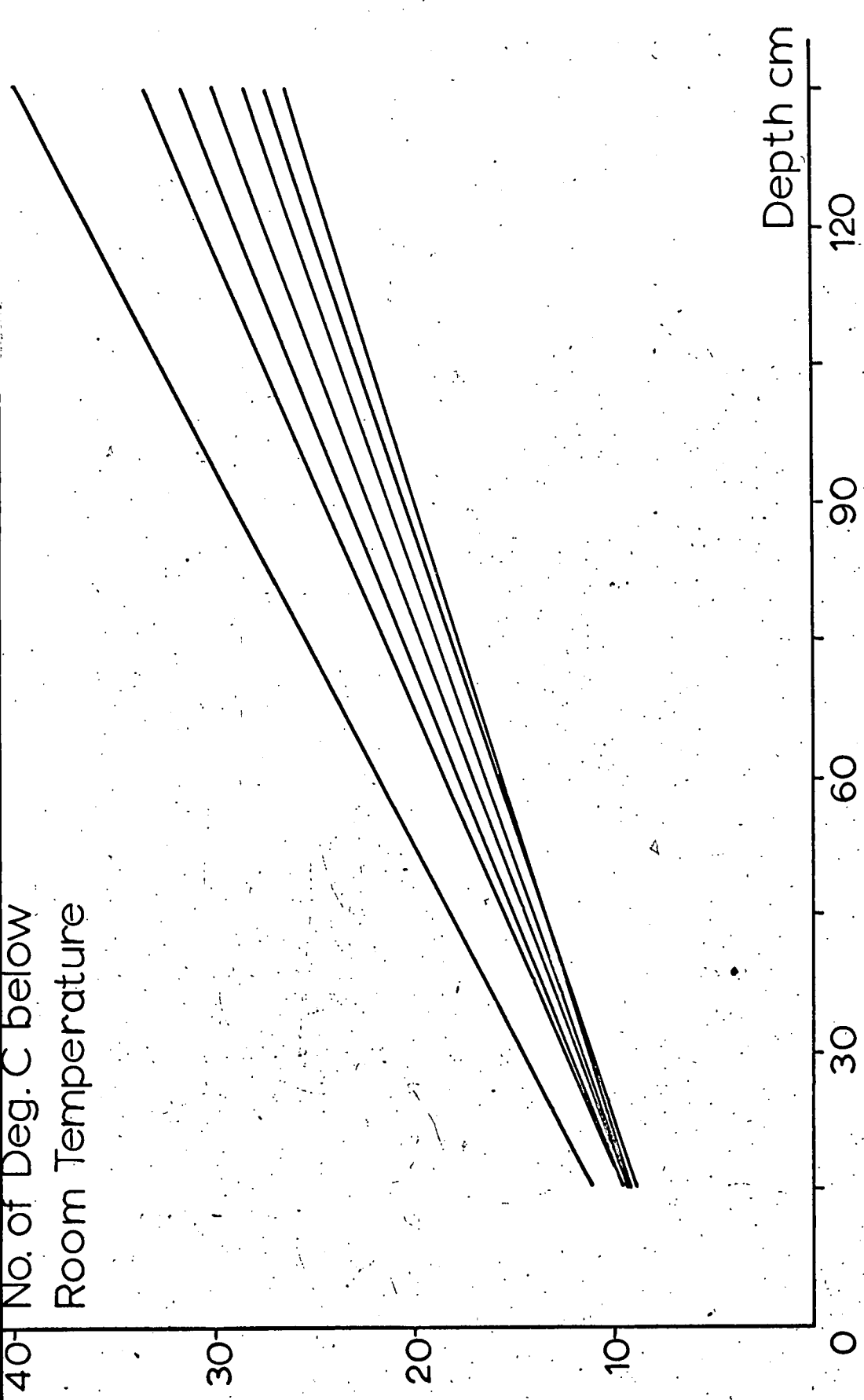


Fig.26 The Variation of Temperature with Depth of the Air in the Vertical Tube for Various Total Temperature Differences.

CHAPTER 7.

THEORETICAL DETERMINATION OF DROPLET TEMPERATURES.

1. INTRODUCTION.

Before proceeding with the charge measurements it was first of all necessary to determine whether the droplets would be supercooled when they encountered the probe. As no method of measuring the droplet temperatures seemed feasible, a theoretical approach was adopted. It was realised, however, that such an approach could not give very accurate results because there were so many uncontrolled parameters which affected the temperature of the droplets.

2. MEASUREMENT OF THE LAPSE RATE IN THE TUBE.

The first step was to find how the air temperature in the main vertical tube varied with height. A thermocouple was suspended along the central axis of the tube and the air temperature was measured at 15 cm intervals. Room temperature was noted. The temperature at the bottom of the tube was then altered, either by running the refrigerator continuously for several hours or by switching it off for several hours, and the readings were repeated. The results were expressed graphically by plotting the difference in temperature between room temperature and that at the bottom of the tube against the height measured from the top of the tube. The results are shown in Fig. 26. These results showed



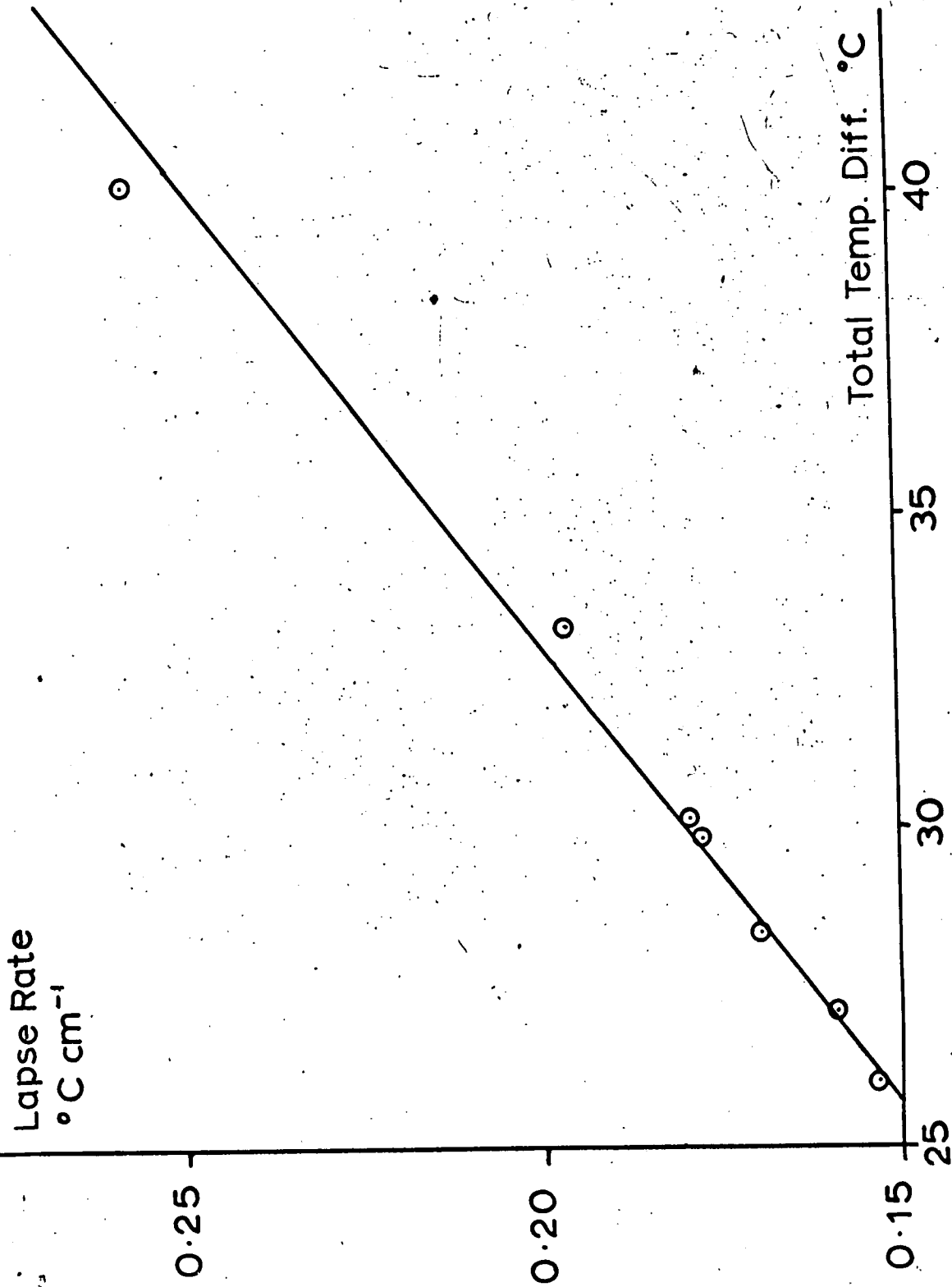


Fig.27 Variation of Lapse Rate with Total Temperature Difference.

that the temperature in the tube varied linearly with height, and that the actual value of the lapse rate depended only on the difference between room temperature and the air temperature in the bottom of the tube. These results were obtained when the air in the tube was still, but it was observed that when the probe was rotating and the small illumination source switched on, the temperature distribution remained virtually unaffected; it was only close to the probe that the temperature was altered slightly, by about  $0.5^{\circ}$  C. On the basis of these results Fig. 27 was drawn in which the lapse rate was plotted against the total temperature difference. Fig. 27 shows that the lapse rate varied linearly with the total temperature difference, and thus for any particular value of the total temperature difference, the lapse rate could be determined by interpolation.

### 5. CALCULATION OF REYNOLDS NUMBERS AND TERMINAL VELOCITIES.

The heat flux at the surface of a falling sphere is increased by virtue of its motion by a factor which is a function of the Reynolds number and which is called the ventilation coefficient. Therefore in order to determine thermal relaxation it was necessary first to determine Reynolds numbers. Because droplets fell through air of varying temperature, it was also necessary to determine terminal velocities. In the calculations certain approximations were made. The first approximation arises from the fact that the Reynolds number and terminal velocity of a water droplet of a particular radius falling in air are not unique, but vary considerably depending on the variation

of the viscosity and density of the air with temperature, atmospheric pressure and humidity. Table 21 in Appendix 2 shows how the Reynolds numbers of droplets falling at their terminal velocities vary just with temperature. The Reynolds number and terminal velocity of a droplet affect its thermal relaxation, and so unless the physical condition of the air is known and maintained precisely, the estimation of both the position of the droplet in space and its surface temperature at any time will be subject to large errors. The first approximation in these calculations was to consider the Reynolds number and terminal velocity as constant for a particular droplet size, even though droplets fell through air in which the temperature varied with height and the other physical quantities varied from day to day. The Reynolds numbers and terminal velocities of droplets were derived for air at  $0^{\circ}\text{C}$ , which was considered to be a suitable intermediate temperature.

A cooling droplet loses heat by conduction to the air, and unless the air is of the exact humidity, there will also be a heat flux due to evaporation or condensation. Droplets falling in laboratory air are evaporating, and assume the wet-bulb temperature of their environment, which may be several degrees colder than the dry-bulb temperature at room temperature. However, as the air becomes colder, the difference between the wet and dry-bulb temperatures becomes smaller and at  $-10^{\circ}\text{C}$  the difference is only  $1.5^{\circ}\text{C}$  for a relative humidity of 50%. Thus the second approximation was that no serious error would be incurred by considering that the droplet cooled to the dry-bulb temperature of

the environment. Any error incurred by this assumption would mean that droplet temperatures were lower than their estimated values. Without this assumption the calculations would have been difficult.

Room temperature varied throughout the investigations, and it might have been thought that if the temperature of droplets entering the vertical tube varied from day to day, the temperature of the droplets when they reached the bottom of the tube would also be different on different days. However, using the theory shown in Appendix 3, a graph was plotted which showed that this is not so, and that for identical lapse rates droplets which, on entering the tube, have surface temperatures in the range 15 to 30° C, will reach the bottom at very nearly the same temperature.

The Reynolds number of a sphere falling at its terminal velocity in air is given by:-

$$\frac{C_d Re^2}{24} = \frac{4}{9\eta^2} a^3 \rho \rho^1 g$$

where:-  
Re = Reynolds number     $\rho^1$  = density of air  
C<sub>d</sub> = drag coefficient     $\eta$  = viscosity of air  
 $\rho$  = density of sphere    a = radius of sphere

The following procedure (see Mason, Physics of Clouds, Page 420) was used to calculate Reynolds number:-

(a) The values of  $\frac{C_d Re^2}{24}$  were found for water droplets of

various radii falling in air at 0° C.

(b) Using the empirical relationship

$$\frac{C_p Re}{24} = 1 + 0.197 Re^{0.63} + 2.6 \times 10^{-4} Re^{1.38}$$

the values of  $\frac{C_p Re}{24}$  corresponding to specific values of Re

were found.

(c) Using the results of (b) a graph was plotted of  $\frac{C_p Re^2}{24}$

against Re.

(d) Using this graph, the values of Re appropriate to the values of  $\frac{C_p Re^2}{24}$  found in (a) were read off.

Having thus found the Reynolds numbers of droplets at 0° C, their terminal velocities and ventilation coefficients were found.

The expression for the terminal velocity is :  $V = \frac{4 Re}{2 a \rho}^{\frac{1}{2}}$

The empirical expression for the ventilation coefficient (see Mason 1956) is given by  $C = 1.6 + 0.5 Re^{\frac{1}{2}}$ . There is some doubt, however, as to whether this expression is valid for  $Re < 10$  and it has been suggested that in such cases  $C = 1$ . The values of Re, V and C are shown in Table 19.

TABLE 19.

The Reynolds Numbers, Terminal Velocities and Ventilation Coefficients  
of Water Droplets falling in Air at 0° C, 1000 mb Pressure.

$a (\mu)$	Re	$V(\text{cm sec}^{-1})$	C
20	0.2	6.6	1.7
30	0.5	11.1	1.8
40	1	18.6	1.9
50	2	26.6	2.0
60	3	33.2	2.1
70	4	37.9	2.2
80	6	51.3	2.5
90	8	59.2	2.4
100	10	66.4	2.5
110	13	78.5	2.7
120	16	88.5	2.8
130	19	97.0	2.9
140	22	104	3.0
150	25	111	3.1
160	29	120	3.2
170	33	129	3.3
180	37	137	3.4
190	42	147	3.5
200	47	156	3.7

4. CALCULATION OF THERMAL RELAXATION TIMES.

The relaxation time of a droplet is the time taken for the temperature difference between the droplet and its surroundings to become  $1/e$  of its former value. It is given by the following expression (see Mason 1956)

$$= \frac{\rho s a^2}{3 C (K_A + E)}$$

where S is the specific heat of water,  $K_A$  is the thermal conductivity of air and E is an evaporation term. As it would have been a difficult matter to determine the rate of evaporation of the droplets this term has been neglected, and so the relaxation times shown in the table are greater than the actual values. The values of the relaxation times are shown in Column 2 of Table 20. It is useful to know also the corresponding relaxation distances, and these are shown in Column 3. Columns 4 and 5 show the same quantities, but for  $C = 1$ .

TABLE. 20.

The Thermal Relaxation Times of Water Droplets falling in air at 0°C.

1000 mb Pressure.

a ( $\mu$ )	$\tau$ (sec)	$d_r$ (cm)	$\tau$ (sec)	$d_r$ (cm)
20	0.014	0.092	0.023	0.15
30	0.029	0.32	0.052	0.58
40	0.049	0.91	0.092	1.7
50	0.072	1.9	0.14	3.7
60	0.099	3.3	0.21	7
70	0.13	4.9	0.28	11
80	0.16	8.2	0.37	19
90	0.19	11	0.47	28
100	0.23	15		
110	0.26	20		
120	0.30	26		
130	0.34	33		
140	0.38	40		
150	0.42	47		
160	0.46	55		
170	0.51	66		
180	0.55	75		
190	0.59	87		
200	0.63	98		



5. CALCULATION OF SURFACE TEMPERATURES.

A water droplet loses heat by conduction at a rate

$$\frac{dQ}{dt} = 4\pi a CK_A (T_A - T_S)$$

where  $T_A$  is the air temperature and  $T_S$  is the surface temperature of the droplet. The heat which is lost in cooling from an initial temperature  $T_0$  to  $T_S$  is given by

$$Q = \frac{4}{3} \pi a^3 \rho s (T_S - T_0)$$

Differentiating this second equation with respect to time and combining it with the first equation gives

$$\frac{dT_S}{dt} = \frac{3 CK_A}{\rho s a^2} (T_A - T_S) = \frac{T_A - T_S}{\tau}$$

When the droplet falls in air in which there is a constant lapse rate, it reaches a steady state condition with the temperature of its surface lagging behind the local air temperature by a constant amount. If this temperature lag is called  $T_L$ , then at any time

$T_A = T_L + T_S$ . Also from Fig. 26 the variation of the air temperature with time, as seen by the droplet is  $T = \alpha vt + \beta$ , where  $\alpha$  is the lapse rate,  $\beta$  is a constant and  $v$  is the droplet terminal velocity.

$$\frac{dT_A}{dt} = \alpha v = \frac{dT_S}{dt} = \frac{T_A - T_S}{\tau}$$

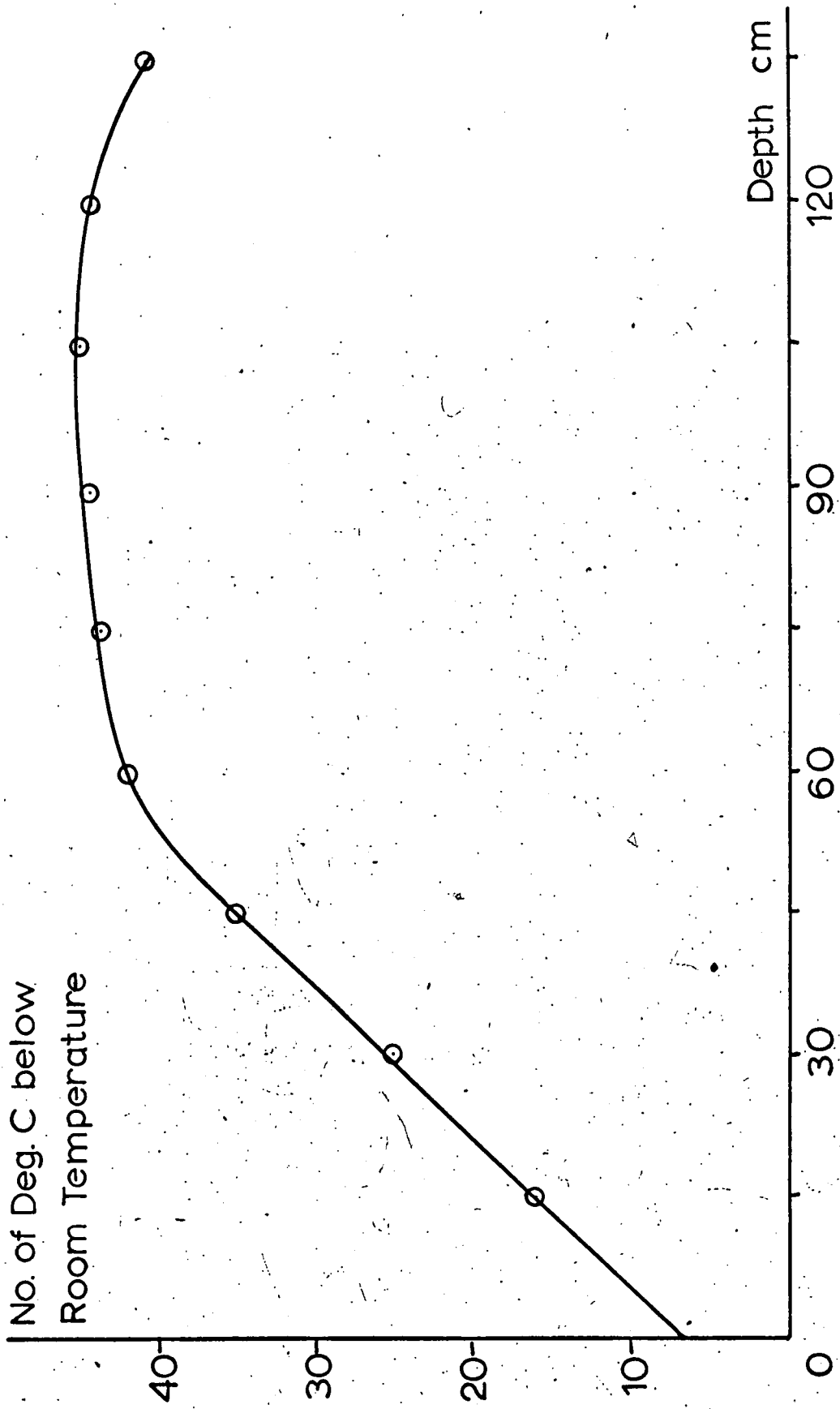


Fig. 28 The Temperature Distribution in the Tube when Using the Liquid Coolant.

Therefore  $T_L = a v \tau = a d \tau$  where  $d \tau$  is the relaxation distance. This result implies that when a droplet, losing heat by conduction only, falls through air which has a constant lapse rate, it lags behind the air temperature by an amount equal to the product of the lapse rate and the relaxation distance. Since these quantities have been evaluated, the temperature lag and hence the surface temperature of any droplet can be found. A typical value for the lapse rate was  $0.25^\circ \text{ C cm}^{-1}$ . The largest droplets used had a radius of  $150 \mu$ . The corresponding relaxation distance was 47 cm, and therefore the temperature lag was approximately  $12^\circ \text{ C}$ . Therefore, providing the temperature at the bottom of the tube is colder than  $-12^\circ \text{ C}$ , and providing the lapse rate does not exceed  $0.25^\circ \text{ C cm}^{-1}$ , all droplets of radii  $150 \mu$  or smaller will be supercooled.

## 6. CALCULATION OF THE HIGHER DEGREES OF SUPERCOOLING.

The above results have been evaluated for water droplets falling through a closed tube in which there was an air inversion. Higher degrees of supercooling were achieved using the liquid coolant. On such occasions the temperature distribution in the tube was not as reproducible as before, and so the errors in estimating the droplets temperatures were larger. Fig. 28 shows a typical variation of temperature with height when the tube was being cooled by refrigerated methylated spirits. This temperature distribution, which was measured about 5 minutes after the coolant was added, remained fairly constant

for at least a further 15 minutes, which was satisfactory since all readings were taken during the first few minutes. Fig. 28 could be approximated to a linear variation of temperature with height for the top 60 cm of the tube, followed by a region of constant temperature for the lower 75 cm. It was on this basis that the droplet temperatures were determined. The procedure was to determine the lapse rate in the upper part of the tube from the individual temperature measurements, and to estimate the mean temperature in the lower part. The result was evaluated using the preceding equations.

#### 7. CONCLUSION.

It was concluded that the droplet surface temperatures estimated in this chapter were subject to substantial errors because of the many variables which occurred in practice, and which could not be included in the calculations. It would have been desirable in practice to have eliminated these variables by being able to maintain constant conditions in the laboratory, and the calculations would have been avoided under conditions where droplets attained thermal equilibrium with their surroundings. The factors which were neglected in the calculations which are probably the largest source of error are that the falling droplets are evaporating and are cooling to their local wet-bulb temperature. However, both these effects cause droplets to be cooler than their calculated temperatures, and since the theory, without taking these effects into account, has indicated

the conditions under which droplets will become supercooled, then under such conditions droplets will still be supercooled, but to a somewhat greater extent. It is considered that the largest supercooled droplets used will not be more than about  $2^{\circ}$  C colder than their calculated temperatures for relative humidities of about 50%.

APPENDIX 2.

TABLE 21.

Variation of Reynolds Numbers with Temperature of Water Droplets  
Falling at Their Terminal Velocities in Air.

Droplet Radius ( $\mu$ )	Temperature $^{\circ}\text{C}$		
	-20	0	+20
20	0.2	0.2	0.1
30	0.6	0.5	0.4
40	1.2	1.0	0.9
50	2.4	1.9	1.6
60	3.5	3.0	2.6
70	5.1	4.4	3.8
80	7.2	6.2	5.4
90	9.4	8.5	7.0
100	11.9	10.3	9.0
110	14.8	12.8	11.1
120	18.0	15.7	13.5
130	21.7	18.7	16.3
140	25.3	22.0	19.2
150	29.7	25.5	22.3
160	33.7	29.3	25.8
170	38.3	33.3	29.3
180	43.1	37.7	33.2
190	48.3	42.0	37.2
200	53.5	47.0	41.4

APPENDIX 3.

The Effect of Room Temperature on the Cooling of the Droplets.

The purpose of the procedure described below was to determine the magnitude of the temperature difference between droplets at the bottom of the tube which had had very different temperatures on entering the tube. On Page 140 the following expression was obtained for the rate of cooling of falling droplets of surface temperature

$T_S$  in air of uniform temperature  $T_A$

$$\frac{dT_S}{dt} = \frac{T_A - T_S}{\tau}$$

For air in which there is a uniform lapse rate  $\alpha$ , this expression

becomes

$$\frac{dT_S}{dt} = \frac{\alpha vt + \beta - T_S}{\tau}$$

where  $\beta$  is a constant, and  $v$  is the terminal velocity of the droplets.

This is a differential equation of standard form, but when boundary conditions are included the solution becomes complicated.

Instead, an approximate solution was obtained by integrating the first equation, including the boundary conditions that at  $t = 0$ ,

$T_S = T_0$ , and then by applying the step by step procedure described below.

The solution of the first equation is

$$T_S = T_A (1 - e^{-t/\tau}) + T_0 e^{-t/\tau}$$

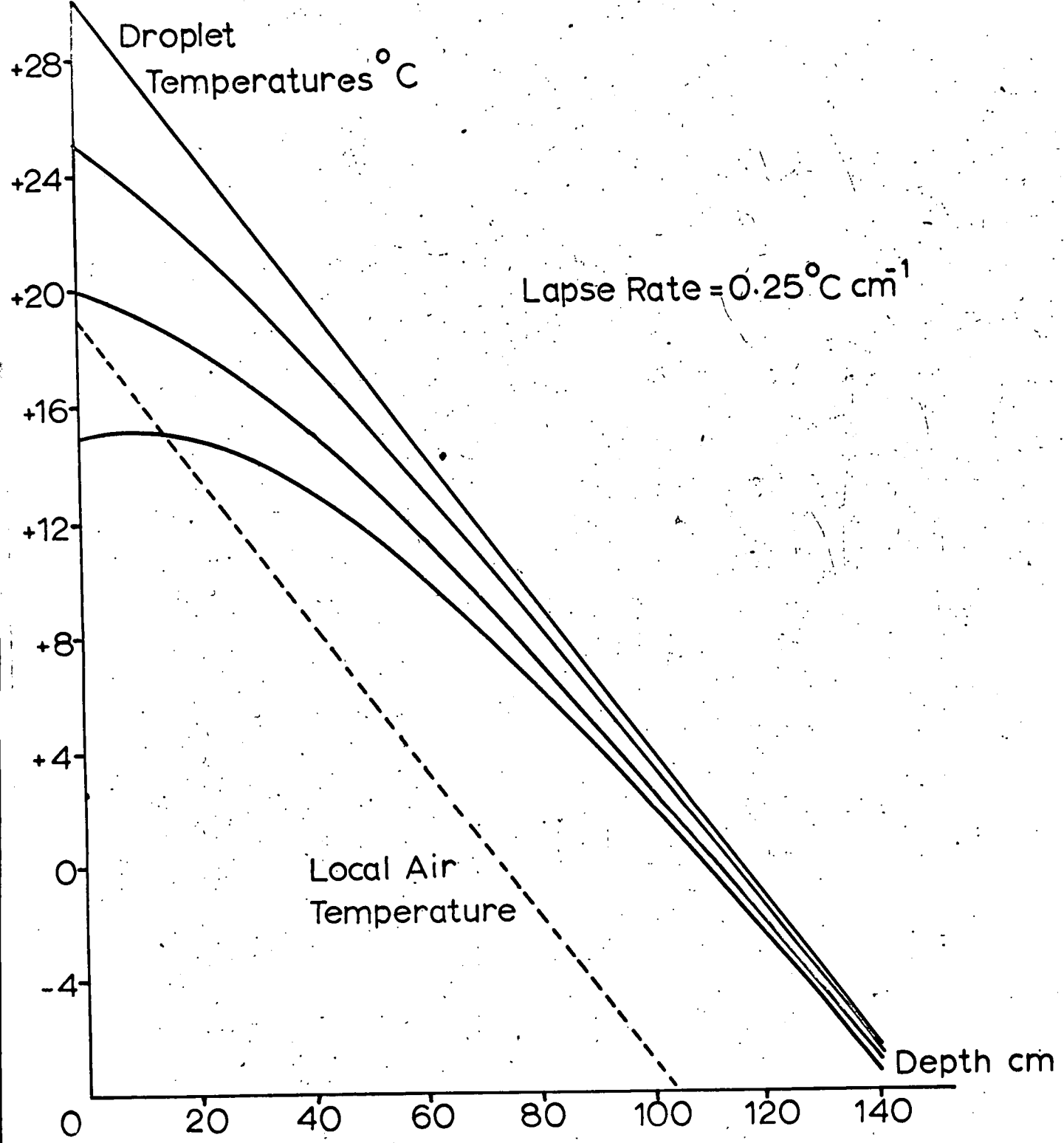


Fig. 29 The Variation of Droplet Temperatures with Depth in the Tube for Various Entry Temperatures.



The main vertical tube was divided into 10 cm lengths, and the procedure was then to apply the above equation to calculate the surface temperatures of  $150 \mu$  radius droplets, entering the tube at temperatures of 15, 20, 25 and  $30^{\circ}$  C, at the end of each 10 cm length of fall. The equation was written in its more particular form:

$$T_{S,n+1} = T_{M,n+1}(1 - e^{-t/\tau}) + T_{S,n} e^{-t/\tau}$$

where  $T_{M,n}$  is the mean air temperature over the nth 10 cm length and  $T_{S,n}$  and  $T_{S,n+1}$  are the surface temperatures at the beginning of the nth and (n + 1) th 10 cm lengths respectively. An approximation was made that over each 10 cm length of the tube a mean temperature  $T_M$ , which was the average of the temperatures at the ends of the 10 cm length, was operative. The various values of  $T_M$  were known for a particular lapse rate. The values of the exponential function were known for droplets of this size, so the temperature  $T_{S,2}$  could be calculated from the initial temperature  $T_0$ , and similarly  $T_{S,3}$  from  $T_{S,2}$  and so on. In this way the surface temperatures of droplets at the bottom of the tube were deduced for various values of  $T_0$ . The results are plotted in Fig. 29, and show that droplets entering the tube with surface temperatures between 15 and  $30^{\circ}$  C will all reach the bottom of the tube within  $0.8^{\circ}$  C of each other. This is a consequence of the length of the tube, and it can be seen from the graphs that if the tube were only one third as long, the temperature

differences between these droplets would be about  $5^{\circ}$  C. The graphs also show that a constant temperature lag between the droplet surfaces and the surrounding air is developed.

The conclusion drawn from the results was that the procedure described in Chapter 7 for determining droplet surface temperatures at the bottom of the tube, was applicable without serious error for droplets entering the tube at different temperatures which were determined by the room temperature.

CHAPTER 8.

EXPERIMENTAL WORK ON WATER DROPLETS.

1. INTRODUCTION.

Water droplets in the radius range 30 to 150  $\mu$  were made to fall through the main vertical tube in which they became cooled. The quantity of charge separated when they encountered the probe and the dependence of the charging on impact velocity, droplet temperature and droplet size was measured. The charge separated by droplets which were in the process of freezing was also measured.

2. GENERAL PROCEDURE.

A thin smooth coating of ice was prepared on the probe rods by alternately cooling them in liquid air and dipping them into cold demineralised water. The thickness of the ice was approximately  $\frac{1}{2}$  mm. The apparatus shown in Fig. 25 was aligned so that water droplets would fall through the stabilising tunnel and main tube and would strike the probe situated at the bottom of the main tube. An area of the floor of the probe casing had been painted white, and when the small illumination source contained in it had been switched on it was possible, by viewing from above, to observe the droplets throughout their entire fall. To ensure that the droplets fell down the tube without touching the sides it was necessary to move the vibrating needle device by hand to the required

position. On a few occasions droplet streams were less stable than on others, and continual adjustment of this position was necessary. It was observed that practically all droplets fell on to an oval area of floor, approximately 3 cm x 5 cm.

It was of primary importance to ensure that the droplets which were produced were uncharged. An induction can which consisted of an electrostatically screened miniature film can attached to the electrometer was used to collect the water droplets which were produced by the needle. The resistance in parallel with the electrometer input circuit was  $10^{10}$  ohms. It was found that the droplets were initially negatively charged, and that 150  $\mu$  radius droplets gave electrometer deflections of up to 30 mV showing that droplets were being produced with mean charges of up to  $4 \times 10^{-5}$  e.s.u. Smaller droplets had smaller charges. Uncharged droplets were obtained by applying the necessary d.c. voltage between the needle and the electromagnet. By critical adjustment of the voltage the electrometer reading was reduced to zero. The charge on the droplets could not be said to be exactly zero, because of the noise level of the electrometer - induction can system. The noise level was about + 0.05 mV or  $1.5 \times 10^{-5}$  e.s.u.  $\text{sec}^{-1}$ , and since 250 droplets were being produced each second, the maximum possible charge per droplet was +  $6 \times 10^{-8}$  e.s.u. Thus it could be said that each droplet had zero charge to within approximately 100 elementary charges. Sometimes the zero level drifted and this was attributed to instabilities

in the satellite (attendant) streams. Usually, however, a stream of neutral droplets could be maintained for several hours.

The sizes of droplets were found by allowing a few of them to fall into a drop of paraffin oil on a microscope slide, and quickly measuring the diameters under a microscope. The diameters were expressed to the nearest  $10 \mu$ .

### 3. VARIATION OF CHARGING WITH DROPLET TEMPERATURE.

#### (a) Experimental Procedure.

The first experiments were performed with the largest droplets of radius  $150 \mu$ . Droplets of this size were comparatively easy to work with because their trajectories were hardly disturbed by slight air currents. A sequence of measurements was made in the following manner.

The refrigerator was allowed to warm up to about  $-5^{\circ}$  C. Room temperature was taken. The illumination source near to the probe was switched on and the probe was set in motion at  $10 \text{ m sec}^{-1}$ . The noise level of the probe was observed, and the temperature adjacent to it was measured. A stream of droplets was selected and the net charge adjusted to be zero. The droplets were made to impinge on the probe. It was observed that a continuously varying electrometer reading was obtained. The deflection showed that the probe was being charged by the droplets and the fact that it varied was because

a varying number of droplets was encountering the probe. A simple geometry calculation was done to determine the maximum collection efficiency of the probe for droplets of different sizes. The calculation showed what fraction of droplets were struck by the probe when they fell through the volume swept out by the probe and how this depended on the fall-speeds of the droplets and the angular velocity of the probe. The results are shown in Table 22. In estimating the quantity of charge separated per droplet collision, the procedure adopted was to observe the fluctuating electrometer deflection for some minutes, noting down the maximum deflection. If this maximum value was recurrent it was assumed that this value corresponded to the maximum rate at which droplets could strike the probe. After the maximum values had been recorded the probe was switched off and a check was made to see if the droplets were still uncharged. The results were rejected if the droplets carried any detectable charge, and further readings were taken.

The refrigerator compressor was switched on and as the refrigerator cooled down over a period of hours towards  $-18^{\circ}$  C, the whole procedure was repeated at temperature intervals of three or four degrees. In order to make droplets more highly supercooled than was possible using the refrigerator alone, chilled methylated spirit was poured into the space between the concentric tubes. The methylated spirits had been cooled by direct contact with pieces of solid carbon dioxide, and contained a great deal of dissolved gas which was released upon

contact with the warmer surfaces. When the gas had escaped through the holes in the top of the tube the holes were closed to prevent any remaining gas from mixing with the air in the main tube. After the coolant had been standing in the tube for about five minutes until a stable temperature distribution had been produced, the temperature of the air adjacent to the probe was taken, and the whole charge measurement procedure was repeated. After one or two readings had been taken, the tube was removed and the coolant poured out.

The entire sequence described above was repeated several times. A Watanabe Type 2L pen-recorder became available during the course of these measurements, and this enabled permanent records of the rapidly varying electrometer readings to be taken, and this greatly facilitated the work. The surface temperatures of the droplets were calculated as described in Chapter 7 and all the results were tabulated in Table 23.

In order to investigate the effect on charging of heating the probe relative to the falling droplets, a brass panel was removed from the probe casing and replaced by a perspex one. The probe was then illuminated by an infra-red lamp. It was found to be necessary to screen the perspex panel with wire gauze, to prevent large electrometer deflections when switching on the lamp. The probe was heated from  $-17^{\circ}\text{C}$  to  $-7^{\circ}\text{C}$  and a record was made of the rate of charging by the falling droplets.

An attempt was made to determine the nature of the fragments which carried away the charge which was equal and opposite to the one given to the probe. This was difficult because of the confined space in the probe casing and because the probe would be throwing off particles in all directions. A panel was removed from the probe casing and some sheet aluminium attached at right angles to it. This aluminium had been bent into a shape which ensured that when several microscope slides were placed upon it they faced in several different directions. Microscope slides coated with 5 to 10% supercooled Formvar solution were placed on the bent sheet. The brass panel was replaced in order to maintain the temperature inversion, and in so doing, the Formvar slides were brought close to the rotating probe. Some of the fragments thrown off from the probe when droplets impinged on it were caught on the slides. The slides were left until the plastic had hardened, and then they were removed and examined under the microscope.

(b) Precautions.

It was necessary to make a few checks to be certain that the electrification of the probe was really caused by collisions with uncharged droplets. Results showed that if the droplets were supercooled the probe became negatively charged, so the droplets were given positive charges of the same magnitude as the observed negative charging to see whether the probe would become positively charged. However the negative charging of the probe persisted, and



it was only when the droplets were given quite high positive charges that the probe became positively charged. There was also the question of whether droplets could become charged before encountering the probe by rebounding from the side of the vertical tube, but it was observed that on the occasions that droplets did hit the side they tended to adhere and freeze slowly. The possibility of ion capture by droplets falling through 2 m of air was also investigated, and it was concluded that the amount of charge acquired by this process was too small to be detected. It was concluded from these observations that when the droplets encountered the probe they were uncharged.

(c) Results.

The maximum collection efficiency of the probe for droplets of various sizes for various probe speeds is shown in Table 22. The measured rates of charging of the probe and the deduced temperatures of the droplets are shown in Table 23. The results of Table 23 are displayed graphically in Fig.30.

TABLE 22.

The Maximum Number of Droplets per Second which can Hit the Probe for Various Speeds of Rotation.

Droplet Radius ( $\mu$ )	Tangential Velocity of Probe ( $m\ sec^{-1}$ )				
	5	10	12.5	15	20
150	65	130	160	195	250
100	120	240	250	250	250
50	250	250	250	250	250

TABLE 23.

Variation of Charging with Temperature for 150  $\mu$  Radius Droplets.

Electro- meter Deflection (mV)	Rates of Charging (e.s.u. sec <sup>-1</sup> )	Room Temp. °C	Probe Temp. °C	Lapse Rate (°C cm <sup>-1</sup> )	Temp. Lag T <sub>L</sub>	Droplet Temp. °C.
-4.1	-12.3x10 <sup>-4</sup>	19	-11.1	0.18	8.5	-2.6
-1.2	- 3.6	"	- 9.5	0.17	8.0	-1.5
-2.9	- 8.7	"	-13.0	0.19	8.9	-4.1
-2.0	- 6.0	"	-16.0	0.21	9.9	-6.1
-1.1	- 3.3	"	-20.0	0.70	33	-16
-2.9	- 8.7	22	-10.8	0.20	9.4	-1.4
-2.6	- 7.8	"	-12.0	0.21	9.9	-2.1
-3.0	- 9.0	"	-12.0	0.21	9.9	-2.1
-3.2	- 9.6	"	-14.6	0.23	10.8	-3.8
-2.7	-8 .1	"	-16.3	0.24	11.3	-5.0
-2.1	- 6.3	"	-17.9	0.25	11.8	-6.1
-1.0	- 3.0	"	-21.3	0.77	36	-17
-3.0	- 9.0	"	-11.2	0.20	9.4	-1.8
-2.5	- 7.5	21	-10.5	0.19	8.9	-1.6
-2.5	- 7.5	"	-11.4	0.20	9.4	-2.0
-2.0	- 6.0	"	-12.2	0.20	9.4	-2.8
-2.3	- 6.9	"	-13.9	0.21	9.9	-4.0
-2.6	- 7.8	29	-16.0	0.28	13.2	-2.8

TABLE 23. (Continued)

Electro- meter Deflection (mV)	Rates of Charging (e.s.u. sec <sup>-1</sup> )	Room Temp. °C	Probe Temp. °C	Lapse Rate (°C cm <sup>-1</sup> )	Temp. Lsg T <sub>L</sub>	Droplet Temp. °C.
-2.9	- 8.7	29	-14.1	0.27	12.7	-1.4
-1.9	- 5.7	"	-11.5	0.25	11.8	+0.3
-0.8	- 2.4	"	- 9.4	0.24	11.3	+1.9
+1.7	+ 5.1	"	- 6.6	0.22	10.3	+3.7
+1.2	+ 3.6	"	- 6.9	0.22	10.3	+3.4
+0.7	+ 2.1	"	- 8.3	0.23	10.8	+2.5
-1.5	- 4.5	"	-10.8	0.25	11.8	+1.0
-2.1	- 6.3	"	-12.6	0.26	12.2	-0.4
-2.4	- 7.2	"	-13.6	0.27	12.7	-0.9
-3.8	-11.4	24	-13.2	0.23	10.8	-2.4
-3.4	-10.2	"	-13.5	0.23	10.8	-2.7
-3.4	-10.2	"	-17.4	0.26	12.2	-5.2
-2.6	- 7.8	"	-21.0	0.28	13.2	-7.8
-1.0	- 3.0	"	-22.8	0.83	39	-18
-4.9	-14.7	"	-13.5	0.23	10.8	-2.7
-4.6	-13.8	"	-14.0	0.23	10.8	-3.2
-3.3	- 9.9	"	-13.4	0.23	10.8	-2.6
-2.1	- 6.3	"	-10.8	0.21	9.9	-0.9
+1.1	+ 3.3	"	- 8.9	0.20	9.4	+0.5
+2.0	+ 6.0	"	- 6.5	0.18	8.5	+2.0
+1.4	+ 4.2	"	- 4.2	0.17	8.0	+3.8

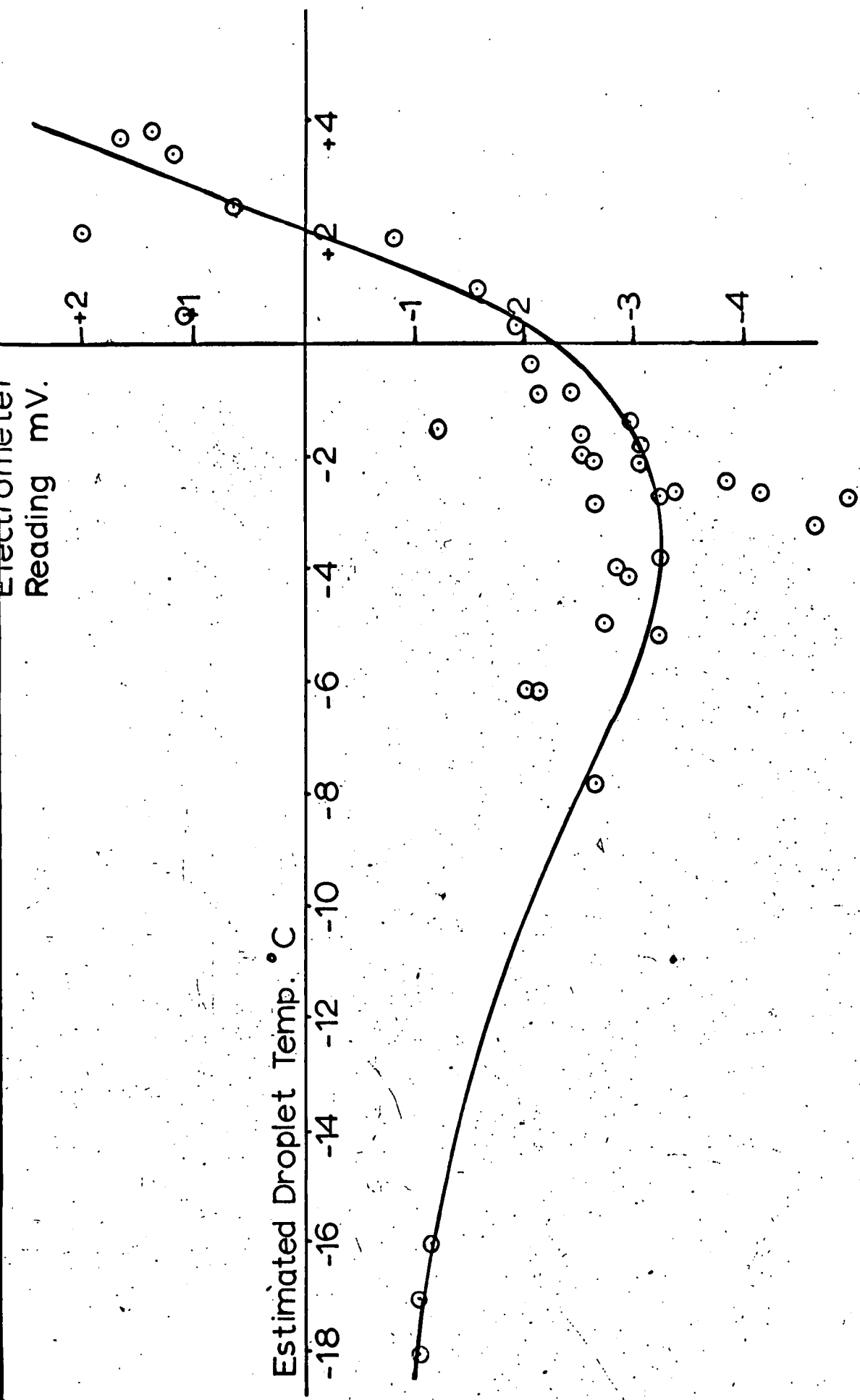


Fig.30 Variation of Charging with Droplet Temperature.

After a number of readings had been taken, the probe was removed and examined. It was observed to have a glassy rippled surface, which suggested that droplets had splashed at its surface and not splintered. If droplets had splintered it would have been expected that a few sharp ice fragments would have adhered to the probe. The Formvar slides were inspected and it was observed that small water droplets with radii down to  $10 \mu$  had been collected. Very few droplets had been caught on the slides and the number of them was certainly too small to be related to the number of droplets which had struck the probe. They merely served to show that splashing had occurred. No ice crystals were ever collected on the slides.

The results showed that when droplets whose temperatures were above about  $+2^{\circ} \text{C}$  encountered the probe, the probe became charged positively, and when the droplets were colder than this it became charged negatively. The rate of charging of the probe reached a maximum for a droplet temperature of about  $-3^{\circ} \text{C}$ , and was much reduced when the probe and the droplets were much colder. The conclusion drawn from heating the probe with an infra-red lamp was that this did not significantly affect the results. The rate of negative charging of the probe was reduced by about 30% on heating the air surrounding the probe from  $-17^{\circ} \text{C}$  to  $-7^{\circ} \text{C}$ . If the results had depended on the temperature of the probe instead of the droplets, then positive charging would have been expected. It was concluded that the charging depended on the temperature of the droplets and not of the probe. The observed

reduction of negative charging may have been caused by the effect of heating on the temperature distribution in the tube.

(d) Calculation.

Taking the maximum electrometer deflection as 4 mV which is equivalent to a rate of charging of  $12 \times 10^{-4}$  e.s.u.  $\text{sec}^{-1}$ , the maximum rate at which droplets collided with the probe was 150 per second.

Hence, for negative charging of the probe, the mean charge separated per  $150 \mu$  radius droplet was  $10^{-5}$  e.s.u.

For positive charging of the probe the maximum observed rate of charging, and hence the mean charge separated per droplet collision, was approximately half the above values.

(e) Discussion of the Results.

The fact that the curve drawn in Fig. 30 does not go through the origin of the graph may only be the result of the droplets having temperatures 1 to  $2^{\circ}$  C colder than their calculated values, and this would lead to the conclusion that droplets above  $0^{\circ}$  C charge the probe positively, and droplets which are supercooled charge it negatively. The points are widely scattered, and again the errors in the droplet temperatures may be responsible for this, since the thermal properties of the air in the laboratory varied from day to day. It should be mentioned that each set of readings showed a similar variation of charging with temperature, and that in representing all the readings

on one graph some of this detail has been lost.

The reason for these results is obscure. The electrification does not appear to be the result of splintering, since the rate of charging was lower, not higher, at lower temperatures. The positive charging is in agreement with the observations of Faraday (1845) and Sohneke (1886), but the mechanism for the charge transfer has not been explained. It might be possible to explain the negative charging in terms of the Workman-Reynolds effect in which a small fraction of the droplet freezes upon contact with the ice, and there is a separation of charge across the freezing interface, which registers as an electrometer deflection when the rest of the droplet is flung off. However, this does not explain the reduction of the negative charging as the temperature becomes lower, and it would be attractive to seek an explanation for the negative charging which would also explain the positive charging.

#### 4. VARIATION OF CHARGING WITH IMPACT VELOCITY.

##### (a) Procedure.

The tangential velocity of the probe was varied by adjustment of the resistances in series with the motor. The probe was set in motion in air at about  $-12^{\circ}$  C, and its tangential velocity was varied over the range 5 to 20 m sec<sup>-1</sup>. Measurements of the rate of charging of the probe by the 150  $\mu$  radius droplets were performed in the manner described in Section 3. The results are shown in Table.24.

(b) Results.

TABLE 24.

The Charging of the Probe by 150  $\mu$  Droplets at Various Impact Velocities

Tangential Velocity of Probe (m sec <sup>-1</sup> )	5	10	12.5	15	20
Maximum rate of droplet collisions (sec <sup>-1</sup> )	65	130	160	195	250
Maximum electrometer deflection (mV)	1.05	1.65	2.10	2.70	2.90

(c) Conclusion.

It can be seen in Table 24 that there is approximate proportionality between the rate of charging of the probe and the rate at which droplets collided with it. It was therefore concluded that in the range of impact velocities 5 to 20 m sec<sup>-1</sup>, the mean charge separated per droplet collision was constant.

5. VARIATION OF CHARGING RATE DROPLET SIZE.

(a) Procedure.

Stable satellite streams of droplets with radii down to 50  $\mu$



were produced. The variation of charging with temperature was determined for each droplet size in the same way as before. However, as the droplets became smaller it became increasingly more difficult to get them all to follow the same fall path, because they were very susceptible to slight air movements. The rotation of the probe caused some turbulence of the air in its vicinity, and at one time it was thought that because of this the 50  $\mu$  radius droplets were not hitting the probe. However it was later shown that a proportion of them, at least, were hitting it. Stable streams of droplets with radii smaller than 50  $\mu$  could not be produced, but small showers of droplets of radii between 30 and 40  $\mu$  were made to fall into the tube. It was not certain what proportion of these hit the probe.

(b) Results.

TABLE 25.

Variation of Charging with Droplet Size.

Droplet Radius ( $\mu$ )	Electrometer Deflection (mV)	Room Temp $^{\circ}$ C	Probe Temp $^{\circ}$ C	Lapse Rate ( $^{\circ}$ C cm <sup>-1</sup> )	Temp Lag $T_L$	Droplet Temp. $^{\circ}$ C
90	None	23	- 7.0	0.18	2.0	- 5.0
90	-0.5	"	- 9.8	0.20	2.2	- 7.6
90	-0.35	"	-12.0	0.21	2.3	- 9.7
90	-0.55	"	-17.0	0.25	2.8	-14.2
90	-0.25	"	-15.0	0.24	2.6	-12.4
55	None	22	-14.0	0.22	0.6	-13.4
55	None	"	-18.0	0.25	0.7	-17.3
30-35	None					
30-40	None					

The observation "None" means that deflections were not significantly greater than the noise level of the electrometer, which for the above readings was  $\pm 0.15$  mV.

(c) Discussion.

The average rate of charging of the probe by 240  $90 \mu$  radius droplets per second was found to be approximately  $10^{-4}$  e.s.u.  $\text{sec}^{-1}$  and hence the mean negative charge imparted to the probe per droplet collision was  $4 \times 10^{-7}$  e.s.u. The results for  $90 \mu$  radius droplets did not indicate any systematic variation with temperature. It also seemed that splashing was the electrification mechanism with these droplets, as Formvar slides did not reveal any ice splinters.

No electrification of the probe by droplets in the radius range 30 to  $55 \mu$  was detected. This meant that the mean charge separated per droplet was not greater than about  $2 \times 10^{-7}$  e.s.u. This result differs from that of Latham and Mason, where the mean charge separated for droplets in the radius range 20 to  $50 \mu$  was  $4 \times 10^{-6}$  e.s.u. In the present experiments, however, it was not known what proportion of droplets in this size range hit the probe, since they were very susceptible to the turbulence caused by the rotating probe. It was concluded that a rotating probe was not a suitable target for droplets of this size, and that in future experiments supercooled droplets should be drawn past a stationary probe.

6. CHARGING BY DROPLETS WHICH HAD BEEN NUCLEATED BEFORE  
ENCOUNTERING THE PROBE.

(a) Introduction.

In the previous experiments it had been noticed when the coolant had just been poured into the tube that a slight mist was visible inside it at the lower end. It was often noticed when droplets fell through this mist and encountered the rotating probe that there was considerable negative charging of the probe - at least an order of magnitude greater than the other results. This phenomenon did not occur on every occasion and could only be observed during the first few minutes after adding the coolant. It was observed that the charging ceased when the supply of droplets was stopped, and so the electrification must have been caused by the droplets. It was surmised that the mist contained small ice crystals which nucleated the supercooled droplets causing them to freeze inwards, and that the resulting charge separation was caused by collisions between partially or wholly frozen droplets and the probe. Steps were then taken to investigate whether this was true.

(b) Investigation of the Effect.

Instead of using the coolant to produce a mist, small quantities of liquid nitrogen were introduced into the column of the tube. This produced a column of microscopic ice crystals which persisted for about a minute. It was observed that these crystals did not cause any detectable charging of the rotating probe. When 150  $\mu$  radius

droplets fell through this fog of crystals and encountered the probe, the strong negative charging was once more observed. It might have been thought that the negative charge occurred as a result of the crystals being charged, in which falling droplets swept up some of the crystals and transferred their charge to the probe. In order to investigate this the tube was allowed to warm up until the temperature at the bottom was  $-6^{\circ}$  C. The corresponding lapse rate was such as to ensure that none of the droplets would become supercooled, and so on falling through a column of ice crystals none would be nucleated. When the droplets fell through the fog of crystals and encountered the probe there was no negative charging, but instead a slight positive charging of the probe. This was in agreement with previous results obtained at this temperature in the absence of a column of ice crystals. It was concluded from this that the high negative charging was not the result of water droplets sweeping up highly charged ice crystals.

Evidence of the physical state of the droplets was obtained by collecting them on microscope slides placed on the floor of the probe case, and examining their shape. It was observed when droplets had fallen through cold air containing no crystals that when they hit the slides they spread out and formed large patches before freezing. When the droplets fell through the same air containing a column of ice crystals and hit the slides they rested on the surface of the slides largely retaining their spherical shape. This gave a strong

indication that in the latter case the droplets were in the process of freezing when they hit the slides. It was also seen that the droplets were intact — that they were not shattered either when falling through the air or landing on the slides. This showed that it was unlikely that the droplets were charged by shattering or splintering before reaching the probe.

In order to determine whether the droplets were wholly or partially frozen by the time they encountered the probe, the freezing times of droplets of various sizes were calculated. The theory of this is shown in Appendix 4. The result was that the largest droplets were only partially frozen.

It was therefore concluded that the observations of large rates of negative charging of the probe were caused by uncharged partially frozen droplets.

(c) Experimental Procedure.

The tube was cooled by the chilled methylated spirits. Prior to each reading a column of ice crystals was formed in the tube. Charge measurements were made as before, using droplets in the radius range 30 to 150  $\mu$  and a probe speed of 10 m sec<sup>-1</sup>. Results were also obtained for 150  $\mu$  radius droplets with the probe stationary. The maximum rate at which droplets struck the stationary probe was determined in a subsidiary experiment by applying known charges to the droplets and measuring the fraction of charge transferred to the

probe. The assumption was made that all the charge on the droplets was transferred in the collisions. The results of the main experiment are shown in Tables 26 and 27.

(d) Results.

TABLE 26.

Charge Separated by Freezing Droplets for a Relative Velocity of 10 m sec<sup>-1</sup>

Droplet Radius ( $\mu$ )	Mean Air Temperature ( $^{\circ}$ C)	Rate of Charging (mV)	Charge per Droplet (e.s.u.)
150	-25	-19	-44 x 10 <sup>-6</sup>
150	-21	-92	-212
150	-25	-19.5	- 45
145	-24	-28	- 64
145	-22	-23	- 53
145	-25	-37	- 85
95	-20	- 5.2	- 7.0
90	-19	- 5.0	- 6.8
90	-22	- 6.9	- 9.4
55	-21	- 2.1	- 2.5
55	-21	- 1.7	- 2.0
50	-24	- 2.0	- 2.4
30-35		No detectable charging	
30-40		(Noise level $\pm$ 0.2 mV)	

Table 7.

Charge Separated by Freezing Droplets for a Relative Velocity of  
Approximately 1 m sec<sup>-1</sup>.

Mean Air Temperature (° C)	Rate of Charging (mV)	Charge separated per Droplet (e.s.u.)
-25	- 9.2	30 x 10 <sup>-6</sup>
-25	- 8.0	26
-25	- 7.9	26
-25	-19.0	62
-22	-18.5	60

The result in Column 3 was derived using the result of the subsidiary experiment, in which it was shown that the greatest fraction of droplets which could hit the stationary probe was 0.37.

(e) Discussion.

The results have shown that this process caused appreciable electrification and that the probe was always negatively charged. The values from Table 26 showed that for an impact velocity of 10 m sec<sup>-1</sup> the average charge separated for 150  $\mu$  radius droplets was  $(8.4 \pm 4.0) \times 10^{-5}$  e.s.u., for 90  $\mu$  radius droplets was

$(7.7 \pm 0.8) \times 10^{-6}$  e.s.u. and for  $55 \mu$  radius droplets was  $(2.3 \pm 0.2) \times 10^{-6}$  e.s.u. Although the number of observations was small, the indication was that the mean quantity of charge separated by each droplet increased approximately as the cube of the droplet radius, assuming that all of the smaller droplets encountered the probe. From Table 27, when droplets hit the stationary probe at a relative velocity of about  $1 \text{ m sec}^{-1}$  the mean charge separated was  $(4.1 \pm 0.8) \times 10^{-5}$  e.s.u., which showed that the effect was not very sensitive to impact velocity.

These results are in qualitative agreement with those of Latham and Mason which were obtained for a range of smaller droplets, and this suggests a similar charge separation mechanism. It is thought that the charge was separated by the shattering of partially frozen droplets on the probe, although the experimental conditions did not allow verification of this. In the work of Latham and Mason it was considered that shattering occurred after droplets had been nucleated by contact with the surface of the probe. The maximum size of droplets which shattered would depend on how the time required for the formation of an ice shell compared with the contact time. In the present experiments freezing had already commenced before the droplets encountered the probe, and it is suggested that this enabled an investigation similar to the earlier work but in a different range of droplet sizes to be carried out.



Two mechanisms which might explain the electrification are the temperature gradient theory and the Workman - Reynolds effect. Applying the temperature gradient theory to a water droplet with a spherical shell of ice of thickness  $x$  cm, with a temperature difference  $T_s$  across it, the maximum charge separated is  $4 \pi a_0^2 \times 5 \times 10^{-5} (T_s - T_w) / x$  e.s.u. where  $a_0$  is the radius of the sphere. The expression for  $T_s$  has been determined in Appendix 4. For a  $150 \mu$  radius droplet with an ice shell  $20 \mu$  thick, and an air temperature of  $-20^\circ \text{C}$ , the surface temperature of the droplet  $T_s$  was calculated to be approximately  $-0.1^\circ \text{C}$ . Consequently the maximum separation of charge according to the temperature gradient theory is  $7 \times 10^{-7}$  e.s.u. The actual value may be somewhat greater than this because of the increased conductivity of ice near to  $0^\circ \text{C}$ . It is, however, clearly insufficient to account for the observed charge separations of up to  $2 \times 10^{-4}$  e.s.u. per droplet. It should be mentioned here that in their calculations Latham and Mason considered that the surface temperatures of freezing droplets approached the air temperature, and this gave estimates two orders of magnitude greater than in the above calculation. However the calculations in Appendix 4 have shown that while droplets are in the process of freezing their surface temperatures are close to  $0^\circ \text{C}$ . The results had shown that the electrification was not critically dependent on impact velocity as had been the case when the probe was electrified by ice crystals, and this indicated that the results could not be explained in terms of an enhanced temperature gradient effect, as was possible in the

ice crystal work. It was concluded that the temperature gradient theory did not seem to be able to account for the observed electrification.

Workman and Reynolds (1950) observed that for very dilute aqueous solutions the quantity of charge separated across the ice-water boundary was typically  $10^{-5}$  e.s.u. for each cubic centimetre of liquid frozen, and that the ice was usually negative with respect to the water. For a  $150 \mu$  radius droplet with a shell  $20 \mu$  thick the volume of ice formed is  $5 \times 10^{-6} \text{ cm}^3$ , and the corresponding charge separated across the boundary is 0.5 e.s.u. This amount of charge would seem to be ample to account for the observed magnitude of charging by the shattering of such droplets on the probe. Workman and Reynolds had observed that when the ammonium ion was present in dilute solutions the sign of the charge on the ice formation was reversed. An attempt to verify whether the present results could be ascribed to the presence of impurities was made by adding sufficient ammonium nitrate to the water supply to make a solution of normality  $3 \times 10^{-6}$ . Allowing  $95 \mu$  radius droplets of this solution to encounter the probe after being nucleated, a negative electrometer reading of about 5 mV was obtained. Thus there had been no sign reversal, and no difference between the magnitude of this and previous results was detectable. It was concluded that the very small quantity of added impurity had not produced any detectable change in the results. However, since the original water was not of the highest purity, it is doubtful whether this result is very significant, as it may be

that an impurity originally present in the water may have been the dominating factor.

It was concluded that when partially frozen water droplets encountered an iced probe the magnitude of the charge separated could be explained more satisfactorily by the Workman - Reynolds effect than by the temperature gradient theory.

#### 7. SUMMARY.

The results obtained in this chapter are not directly comparable with those of Latham and Mason because readings were only obtained here for droplets in the radius range 150 to 50  $\mu$  . However it is thought that results bearing an indirect comparison to theirs were obtained.

It was shown for uncharged droplets which had fallen through clear air that the probe became positively charged if the droplet temperatures were above 0° C and negatively charged if the droplets were supercooled. It was concluded that the electrification was caused by splashing. The negative charging became reduced as the degree of supercooling of the droplets increased. The average maximum charge separated by a 150  $\mu$  radius droplet was  $10^{-5}$  e.s.u. and by a 50  $\mu$  radius droplet was  $4 \times 10^{-7}$  e.s.u. No charge separation was observed for 50  $\mu$  radius droplets or for droplets in the range 30 - 40  $\mu$  . Readings which were taken later showed that some or all of the droplets were hitting the probe, but that it was not

known whether a significant proportion of the 30 - 40  $\mu$  droplets were hitting it. The observation for 50  $\mu$  radius droplets is at variance with the quantity of charge  $3 \times 10^{-6}$  e.s.u. per droplet measured by Latham and Mason. This cannot be readily explained.

Droplets which investigations had indicated were uncharged and in the process of freezing caused the probe to become negatively charged by a process which gave approximately one order of magnitude more charge than the splashing process. It was considered that this was the same process as was observed by Latham and Mason. It was concluded that the electrification was most readily explained by the Forknan - Reynolds effect.

APPENDIX 4.

Calculation of Droplet Freezing Times.

The following approach is a completely classical one and does not take into account the presence of dissolved gases in water, the difference in densities of water and ice, or the crystalline nature of ice which causes droplets to freeze in a complex manner. However, these factors cannot cause the freezing to proceed faster than is dictated by the rate at which heat can be conducted from the droplet surface.

When a water droplet of radius  $a_0$  is nucleated at  $-T^\circ \text{C}$ , a spherical shell whose mass is  $\frac{ST}{L}$  of the total mass is formed instantly, and the whole drop acquires a temperature of  $0^\circ \text{C}$ . The radius of the sphere of liquid water may be called  $\beta a_0$ . Since  $\beta = \sqrt{1 - \frac{ST}{L}}$ , it can be approximated to unity for  $T < 10$ ,  $L$ , the latent heat of fusion being  $80 \text{ cal gm}^{-1}$  and  $S$ , the specific heat of water being  $1.0 \text{ cal gm}^{-1} \text{ }^\circ\text{C}^{-1}$ . Upon nucleation the droplet proceeds to freeze inwards. After a certain time the liquid radius has become  $a(t)$ . The freezing rate and the surface temperature of the droplet vary in order to maintain a balance between the conduction of heat from the surface, the conduction of heat through the ice shell, and the production of latent heat at the freezing surface.

The calculation is based on the following three standard equations:

1) Rate of conduction of heat from the surface =

$$\frac{-4 \pi a_0 C K_A (T_A - T_S)}{}$$

2) Rate of conduction of heat through the ice shell =

$$\frac{-4 \pi K_i (T_S - T_W)}{\left( \frac{1}{a(t)} - \frac{1}{a_0} \right)}$$

3) Rate of production of latent heat =

$$\frac{4 \pi a(t)^2 \frac{d a(t)}{d t} \rho_i L}{}$$

where C is the ventilation coefficient,  $K_A$  is the thermal conductivity of the air,  $K_i$  is the thermal conductivity of ice,  $\rho_i$  is the density of ice and  $T_A$ ,  $T_S$  and  $T_W$  are the air, surface and water temperatures respectively, the latter being measured in degrees Absolute. By equating 1) and 2),  $T_S$  can be found:

$$T_S = T_W + \frac{T_A - T_W}{1 + \lambda}$$

where

$$\lambda = \frac{K_i a(t)}{C K_A (a_0 - a(t))}$$

Since the thermal

conductivity of ice is greater than that of air by a factor of approximately 100, it can be seen that throughout freezing until the droplet is very nearly completely frozen,  $\lambda$  will have a high numerical value. Since  $T_W = 273^\circ \text{K}$  it can be seen from the above expression that for high values of  $\lambda$  the surface temperature of the droplet will be only a fraction of a degree below  $0^\circ \text{C}$ . This result may have some bearing on the attempts which have been made to explain the electrification of shattering water drops by the temperature gradient theory.

Equating 3) and 1) and eliminating  $T_S$  gives:

$$a(t) \left[ a(t) K_1 + (a_0 - a(t)) CK_A \right] \frac{da(t)}{dt} \rho_i L = - a_0 C K_A K_1 (T_A - T_W)$$

Integrating this expression between  $a_0$  and  $a(t) = 0$  gives the expression for the freezing time  $t_F$  :

$$t_F = - \frac{\rho_i L a_0^2}{3(T_A - T_W)} \left( \frac{1}{CK_A} + \frac{1}{2K_1} \right)$$

The only approximation in this expression is that  $\beta = 1$ .

Using this expression the value of the quantity  $-t_F (T_A - T_W)$  was evaluated for various droplet sizes. The units are  $\text{sec}^\circ \text{C}$  and the significance of the quantity is that it can be used to determine the freezing time at any specified air temperature. The values are

given in Table 28.

TABLE 28.

The Quantity  $-t_F (T_A - T_W)$  for Various Droplet Sizes.

$a_d (\mu)$	$-t_F (T_A - T_W) \text{ sec } ^\circ \text{C.}$
20	1.0
50	5.4
100	17.4
150	31.6
200	47.3

Thus, from the table, a  $150 \mu$  radius droplet takes approximately  $1\frac{1}{2}$  sec to freeze when the air temperature is  $-20^\circ \text{C}$ . A  $150 \mu$  droplet falling through the 140 cm tube at  $111 \text{ cm sec}^{-1}$  was supercooled for only a fraction of this time, and therefore it was concluded that droplets of this size were not completely frozen.



CHAPTER 2.

CONCLUSIONS AND SUGGESTIONS FOR FURTHER WORK.

The results for the collision of  $20\ \mu$  size ice crystals with a pre-cooled and pre-heated stationary probe showed that  $2.5 \times 10^{-7}$  e.s.u. of charge were separated for a measured temperature difference of  $10^{\circ}$  C, but the results indicated that because of the ventilation of the probe surface, the mean effective temperature difference was much less than this. It was considered that the fact that the mean charge was greater than was found by Latham and Mason could be explained by the differences in details of the experimental techniques. It was concluded that the presence of impurities in the probe ice did not have a dominating influence on the rate of charging of the probe, and it was shown that the charge separated per crystal collision increased rapidly as the impact velocity increased. The main limitation of the apparatus was in the size of the crystals produced. They were approximately  $20\ \mu$  in diameter and it is difficult to compare accurately their effect on iced probes with that of natural ice crystals of  $100\ \mu$  diameter on hailstones because there will be differences in charging due to the different areas of contact and also the different surface structures. It is thought that little further information would be gained by adopting these experimental techniques in future studies of the electrification produced between impacting ice particles, but it is considered that further study would be valuable. What is required is to observe the charge separation

produced by projecting ice particles at impact velocities of up to  $10 \text{ m sec}^{-1}$  at an unventilated probe whose temperature could be varied. If the ice particles were spheres, results might be more reproducible. Although this would be a departure from reproducing atmospheric conditions it would help to establish the parameters governing electrification more precisely.

From measurements with a rotating probe it was concluded that there was negligible charging by the accretion of water droplets of estimated diameter  $3 - 5 \mu$ , and that large quantities of charge were separated by rebounding ice crystals in the presence of supercooled droplets. When the pre-cooled or pre-heated rotating probe encountered ice crystals in which the water droplet concentration was low the results were qualitatively in agreement with the temperature gradient theory. A value of  $10^{-6}$  e.s.u. for the charge separated per crystal collision was obtained. It was considered that this value corresponded to only a small temperature difference. Further investigations showed that the negative charging of the probe could be augmented to  $5 \times 10^{-6}$  e.s.u. per crystal collision if some supercooled droplets were present, although it was thought that if a greater number of droplets could have been supplied to the probe surface, the mean charge separated would have been greater. The rate at which droplets at a low temperature would be supplied was limited by the size of the refrigerator, which also prevented conditions in the cloud from staying constant for very long. It was difficult to explain the results quantitatively in terms of the temperature gradient theory because of several unknown factors.

Hitherto it has been recognised that quantitative verification of the theory in experiments of this type has been limited by insufficient knowledge of the area of contact and time of contact for ice crystal impacting on hailstones. To these, it is now suggested, may be added the insufficient knowledge of the temperature difference between the surfaces when the probe is ventilated. Even by considering values for these factors which were most favourable to the theory, it was seen that the observed rate of charging was much greater than could be explained by the temperature gradient theory. It is possible that an explanation for this may be sought in the increase of charging with impact velocity, although at the present time the reason for this enhancement is obscure.

In relating these laboratory results to the behaviour of particles in thunderclouds there is always the problem that the crystals which can be produced in the laboratory are smaller than those to be found in the atmosphere and there is consequently uncertainty as to their relative contact areas. It is probably this which has led workers such as Latham and Miller (1965) to perform experiments in natural clouds containing ice crystals, and which probably gave more meaningful quantitative results than laboratory measurements. The mean diameter of crystals used in the present experiments was  $40 \mu$ , whereas the most common sizes in thundercloud are 80 to  $175 \mu$ . It is difficult to make an estimate of the effect on the magnitude of charging of these increased crystal sizes, but it is thought that this would not

exceed one order of magnitude. Although one can surmise that if sufficient numbers of water droplets could have been supplied to the surface of the probe to heat it further but not enough for it to become wet, the charge separation would have been higher, this matter has not been proved here, and so the value of  $5 \times 10^{-6}$  e.s.u. will be taken as the maximum charge separated per crystal - hailstone collision. This is less by a factor of 100 than the value of Reynolds et al which was just sufficient to account for the electrification of a thundercloud, and even by taking into account the larger crystal sizes in thunderclouds, the present results cannot be considered to account for the electrification of thunderclouds. It was therefore concluded that in the light of the present experiments under atmospheric conditions in which there were high concentrations of hailstones, ice crystals and supercooled cloud droplets it was possible that large quantities of charge could be separated but that it was insufficient to explain thunderstorm electrification.

From the work on droplets it was concluded that when droplets in the radius range  $90 - 150 \mu$  struck the iced probe moving at  $10 \text{ m sec}^{-1}$ , the electrification observed was associated with splashing. It was shown that for droplets above about  $0^\circ \text{ C}$ , the probe was positively charged in accordance with the so-called Faraday effect, but that when the droplets were supercooled the probe was charged negatively, the mean charge per droplet decreasing as the degree of supercooling increased. The charge separated by this process depended critically on droplet size, being  $10^{-5}$  e.s.u. per droplet for  $150 \mu$  radius

droplets and  $4 \times 10^{-7}$  e.s.u. for  $90 \mu$  droplets. No charge separation for  $50 \mu$  droplets could be detected.

For droplets which were in the process of freezing the electrification was much greater. For  $150 \mu$  droplets the mean charge separated was up to  $2 \times 10^{-4}$  e.s.u., the average value being  $(8.4 \pm 2.6) \times 10^{-5}$  e.s.u. The average values for  $90 \mu$  and  $55 \mu$  radius droplets were  $(7.7 \pm 0.8) \times 10^{-5}$  and  $(2.3 \pm 0.2) \times 10^{-6}$  e.s.u. respectively. The magnitude of the charge separated was not sensitive to the impact velocity of the droplets on the probe.

The above measurements were made for droplets in a range of sizes greater than those investigated by Latham and Mason, and it would seem to be of value to repeat experiments using the smaller droplets. It is of particular interest to see whether any electrification produced would be influenced by the presence of small quantities of impurities. Particularly significant might be the effect of the presence of the ammonium ion in the droplets. The practical requirements of such an investigation are the production of sufficient uniformly - sized supercooled droplets which ideally should be in thermal equilibrium with their surroundings, and whose sizes can be adjusted at will and kept constant during their fall by control of humidity. A relative velocity of about  $10 \text{ m sec}^{-1}$  between the droplets and the probe must be effected. The present measurements have indicated that for droplets with radii less than  $50 \mu$  the probe must be stationary. It will be difficult to satisfy these requirements in an ordinary laboratory,

and although certain compromises in experimental procedure were possible for droplets greater than  $50 \mu$  radius, it becomes increasingly difficult to compromise as the droplets sizes become smaller.

Substantial electrification has been observed with partially - frozen droplets and whether these results are of direct significance to the electrification of clouds will depend on whether a significant number of such droplets encountered by a hail pellet in a thundercloud will be in the process of freezing. However the measurements may have served a purpose in providing a comparison with the droplet shattering work of Latham and Mason. It was considered that the separation of charge which was observed here, and which was also observed by Latham and Mason, could be explained more readily in terms of the Workman-Reynolds effect than the temperature gradient theory.

### ACKNOWLEDGEMENTS.

I am grateful to Prof. G.D. Rochester for the opportunity of doing research at Durham, and to Prof. J.A. Chalmers for his interest in the work and for allocating a research grant provided by the United States Navy.

I am indebted to my supervisor Dr. W.C.A. Hutchinson for his help and advice during the research work and in the preparation of this thesis.

I would like to thank Dr. J.V. Major and Dr. A. J. Apostalakis of the Physics Department for the loan of optical equipment and refrigerators.

I appreciate the assistance of the technical staff of both the Physics and Chemistry Departments during this period of research.

I finally wish to thank Mrs. E.W. Lincoln for the speed and accuracy with which she produced this typescript.

REFERENCES.

- BERNAL J.D.  
& FOWLER R.H. 1933 J. Chem. Phys. vol.1, p.515.
- BJERRUM N. 1951 K. Danske Vid. Selsk. fys. Medd.  
vol.27, p.56.
- BROOK M. 1959 R.A.A.E. p.383
- BYERS H.R. &  
BRAHAM R.R. 1949 The Thunderstorm (Washington, D.C.  
U.S. Weather Bureau)
- CHALMERS J.A. 1947 Q.J.R. Met. Soc. vol.73, p.324
- 1953 J. Atmosph. Terr. Phys. vol.3, p.346
- 1965 P.A.S.E. p.304.
- COSTA RIBEIRO J. 1945 Anais Acad. bras. Cienc. vol.17, p.2.
- DINGER J.E.  
& GUNN R. 1946 Terr. Magn. Atmos. Elect. vol.51, p.477.
- DINGER J.E. 1964 *Q.J.R. Met. Soc. vol. 90, p. 208.*
- EIGEN M &  
DE MAEYER L. 1958 Proc. Royal Soc. A. vol.247, p.505.
- ELSTER J. &  
GEITEL H. 1913 Phys. Z. vol.14, p.1287.
- FARADAY M. 1845 Ann. Phys. vol.60, p.342
- FINDEISEN W. 1940 Met. Z. vol.57, p.201.
- FINDEISEN W.  
& FINDEISEN E. 1943 Met. Z. vol.60, p.145.
- GISH O.H. &  
WAIT G.R. 1950 J. Geophys. Res. vol.55, p.473
- GRENET G. 1947 Ann. Geophys. vol.3, p.306.
- HOSLER.  
& HALLGREN. 1960 M.S. Thesis, Dept. of Meteorology,  
Pennsylvania State Univ.
- JACCARD C. 1963 Physik der Kondens. Materie vol.1, p.143



REFERENCES (Continued)

- JONES R.F. 1960 Q.J.R. Met.Soc. vol.86, p.187
- KIKUCHI K. 1965 I.C.C.P. p.338
- KOBAYASHI T. 1955 Contrib. Inst. Low. Temp. Sci.,  
Hokkaido Univ. vol. 8, p.75
- KRAMER C. 1948 Kon. Ned. Met. Inst. No.102  
Med. en Verh. Series A. Vol.52.
- KÜTTNER J.P. 1950 Met. Rundschau. vol.3, p.145
- LATHAM J.R. & 1961A Proc. Royal Soc. A vol.260, p.523  
MASON B.J. 1961B Proc. Royal Soc. A vol.260, p.537.
- LATHAM J. 1964 Q.J. R. Met. Soc. vol.90, p.266  
1965 Tellus vol.17, p.204.
- LATHAM J. & 1965A I.C.C.P. p.352.  
STOW C.D. 1965B Q.J.R. Met. Soc. vol.390, p.462.  
1965C Q.J.R. Met. Soc. vol.390, p.539.
- LATHAM J. & 1965 J. Atmos. Sci. vol.22, p.505.  
MILLER A.H.
- LATHAM J. MYSTROM 1965 Nature vol. 206, no.4991, p.1344.  
R. E. & SARTOR J. D.
- MACCREADY P.B. & 1965 Q.J.R. Met. Soc. vol.91, p.44  
PROUDFIT A. 1965 Q.J.R. met. Soc. vol.91, p.54.
- MAGONO C. & 1963 J. Met. Soc. Japan vol.41, p.270  
KIKUCHI K. 1965 J. Met. Soc. Japan vol.43, p.331.
- MAGONO C & 1963 J. Met. Soc. Japan vol.41, p.197  
TAKAHA SHI T.
- MASON B.J. 1953 Tellus vol, 5, p.446  
1956 Q.J.R. Met. Soc. vol.82, p.209

REFERENCES (Continued)

- MASON B.J. & OWSTON P.G. 1952 Phil. Mag. vol.43, p.911
- MASON B.J. JAYARATNE O.W. & WOODS J.D. 1963 J. Sci. Inst. vol, 40. p.247
- MATTHEWS B.J. & MASON B.J. 1963 Q.J.R. Met. Soc. vol. 89, p.376.
- MEINHOLD H. 1951 Geofis. Pura e App. vol. 19, p.176.
- MOORE C.B. 1965 P.A.S.E. p.255
- MÜLLER - HILLEBRAND D. 1954 Tellus vol.6, p.367
- PAULING L. 1960 Nature of the Chemical Bond 3rd edition p.466.
- PIERCE E.T. 1955 Q.J.R. Met. Soc. vol.31, p.211
- REITER R. & CARNUTH W. 1965 J. Atmosph. Terr. Phys. vol,27, p.673.
- REYNOLDS S.E. BROOK M. & GOURLEY R.F. 1957 J. Met. vol. 14, p.426.
- SARTOR J.D. 1961. J. Geophys. Res. vol. 66, p.831 and 3070.
- SCHAEFER V.J. 1946. Science, vol. 104, p.457.
- SOHNCKE L. 1886. Ann. Phys. vol.28, p.551.
- STERGISC. G., REIN G.C. & KANGAS T. 1957 J. Atmosph. Terr. Phys. vol.11, p.83
- TEICHMANN & SCHMIDT 1965 Phys. Status Solidi vol.6, p.145
- VONNEGUT B. 1955 Wentworth Conference p.169.
- VONNEGUT B. & MOORE C.B. 1958 R.A.A.E. p.317.

REFERENCES ( Continued )

- WEICKMANN H.K. & AUFM KAMPE H.J. 1950 J. Met. vol. 7, p.404.
- WHIPPLE F.J.W. & CHALMERS J.A. 1944 Q.J.R. Met. Soc. vol.70, p.103.
- WILSON C.T.R. 1929 J. Franklin Inst. vol.208, p.1.  
1956 Proc. Royal Soc. A. vol.236, p.297
- WORKMAN E.J. & HOLZER R.E. 1942 N.A.C.A. Washington, Tech. Note No.850.
- WORKMAN E.J. & REYNOLDS S.E. 1948 Phys. Rev. vol. 74, p.709  
1949 Bull. Amer. Met. Soc. vol.30, p.142.  
1950 Phys. Rev. vol. 78, p.254.
- WORMELL T.W. 1953 Q.J.R. Met. Soc. vol. 79, p.3.

Textbooks and Collected Papers.

- BERNAL J.D. et al. A Discussion on the Physics of Ice and Water.  
Proc. Royal Soc. A. vol.247, (1958) p.421.
- CHALMERS J.A. Atmospheric Electricity. Pergamon 1957.
- CORONITI S.C. (Ed.) Problems of Atmospheric and Space Electricity  
(P.A.S.E.) Elsevier 1965.
- HATA KEYAMA H.  
(Chairman) International Conference on Cloud Physics  
Tokyo and Sapporo (I.C.C.P.), 1965.
- HENRY P.S.H. Brit. J. App. Phys. Supplement 2 p. S 31, 1953.
- LOEB L.B. Static Electrification, Springer, 1958.
- MASON B. J. The Physics of Clouds, Oxford, 1957.
- SMITH L.G. (Ed.) Recent Advances in Atmospheric Electricity  
(R.A.A.E.), Pergamon, 1958.